Development and application of mass spectrometric methods for the investigation of organocatalytic reactions

Dissertation

zur Erlangung des akademischen Grades eines

Doktors der Naturwissenschaften

– Dr. rer. nat. –

vorgelegt von

MOHAMMED WASIM ALACHRAF

geboren in Damaskus

Fakultät für Chemie

der

UNIVERSITÄT DUISBURG-ESSEN

MÜLHEIM AN DER RUHR

2013

Die vorliegende Arbeit wurde im Zeitraum von März 2009 bis Februar 2013 im Arbeitskreis von PD Dr. Wolfgang Schrader am Max Planck Institut für Kohlenforschung durchgeführt.

Tag der Disputation: 09.09.2013

Gutachter:	PD Dr. Wolfgang Schrader
	Prof. Dr. Carsten Schmuck
Vorsitzender:	Prof. Dr. Oliver J. Schmitz

Acknowledgements

My greatest thanks are devoted to PD Dr. Wolfgang Schrader, Prof. Dr. Benjamin List, and Prof. Dr. Peter Schreiner for their continuous encouragement and helpful advice throughout this work.

Furthermore, I would like to thank all friends and colleagues at Max Planck Institut für Kohlenforschung, who helped and supported me during my studies.

Most importantly, I would like to thank my family for all their support and endless encouragement.

„Hohe Bildung kann man dadurch beweisen,

dass man die kompliziertesten Dinge auf einfache Art zu erläutern versteht"

George Bernard Shaw

Abstract

In the last few years organocatalysis has emerged as a new catalytic method based on metal-free organic molecules. In many cases these often small compounds give rise to extremely high enantioselectivity. Usually the reactions can be performed under an aerobic atmosphere with non-anhydrous solvents. The catalysts can be easily synthesized in both enantiomerically pure forms and are often more stable than enzymes or other bioorganic catalysts. Despite the significant growth in the number of organocatalytic researches, still the mechanistic details of many reactions are not fully understood. The knowledge of the reaction mechanism on the other hand is important to optimize the reaction conditions toward higher reaction efficiency.

Structural elucidation of organic compounds is commonly achieved by analytical techniques such as NMR-, UV/Vis- or IR-spectroscopy. The information gained from these methods is essential for the characterization of the reactive intermediates and thus the reaction mechanism investigation. These spectroscopic methods however have enormous limitations when the compounds of interest are existent only in low concentrations or have very short life times.

Mass spectrometry is the method of choice for the analysis of rapid and complex catalytic reactions. Because mass spectrometry is generally a very fast and sensitive technique, it is capable of investigating compounds with short life times and in low concentrations. In addition it is also possible to characterize different analytes at the same time without separation and, with MS/MS experiments, to perform a structural elucidation of each of these directly from the reaction solution.

High resolution MS can be used to gain the elemental composition of the unknown analyte(s), which can give further insight into the studied mechanisms and the compounds that are involved.

Different mechanistic studies of complex organocatalyzed reactions are presented in this work. These reactions have been investigated using unique methods of mass spectrometry such as isotopic labeling, online monitoring and ion/molecule reactions in the collision cell of the mass spectrometer.

Kurzfassung

In den letzten Jahren wurden mit der Organokatalyse neue, katalytische Methoden entwickelt, die auf metallfreien organischen Molekülen basieren. In vielen Fällen wird durch diese oft kleinen Verbindungen eine extrem hohe Enantioselektivität erreicht. Normalerweise können die Reaktionen hierbei an Luft mit nicht wasserfreien Lösungsmitteln durchgeführt werden. Die Katalysatoren können problemlos in beiden enantiomerenreinen Formen synthetisiert werden und sind oft stabiler als Enzyme oder andere bioorganische Katalysatoren. Trotz der deutlichen Zunahme an Forschungsaktivitätenen auf dem Gebiet der Organokatalyse sind die mechanistischen Details vieler Reaktionen noch nicht völlig verstanden. Die Kenntnis der Mechanismen hingegen ist wichtig, um die Reaktionsbedingungen zu optimieren und die Effizienz der Reaktionen zu steigern.

Strukturaufklärung bei organischen Verbindungen wird üblicherweise mit Hilfe analytischer Techniken wie NMR-, UV/Vis- oder IR-Spektroskopie erreicht. Die Informationen, die aus diesen Methoden gewonnen werden können, sind wesentlich für die Charakterisierung der reaktiven Zwischenprodukte bzw. des Reaktionsmechanismus. Diese spektroskopischen Methoden haben allerdings enorme Einschränkungen, wenn die interessierenden Verbindungen nur in geringen Konzentrationen vorhanden sind oder sehr kurze Lebenszeiten haben.

Für die schnelle Analyse von komplexen katalytischen Reaktionen ist die Massenspektrometrie die Methode der Wahl.

Da MS in der Regel eine sehr schnelle und empfindliche Technik ist, ist sie in der Lage Verbindungen auch in sehr niedrigen Konzentrationen und mit kurzen Lebensdauern zu untersuchen. Außerdem ist es möglich, verschiedene Analyten gleichzeitig, ohne vorherige Trennung, zu charakterisieren und mit Hilfe von MS/MS-Experimenten eine Strukturaufklärung von diesen direkt aus der Reaktionslösung durchzuführen.

Hochauflösende MS ermöglicht die Bestimmung der Summenformel unbekannter Analyten und gibt dadurch einen zusätzlichen Einblick in die untersuchten Reaktionsmechanismen und Verbindungen.

Verschiedene mechanistische Studien komplexer organokatalysierter Reaktionen werden in dieser Arbeit vorgestellt. Diese Reaktionen wurden unter Verwendung einzigartiger Methoden der Massenspektrometrie, wie Isotopenmarkierung, Online-Überwachung und Ion / Molekül-Reaktionen in der Kollisionszelle des Massenspektrometers untersucht.

Contents

1. Introduction

Asymmetric synthesis

Asymmetric synthesis is one of the most important fields of research and development in organic chemistry. The importance of asymmetric synthesis comes from the fact that the living systems are chiral. Therefore bioactive drug molecules which interact with receptors and enzymes in the living systems must have the proper chirality to be able to make this interaction.[1] Additionally it is known that two bioactive enantiomers can have very different pharmacological effects. For example (-)-Propranolol **A** was introduced in the 1960s as betABlocking drug used in the treatment of heart disease while the (+) enantiomer **B** is a contraceptive.[2] (See Figure 1.1)

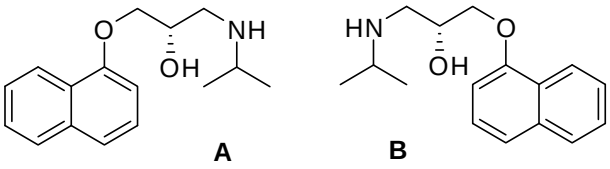

Figure 1.1 (-)-Propranolol **A** was introduced in the 1960s β-blocker used in the treatment of heart disease. The (+) enantiomer **B** is a contraceptive.

Another example of the different pharmacological effects of the different molecule chirality is thalidomide. (R)-Thalidomide works as an anti-nausea and sedative drug[3], while (S)-Thalidomide causes birth defects.[4] (See Figure 1.2).

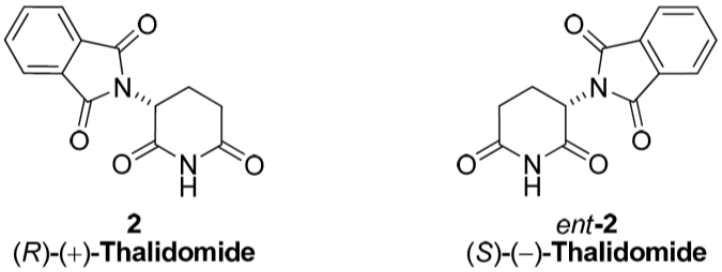

Figure 1.2 (R)-Thalidomide and (S)-Thalidomide.

That explains the importance of enantioselectivity of chemical production with regard of clinical issues.

Organocatalysis

Until a few years ago there were two major methods available for asymmetric synthesis the transition metal catalysis, where transition metals were used with chiral ligands, and bio-catalysis. A third approach to the catalytic synthesis of enantiomerically pure organic compounds has emerged in the last few years – organocatalysis. Organocatalysts are mostly small organic molecules, i.e. composed of mainly carbon, hydrogen, nitrogen, sulfur and phosphorus, that accelerate chemical reactions with a substoichiometric amount of organic molecules and do not contain any metals, thereby reducing toxic effects and have several important advantages over transition metal- and bio-catalysis, since they are usually robust, inexpensive, readily available and non-toxic. Because of their inertness towards moisture and oxygen, demanding reaction conditions, like inert atmospheres, low temperatures, absolute solvents, etc., are not required. Thus, the catalysts are more stable than enzymes or other bioorganic catalysts. They are to synthesize and allow easy separation from the product without racemization.[5, 6]

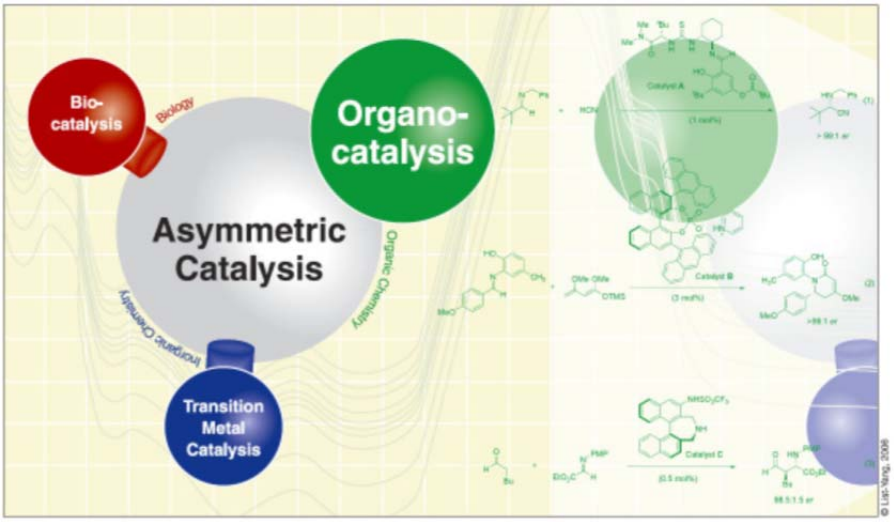

Figure 1.3 The three pillars of asymmetric catalysis: Bio-catalysis, metal catalysis and organocatalysis.[7]

The first reported asymmetric organocatalytic reaction was an intramolecular asymmetric aldol reaction of a triketone catalyzed by L-proline in 1971 by two industrial research groups from Hajos and Parris[8] at Hoffmann-La Roche while the group of Eder, Sauer and Wiechert[9] at Schering AG reported an intramolecular aldol reaction catalyzed by the same catalyst (Figure 1.4).

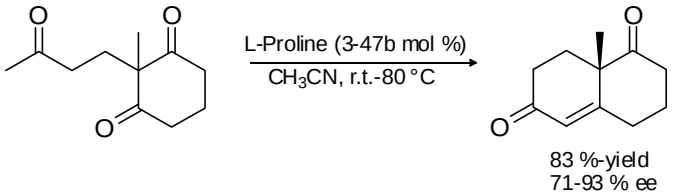

Figure 1.4 The Hajos-Parrish-Eder-Sauer-Wiechert reactions.

Organocatalytic reactions can be classified into two main categories, the first one is the reaction that involves the formation of covalent adducts between catalyst and substrate(s) such as enamine and iminium ion formation.

The second one is the reaction that relies on non-covalent interactions such as hydrogen bonding formation. The former interaction has been termed as "covalent catalysis" and the latter is usually known as "non-covalent catalysis"[10].

According to the mechanistic classification by List[11] as shown in Figure 1.5, the formation of covalent substrate-catalyst adducts occur as a result of Lewis acid - Lewis base interaction. In many instances, non-covalent catalysis relies on the interaction of Brønsted base - Brønsted acid catalysts.

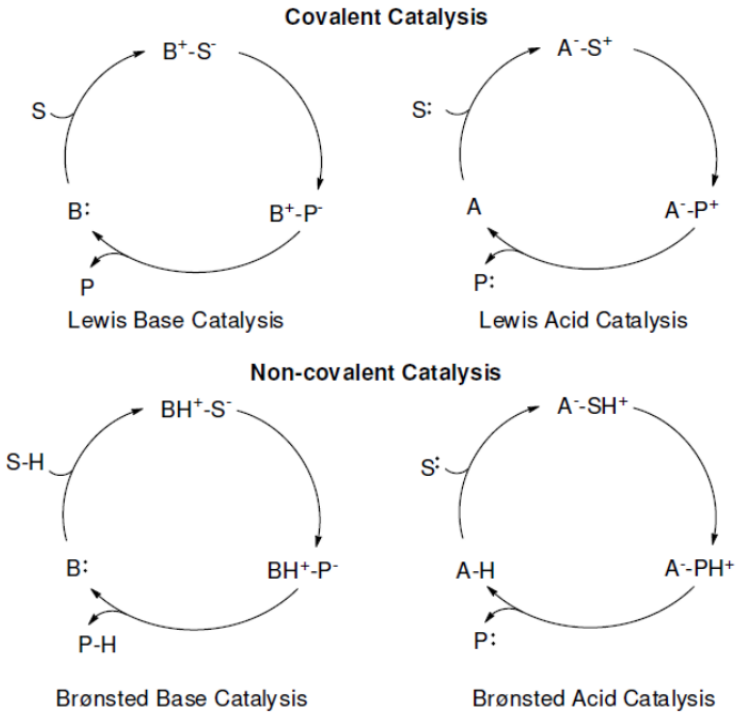

Figure 1.5 Scheme of Organocatalytic Cycle; A: Acid, B: Base, S: Substrate, P: Product.

1.2.1. Lewis Base Catalysis

Lewis base catalysts (B:) begin the catalytic process via nucleophilic addition to the substrate (S). The formed complex undergoes a reaction leading to release the product (P) and the catalyst for more turnover. The typical examples of such kind of catalysis are the enamine catalysis or iminium ion catalysis.

1.2.2. Lewis Acid Catalysis

Lewis acid catalysts (A) attack nucleophilic substrates (S:) leading to the formation of the adduct (A^{-}-S^{+}). which converted to (A^{-}-P^{+}), followed by liberation of the product (P). The catalyst (A) re-enters the catalytic process. Phase transfer catalysts are typical example of Lewis acid organocatalysts which can be successfully used for enantioselective amino acid synthesis.[12]

1.2.3. Brønsted Base Catalysis

Brønsted base catalyzed reactions start with a deprotonation of the substrate S-H, followed by forming of the intermediates ($B^{+}H$-S^{-}) and further to ($B^{+}H$-P^{-}). Elimination of the product (P-H) takes place and the catalyst (B) re-enter the catalytic cycle. The Strecker reaction is a typical examples of organic Brønsted base catalysis in asymmetric synthesis as shown by Lipton who used a cyclopeptide as organocatalyst.[13]

1.2.4. Brønsted Acid Catalysis

Organocatalytic processes starting with a protonation of the substrate (S:). The reaction continues through the formation of ($A^{-}SH^{+}$) which converts into ($A^{-}PH$). Product (P) is liberated from the complex and (A-H) continues the reaction cycle. Catalysis via hydrogen bonding[14] has been presented recently as a new method for asymmetric catalysis. Typical example for the Brønsted acids catalysis is using urea and thiourea compounds as chiral Brønsted acids to activate carbonyl- and imine groups in extending the Strecker reaction[15] as shown by Jacobsen.

1.3. Reaction mechanism investigation and reactive intermediate characterization

In chemistry, to gain accurate information about catalytic reactions, and to understand the reaction more deeply than just its reactants and products, it is important to study the different steps of the reaction thoroughly and investigate its mechanism.
A reaction mechanism is an exact step-by-step description of the reaction pathway of the reactant(s) to the products involving all atom and electron positions of reactants, products as well as the solvent and the catalysts.[16]
The aim of mechanistic reaction studies is to

- synthesize the desired products in high yield and minimize the side products.
- increase reaction efficiency in regard to energy, solvents and time.

The investigation of the reaction pathway is achieved by splitting an overall reaction into a series of intermediate reactions. These intermediate properties can then be characterized individually and can collectively tell us much about the properties of the overall reactions.[17] Intermediates can be short lived or present only in small concentrations, therefore demanding sensitive methods for investigation.

1.4. Analytical techniques for the investigation of organocatalytic reaction mechanisms

Structural elucidation in the organic reactions is achieved by analytical techniques such as NMR, UV/Vis, IR, MS. In this chapter, a short outline of different analytical techniques for structural elucidation of the reactants, the products and even the reactive intermediates which assist in the mechanistic investigation of organocatalytic reactions is given.

1.4.1. Nuclear magnetic resonance (NMR)

Nuclear magnetic resonance (NMR) was first described by Isidor Rabi in 1938[18]. In the 1950s after discovering of the chemical shift the NMR signals carried information about the structural details due to the different hydrogen, carbon, and heteroatom environments of the nucleus.[19] ^{1}H NMR directs the hydrogen nuclei in the studied molecule. ^{13}C NMR focuses on the detection of carbon atoms in the studied molecule. By NMR, organic compounds mostly

can be characterized and easily elucidated. Thus, it makes NMR a brilliant analytical tool for distinguishing and studying structures of organic compounds. However, one disadvantage of this analytical technique is the detection limit of NMR spectroscopy. Accordingly, NMR spectroscopy cannot be employed when desired compounds are existent in low concentrations or have very short life times. Many reports using NMR in the mechanistic studies of organocatalytic reactions are published in the last decades. Page et al.[20] studied the mechanism of an organocatalytic reaction for asymmetric epoxidation with NMR. However, they faced difficulties to detect some of the reactive intermediates due to peak overlapping and their low concentrations. In another report, Gschwind[21] focused on enamine intermediate pathway in proline catalyzed aldol reaction. This work presented a first report to detect the enamine intermediates in situ by NMR. In contrast only product enamines[22] or dienamines,[23] and dienamine intermediates[24] have been reported before.

1.4.2. Ultraviolet-visible spectroscopy (UV/Vis)

Ultraviolet-visible spectroscopy (UV/Vis) indicates to absorption spectroscopy in the ultraviolet-visible spectral region. This wavelength range is absorbed particularly by the conjugated double bond systems. So this method can help to characterize conjugated species such as alkenes, alkynes and aromatic ring systems. However, UV/Vis suffers from the fact that it does not give details structural information.

1.4.3. Infrared spectroscopy (IR)

Infrared spectroscopy (IR) deals with the radiation in the frequency range 4000- 400cm^{-1}. IR spectroscopy is essentially tool for detecting specific functional groups which have a high IR-absorbance such as carbonyl group, nitriles, ketenes, and ammonium ions. In fact molecules have certain frequencies of rotation or vibration of bonds corresponding to specific energy levels[25]. Unfortunately the rotational energies of a given vibrational band for a complex organic molecule can be usually difficult resolved.

1.4.4. Mass spectrometry (MS)

Mass spectrometry has shown in recent years that it can be the method of choice for fast and detailed studies of chemical reactions *Atmospheric Pressure Ionization Mass Spectrometry* (API-MS) and especially *Electrospray Ionization Mass Spectrometry* (ESI-MS) have developed for the analysis of rapid and complex catalytic reactions.[26-28] The main advantage of this technique is its ability to transfer starting materials, intermediates and products as intact ions, with single or multiple charges, from complex and labile species, softly,

selectively and very sensitively from reaction solution to gas phase in ionic form in order to measure their masses and elucidate their structure using tandem-MS. A lot of mechanistic studies in chemistry have been carried out in the last few years using ESI-MS to investigate chemical reactions in the gas phase [29, 30] or in the solution.[31-34]

In some cases the ESI-MS has shown some limitation especially in the case of low-polar analytes. *Atmospheric Pressure Chemical Ionization Mass Spectrometry* (APCI-MS) and *Atmospheric Pressure Photo Ionizations Mass Spectrometry* (APPI-MS) have been chosen to detect non-polar or aromatic analytes respectively. These ion sources (ESI, APCI, and APPI) give the ability to cover the broad spectrum of different polarities and volatilities of the analytes (Figure 1.6).

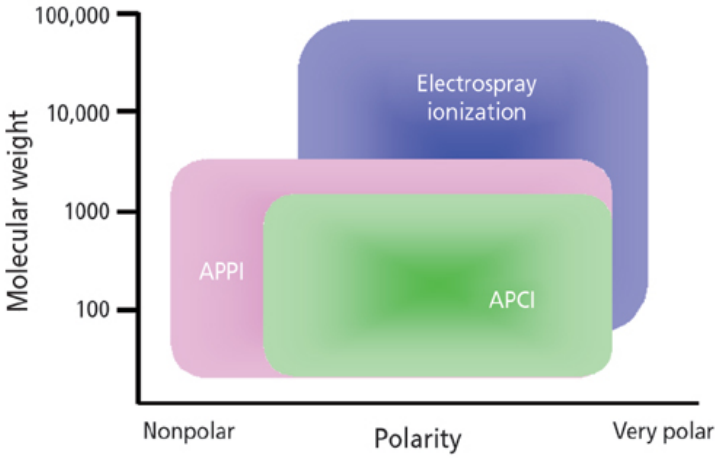

Figure 1.6 Ionization Methods and Applicable Compounds.[35]

In addition to the flexibility, usage of the suitable ion source is dependent upon the desired analyte. Additionally it is possible to choose different mass spectrometric analyzers depending on the measurement requirements. The two major mass spectrometric systems used in this work are a triple quadrupole MS (TSQ Quantum Ultra) as standard analytical tool for the measurement with good sensitivity and ability to use it for tandem-MS (MS/MS), and a hybrid quadrupole ion trap / Orbitrap mass spectrometer (Orbitrap Elite) which allowed high resolution and high accuracy mass measurement. All details about the different analyzers will be explained in the next chapter.

An additional important advantage of using mass spectrometry over other analytical techniques as tool for mechanistic studies of organic reactions is the different possibilities to introduce the reaction mixture sample and screen it in the MS-system depending of the requirement of the experiments.

In principle, there are two different methods to introduce and monitor the reaction mixture sample in API-MS to study a reaction: offline and online monitoring. For offline monitoring, the reaction starting material with catalyst are mixed to produce the different intermediates, products and by-products which determined over time as the reactants are progressively transformed into products.[36] The limitation of this technique is that intermediates have to have a reasonable concentration and have enough life time before degradation to be detected.

When the reaction rate is high online-monitoring can be used. The reactants with catalyst are mixed in a vial, transferred to a syringe and then injected into the MS-system. The reaction occurs in the syringe, so that it can be studied online within approximately 30 minutes (subject to the syringe capacity and the flow rate).

In the case of high reaction rates, it is possible to gain the mechanistic information about the reactions in solution by using so called tubular reactor coupled to the ion source. The main advantage of this technique is that it grants the ability to detect reaction intermediates, which have very short life times, by using a mixing -T, which combines the different solutions of the reactants continuously and direct them to the ion source.[37] It is possible to adjust the reaction time depending of the length of capillary between the reactor and the ion source (Figure 1.7).

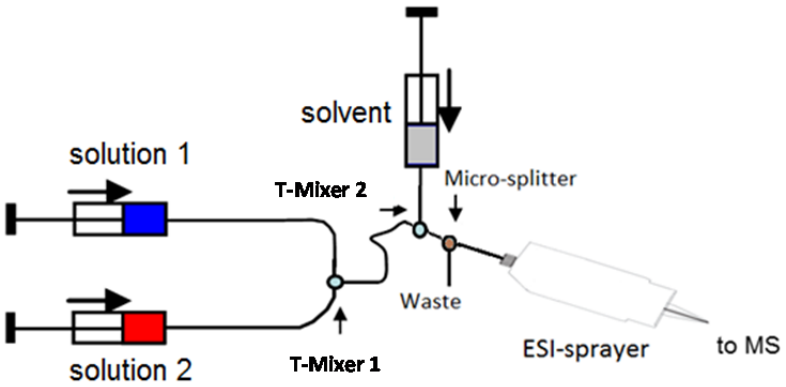

Figure 1.7 Schematic drawing of online tubular reactor.

In the case of a very high reaction rate of some active intermediates (life time is very short) the reaction can be done in the sprayer of the ionization source itself. The different reactants solutions are injected cautiously using two different syringes and mixed unlike the previous technique in T-mixer but in the end of the fused silica capillary of the ESI-source. So the MS-screening is done immediately after the building of the active intermediate and before it is converted to the end product. As explained in Figure 1.8.

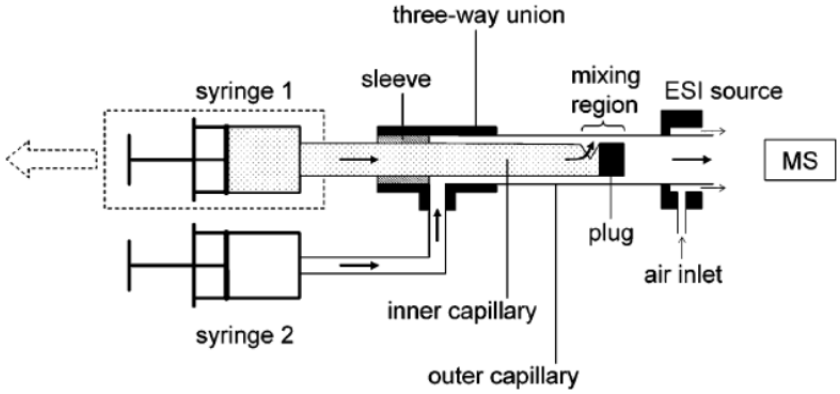

Figure 1.8 Schematic cross-sectional diagram of the experimental apparatus for time-resolved ESI-MS experiments. Syringes 1 and 2 deliver a continuous flow of reactants; mixing of the two solutions initiates the reaction of interest. The inner capillary can be automatically pulled back together with syringe 1, thus providing a means to control the average reaction time. Small arrows in the electrospray (ESI) source region represent the directions of air flow.[38]

Another important advantage of MS is the ability to apply isotopic labeling technique. Isotopic labeled molecule is a term used to describe such an ion which has an abundance of certain nuclide increased above the natural level at one or more (specific) positions. The isotopic labeling has different application in mass spectrometry as ordering to tracking metabolic pathways, serving as internal standard for quantitative analysis, or elucidation of fragmentation mechanisms of ions in the gas phase.[39, 40]

1.5. Mass Spectrometry

Since the beginning of the last century, mass spectrometry has developed into a powerful technique for characterization of unknown organic small molecules, and probing the fundamental aspects of chemistry. In the last two decades, mass spectrometry evolved and changed dramatically in all its components and became the prime analytical tool for the chemical and life sciences. Typical mass spectrometric research focuses on the formation of ions in the gas phase, ions chemistry, and applications of mass spectrometry which is the aim of this work.

All mass spectrometric systems have the same components, where the analytes transferred from liquid or solid state into the gas phase as ionized molecules by an ionization source and then analyzed and detected depending on their *m/z* ratio. In general we can divide the MS into six parts (Figure 1.9).

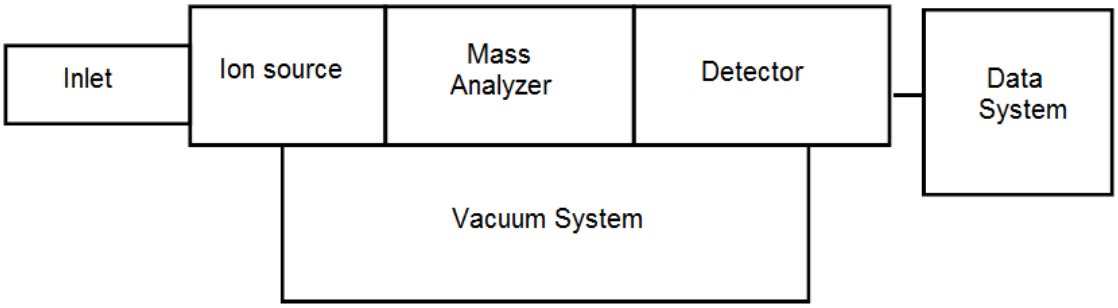

Figure 1.9 Schematic representations of mass spectrometry different parts.

1. The inlet system: where the sample is transferred to the ion source
2. The ion source: in the ion source neutral sample molecules are ionized and then accelerated into the mass analyzer
3. The mass analyzer: this is the heart of the mass spectrometer. In this part ions are separated, either in space or in time, according to their mass to charge ratio.
4. Detector: where the separated ions are detected
5. Data systems: where the information signals from the detector are analyzed to give the spectrum
6. Vacuum system: The high vacuum is required for operation of mass spectrometer to minimize the ion molecule reaction, scattering and neutralization of ions.

Here, the focus will be on ion sources and analyzers that have been explained in this work.

1.5.1. Ion sources

Mass analyzers cannot deal with the neutral analytes. Thus it is a basic requirement to convert the desired sample to corresponding ions by ion source part to be later analyzed depending on the *m/z* ratio by the analyzer.

The classical method of the ionization is electron impact (EI). In this technique a high energetic electron beam of 70 eV is interact with the analyte which is evaporated to the gas phase. Due to the high energy in this technique the anlyte tends to be fragmented which can be useful for the structure elucidation of the analyte.

The basic ionization technique used in this work is *Electrospray Ionization* (ESI). ESI is the most common atmospheric pressure ionization (API) source due to its advantages over the other ionization technique. It is a soft ionization method with minimum fragmentation. This allows ionizing big, thermally labile or non-volatile molecules. Therefore, nowadays, it is the preferred method used to ionize peptides, proteins and polymers.

The electrospray is achieved by applying a large potential difference (a few kV) between the tip of the metal needle and the inlet of the mass spectrometer. The produced electric field from the high voltage causes charge separation in the liquid. This forms a Taylor cone. When the surface tension of the liquid is exceeded by the applied electrostatic force in the cone, charged droplets are produced. These charged droplets include a large amount of ions. Then a desolvation of the droplets is taken place. This leads to a reduction in their diameter. Due to their charge, the droplets are subdivided by Coulomb explosion, which will take place at the point called Rayleigh limit.[41]

To describe this phenomenon there are two different theories discussed in the literatures. *The Ion Evaporation Model* (IEM) describes that the ions are transferred from the droplet to the gas phase directly.[42, 43] The second model called *the charge residue model* (CRM) where produced nanodroplets from the Coulomb fission containing only a single analyte molecule and surrounding with some solvent molecules which retain the charge state of the nanodroplet. Desolvation takes place completely to the droplets, leads analyte ion in the gas phase.[44] (See Figure 1.10).

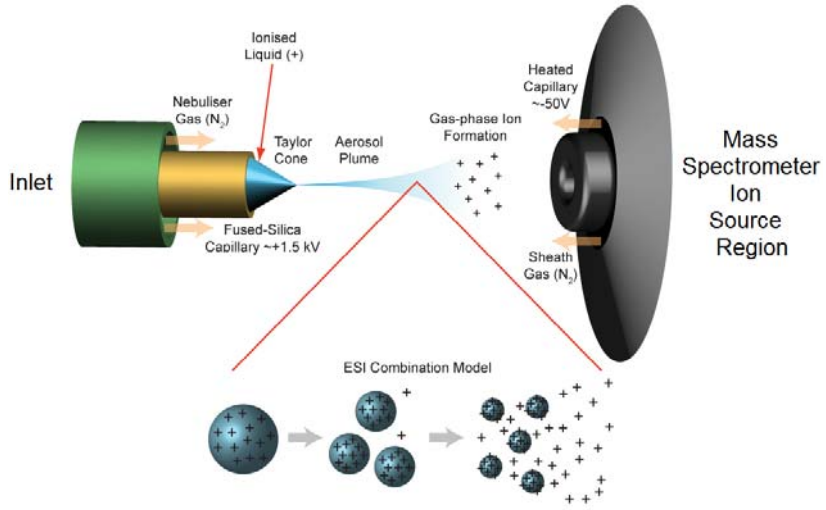

Figure 1.10 Schematic drawing of an ESI interface.[45]

Other techniques which are considered as soft ionization methods and are working under atmospheric pressure conditions API are:

- Atmospheric pressure chemical ionization[46] (APCI): the analyte is ionized by an ion-molecule reaction where the primary ions are produced by a corona discharge
- Atmospheric pressure photo ionization[47] (APPI): the analyte is ionized by single-photon using UV-lamp
- Atmospheric pressure laser ionization[48] (APLI): the analyte is ionized by two photon ionization using a UV-laser source.

The other group of the ionization methods are classified as desorption techniques, as the ions are produced when fast primary particles bombard the analyte.
Examples for this technique with primary particles are as follows:

- Secondary Ionization method (SI): ions like Cs^+ , Ar^+
- Fast Atom Bombardment (FAB): neutral atoms like Xe, Ar
- Matrix Assisted Laser Desorption (MALDI): photons

1.5.2. Analyzers

In addition to a number of new ionization methods developments in analyzers technologies have shown that MS is very innovative analytical technique. In general there are two categories of analyzers depending on the way of separation of ions. The first one called tandem in space, where the separation elements are physically separated and distinct, like quadrupoles, sector field, and time of flight (TOF). The other one called tandem in time, the ion separation is achieved in the same place with multiple separation steps over time, like quadrupole ion trap, Orbitrap, and Fourier transform-ion cyclotron resonance MS (FT-ICR MS).
We will focus on three types of analyzers: triple quadrupoles, quadrupole ion trap (QIT) and Orbitrap which are used in this work.

1.5.2.1. Quadrupole Mass Analyzer

The quadrupole mass analyzer developed in the 1950s[49] and it is the most common analyzer nowadays due to its fast scan rate, compact size, high transmission efficiency, and low vacuum requirement.[50] This leads to a small and inexpensive mass spectrometer. It is comprised of four cylindrical rods, set parallel quadratic. Radio frequency (RF) and direct current (DC) voltages (negative for negative scan modus or positive for positive one) applied to each opposing pair of rods by crossing way to gain an electric quadrupole field (Figure 1.11).

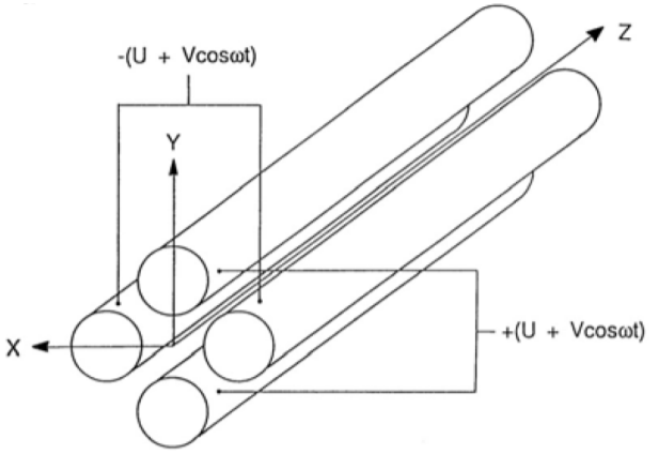

Figure 1.11 Schematic representation of quadrupole analyzer.

Depending on the ratio between DC and RF values only ions with a certain *m/z* can pass the analyzer to the detector while all other ions will have unstable trajectories and hit the rods.

1.5.2.2. Triple Quadrupole analyzer (QqQ)

A series of three quadrupoles can be used as triple quadrupole analyzer in order to perform tandem mass analysis,[39] which is a tool for a structure elucidation of the desired analytes. That overcomes the disadvantages of using a soft ionization method like electrospray ionization ESI which leads a minimum fragmentation. This fragmentation is necessary for structural elucidation of desired ions (see Figure 1.12).

The analyzer consists of a quadrupole mass filter (Q1) a quadrupole (q2) used as a collision cell and filled with a collision gas, and a second quadrupole mass filter (Q3). In the MS/MS mode, the first and third quadrupoles are run with the combination of both RF and DC potentials, thus they are critical for mass selection. The mass filter (Q1) is set on certain potential value to isolate a desired parent ion. The selected ions are then transmitted toward q2. The ions are collided in this collision chamber with a neutral inert gas such as Ar or He at adjustable collision energies (1-100 eV). The produced fragments are then transmitted out of the collision cell into the second mass filter Q3, which scans resulting fragments. Structural information of the molecules can be provided from the produced fragmentation pattern of the desired ion from the CAD fragments. In the normal MS-mode measurement either Q1 or Q3 can be set to RF-only mode, thereby it just acts as an ion transfer element. The analyzer set then behaves as a single quadrupole filter.

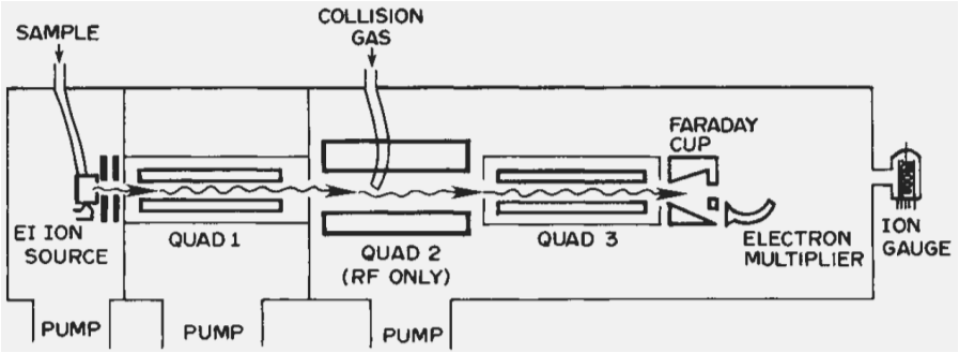

Figure 1.12 Schematic representation of triple quadrupole mass spectrometer.[51]

1.5.2.3. The 2D ion trap or linear ion trap (LIT)

The 2D ion trap is constructed like a quadrupole with the exception that the rods are separated into three different segments. The front and back of all rods together act as trapping electrodes. The trapped ions are slowed down or cooled by cooling gas (inert gas like He) and oscillating in the xy axes in the middle section due to the application of RF potential on the rods. Ions with certain *m/z* value are ejected through slots cut in two opposite rods by variation of RF-potential and received by the electron multiplier to be detected (Figure 1.13). It is also possible to achieve tandem MS experiments with a linear ion trap. The desired precursor ion can be isolated through adjusting of the applied RF potential value and fragmented in the same cell (tandem in time). The corresponding fragments are scanned with variation of RF potential again and detected by the detector. One fragment from the previous fragmentation experiment can be selected and fragmented again in a new tandem MS experiment. This procedure can be repeated again and again (MS^n) instead of just MS/MS as in the case of triple quadrupole MS. Other scan modes like parent ion scan or neutral loss scan cannot be carried out by tandem in time analyzers.

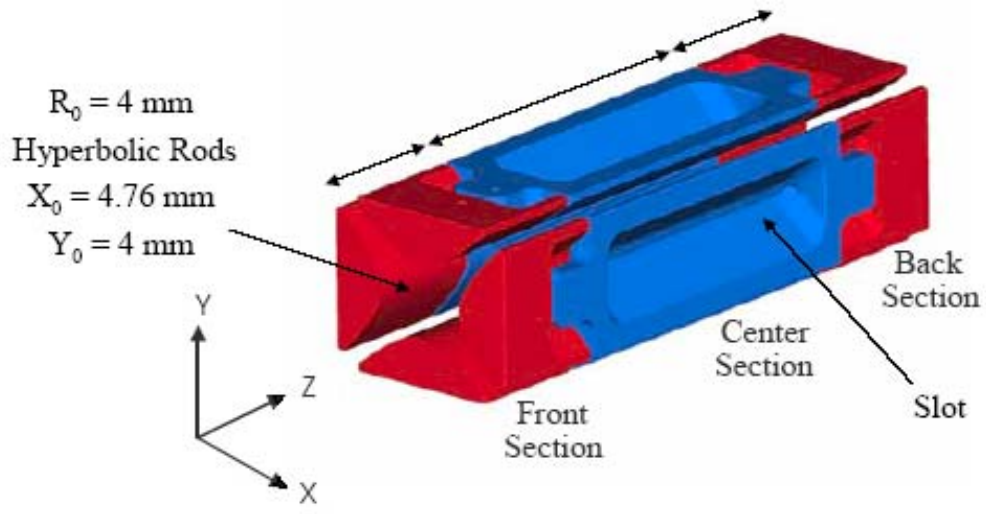

Figure 1.13 Basic design of a two dimensional linear quadrupole ion trap.[52]

1.5.2.4. Orbitrap analyzer

The Orbitrap is a new type of mass analyzer invented by Alexander Makatov.[53]

The Orbitrap cell consists of two electrodes, an outer barrel-like one and coaxial inner spindle-like electrode. The coaxial inner electrode induces an electrostatic field with quadro-logarithmic potential distribution (Figure 1.14). Because of the balance between the electrostatic attraction force and the centrifugal force ions are trapped in the cell and circle around the inner electrode in orbits on elliptical trajectories. These oscillations of ions can be detected by their image current induced on the outer electrode which is divided to two symmetrical pick-up sensors. The detected transient signals can be Fourier transformed into a mass spectrum.

The big advantage of the Orbitrap is the ability to measure with high resolution and high mass accuracy (resolving power about 800 at *m/z* 400 and mass error less than 1 ppm) with lower cost of operation when compared to FT-ICR MS (no liquid helium and liquid nitrogen required for cooling). Due to the fact that two different analytes with the same nominal mass and different elemental composition have different exact masses, the element composition of the desired analyte from the high resolution Orbitrap can be obtained.

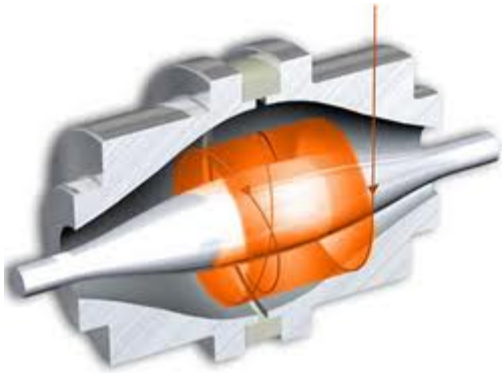

Figure 1.14 Cutaway through an Orbitrap mass analyzer. The orange arrow shows the ions oscillating trajectory.

1.5.2.5. LTQ-Orbitrap

The LTQ-Orbitrap instrument is a hybrid mass spectrometer which is a combination of two different mass analyzers (Figure 1.15). By using the hybrid mass spectrometer the advantages of each different mass analyzer can be combined in one instrument. The LTQ-Orbitrap analyzes the ions in the ion trap-mode of LTQ (Linear trap quadrupole) with the possibility to isolate and fragment the desired ions up to (MS^n) with relative fast scan time. Switching the mass spectrometer to the FT-mode (high resolution mode), collects the LTQ analyzer the ions and send as packet to C-trap. The C-trap device is a C-shaped ion trap accumulates the ions from the LTQ and let them pass into the Orbitrap-cell where the ions are analyzed and detected with very high resolving power.

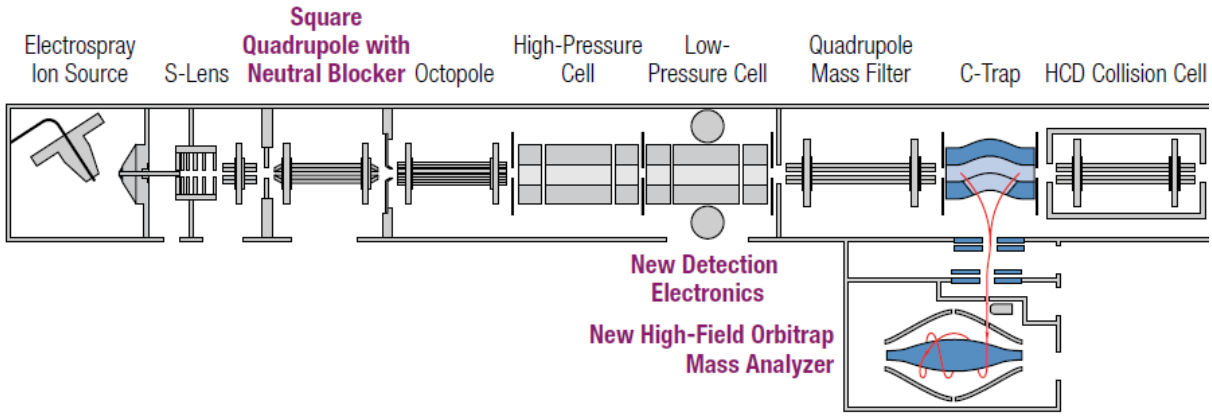

Figure 1.15 Schematic of the LTQ Orbitrap Velos MS instrument with three new hardware implementations.[54]

.

1.6. Scope of the Study

The major topic of this work was developing of mass spectrometric methods to study complex organocatalytic reactions in detail. The reactions were investigated via the fishing and elucidating of the active reaction intermediates, which play a major rule in the reaction path, as reaction keys using unique mass spectrometric methods.

One unique way of using organocatalysis is a methodology where different reactions are combined in a reaction sequence in a one-pot synthetic set-up, usually described as tandem or cascade reaction. Here, all potential reactands are present all the time and are supposed to react at a certain point in the sequence without a cleanup step in between. Therefore, the different steps need to be adjusted to each other to avoid cross reactivities which nonetheless still can occur. The mechanistic investigation of organocatalyzed cascade reactions is challenging because the reactants especially the intermediates are present in small concentrations and are often short lived. These intermediates are continually carrying out several chemical transformations in the same reaction media. Therefore it is a difficult task to elucidate and characterize such reaction components.
In **Chapter 2** a detailed mechanistic investigation was carried out studying a complex organocatalyzed triple cascade reaction. This complex cascade reaction constructs *tetra*-substituted cyclohexene carbaldehydes with four stereogenic centers. The stereochemistry of all steps has been studied thoroughly by ESI-MS using collision activated dissociation (CAD) techniques for structural elucidation of components formed during the reaction. The investigation focused on the reaction process at different reaction conditions and the relationship of the temperature on the side-reactions. It was possible to characterize all products and side-products.

The cascade reaction described above in Chapter 2 shows both the intrigue and the difficulty that summarize the concept of organocatalytic cascade reactions. Due to the fact that all catalytic active components are active from the beginning side reactions can occur. A new concept of multifunctional organocatalyzed cascade reactions has been presented by Schreiner a few years ago that can circumvent the problems. In this case the catalyst is based on different catalytic moieties for different chemical transformations combined in one molecule, coupled by a peptide backbone. In this multifunctional organocatalyst each catalytic moiety needs to be activated individually in the reactions sequence by adding a chemical reagent, allowing combinations of reactions that are otherwise not possible in a cascade. This should

minimize the potential formation of side-products unlike the classic domino reactions. Structural elucidation of big and complex molecules like these multifunctional catalysts is very difficult task especially when these molecules are present in low concentrations in the reaction solution. Chapter 5, 6 present mechanistic investigation of two different reaction systems catalyzed by multifunctional organocatalysts in a one-pot synthesis.

A multifunctional organocatalyzed reaction has been described in **chapter 3**. This reaction consists of two steps, an enatioselective monoacylation of cyclohexanediol and an oxidation of the second hydroxyl group to the corresponding ketone. The problem here was that the reaction suffers from a low product yield. When the reaction is carried out at room temperature the yield is reduced while the yield is increasing when working under colder conditions at 0 °C. The investigation of all details of the reaction allows concluding that at elevated temperatures lactone as unknown side-product is being formed thus reducing the yield of the desired product. When the reaction is carried out at lower temperatures the formation of the side-product is suppressed. The reactive intermediates, product as well as side-product were successfully characterized and the effect of temperature in regard of side-reaction is now well understood using ESI-MS(/MS) as well as high resolution MS to gain better structural data.

Chapter 4 focusses on an asymmetric triple cascade reaction of cyclohexene to produce cyclohexanediol monoacetate with high (*ee*) yield catalyzed by a chiral multifunctional organocatalyst. All reaction steps are fully studied by ESI-MS(/MS) as well as high resolution MS for more structural elucidation. The most interesting part of this reaction was the activation process of each catalytic moiety. Because of the hard oxidation condition in the first reaction step the catalytically moieties N-methylimidazole of the acylation reaction in the second step suffered under oxidation side-reaction. This has been characterized and the results explain the low efficiency of the catalyst in this step. All reactive intermediates of the reaction steps and the side reactions as well as product can be monitored and the mechanistic cycle of the reaction is presented.

The L-proline catalyzed asymmetric aldol addition reaction is one of the first and typical organocatalytic reactions that are a reason why organocatalysis has developed into such an innovative tool for chiral synthesis. Although this reaction has been discussed for more than 10 years, still some questions are not solved regarding the mechanism of this reaction. The major point is that in addition to the chiral aldol product a condensation product as side

product is formed with relatively high yields thus disturbing the reaction. The formation mechanism of this undesired product is not yet fully understood.

Chapter 5 presents a mechanistic investigation of the aldol addition reaction catalyzed by L-proline. The aim of this study was to understand and follow all chemical transformations of this reaction. Additionally to standard ESI-MS(/MS) techniques other more specific techniques such as isotopic labeling, ion/molecule reaction in the collision cell of the MS triple quadrupole analyzer for characterization of the reactive reaction intermediates and the determination of the reaction pathways of the product and side product were applied.

Secondary amines are commonly used as catalysts in organocatalytic reactions. There is a debate in the literature about reaction mechanisms of these catalysts, especially for aldol condensation reactions which allow different potential formation pathways.

Chapter 6 describes a mechanistic study of aldol condensation reaction of acetone with different aromatic aldehydes catalyzed by a new secondary amine organocatalyst morpholinium trifluoroacetate. Many MS methods have been implemented in this study, such as micro-flow reactor, isotopic labeling and ion/molecule reaction in the collision cell to illustrate each component of the catalytic-cycle of this reaction. It was possible to determine the reactive intermediates for this reaction by ESI-MS and ESI-MS/MS under different reaction conditions. The reaction is controlled not only by one mechanism but depending on the reaction condition there are two different pathways for this reaction system that lead to the same end product, the aldol pathway as kinetic controlled mechanism and Mannich pathway as thermodynamic controlled mechanism. Therefore this reaction can be considered as a bi-mechanistic reaction.

Chapter 7 presents a general conclusion of this work.

References

[1] R. A. Aitken, S. N. Kilenyi, *Asymmetric Synthesis, Vol. 1*, Blackie Academic and Professional, Glasgow, UK, **1992**.

[2] H. S. Bevinakatti, A. A. Banerji, *Journal of Organic Chemistry* **1991**, *56*, 5372.

[3] G. W. Mellin, M. Katzenstein, *New England Journal of Medicine* **1962**, *267*, 1238.

[4] G. Blaschke, H. P. Kraft, K. Fickentscher, F. Kohler, *Arzneimittel-Forschung/Drug Research* **1979**, *29-2*, 1640.

[5] H. Pellissier, *Tetrahedron* **2007**, *63*, 9267.

[6] P. I. Dalko, L. Moisan, *Angewandte Chemie-International Edition* **2001**, *40*, 3726.

[7] M. T. Reetz, B. List, S. Jaroch, H. Weinmann, *Organocatalysis*, Springer, **2008**.

[8] Z. G. Hajos, D. R. Parrish, *Journal of Organic Chemistry* **1974**, *39*, 1615.

[9] U. Eder, G. Sauer, R. Weichert, *Angewandte Chemie-International Edition* **1971**, *10*, 496.

[10] A. Berkessel, *Asymmetric Organocatalysis From Biomimetic Concepts to Applications in Asymmetric Synthesis, Vol. Vol. 1*, Wiley-VCH Verlag GmbH & Co. KGaA, Weinheim, Germany, **2005.**

[11] J. Seayad, B. List, *Organic & Biomolecular Chemistry* **2005**, *3*, 719.

[12] T. Ooi, K. Maruoka, *Journal of Synthetic Organic Chemistry Japan* **2003**, *61*, 1195.

[13] M. S. Iyer, K. M. Gigstad, N. D. Namdev, M. Lipton, *Journal of the American Chemical Society* **1996**, *118*, 4910.

[14] P. R. Schreiner, *Chemical Society Reviews* **2003**, *32*, 289.

[15] M. S. Sigman, E. N. Jacobsen, *Journal of the American Chemical Society* **1998**, *120*, 4901.

[16] M. B. Smith, J. March, *Advanced Organic Chemistry: Reactions, Mechanisms, and Structure*, 5 ed., A Wiley-Interscience Publication, **2001**.

[17] Fábián, István, *Reaction Kinetics, Mechanisms and Catalysis*, Springer, **2009**.

[18] I. Rabi, S. Millman, P. Kusch, J. Zacharias, *Phys. Rev* **1938**, *53*, 318.

[19] J. Keeler, *Understanding NMR Spectroscopy, Vol. 1*, University of Cambridge, **2007**.

[20] P. C. Bulman Page, D. Barros, B. R. Buckley, B. A. Marples, *Tetrahedron: Asymmetry* **2005**, *16*, 3488.

[21] M. B. Schmid, K. Zeitler, R. M. Gschwind, *Angewandte Chemie International Edition* **2010**, *49*, 4997.

[22] S. Lakhdar, R. Appel, H. Mayr, *Angewandte Chemie International Edition* **2009**, *48*, 5034.

[23] Á. L. F. de Arriba, L. Simón, C. Raposo, V. Alcázar, J. R. Morán, *Tetrahedron* **2009**, *65*, 4841.

[24] S. Bertelsen, M. Marigo, S. Brandes, P. Dinér, K. A. Jørgensen, *Journal of the American Chemical Society* **2006**, *128*, 12973.

[25] W. Lau, *Infrared characterization for microelectronics*, World Scientific Publishing Company, **1999**.

[26] J. B. Fenn, M. Mann, C. K. Meng, S. F. Wong, C. M. Whitehouse, *Science* **1989**, *246*, 64.

[27] C. M. Whitehouse, R. N. Dreyer, M. Yamashita, J. B. Fenn, *Analytical Chemistry* **1985**, *57*, 675.

[28] C. Trage, D. Schroder, H. Schwarz, *Chemistry-a European Journal* **2005**, *11*, 619.

[29] D. Schroeder, *European Journal of Mass Spectrometry* **2012**, *18*, 139.

[30] S. M. Polyakova, R. A. Kunetskiy, D. Schroeder, *International Journal of Mass Spectrometry* **2012**, *314*, 13.

[31] W. Schrader, P. P. Handayani, J. Zhou, B. List, *Angewandte Chemie-International Edition* **2009**, *48*, 1463.

[32] C. Marquez, J. O. Metzger, *Chemical Communications* **2006**, 1539.

[33] L. S. Santos, L. Knaack, J. O. Metzger, *International Journal of Mass Spectrometry* **2005**, *246*, 84.

[34] T. D. Fernandes, B. G. Vaz, M. N. Eberlin, A. J. M. da Silva, P. R. R. Costa, *Journal of Organic Chemistry* **2010**, *75*, 7085.

[35] APPI: The Second Source for LC-MS http://chromatographyonline.findpharma.com/lcgc/article/articleDetail.jsp?id=504702&pageID=1&sk=&date=, **2008**.

[36] A. O. Aliprantis, J. W. Canary, *Journal of the American Chemical Society* **1994**, *116*, 6985.

[37] J. W. Sam, X. J. Tang, R. S. Magliozzo, J. Peisach, *Journal of the American Chemical Society* **1995**, *117*, 1012.

[38] D. J. Wilson, L. Konermann, *Analytical Chemistry* **2003**, *75*, 6408.

[39] J. H. Gross, *Mass Spectrometry A Text Book*, Springer, Berlin, **2004**.

[40] A.F.Thomas, *Deuterium Labeling in Organic Chemistry*, Appleton-Century-Crofts: , New York, **1971**.

[41] J. B. Fenn, *Angewandte Chemie-International Edition* **2003**, *42*, 3871.

[42] J. V. Iribarne, B. A. Thomson, *Journal of Chemical Physics* **1976**, *64*, 2287.

[43] S. Nguyen, J. B. Fenn, *Proceedings of the National Academy of Sciences of the United States of America* **2007**, *104*, 1111.

[44] M. Dole, L. L. Mack, R. L. Hines, *Journal of Chemical Physics* **1968**, *49*, 2240.

[45] http://www.lamondlab.com/MSResource/LCMS/MassSpectrometry/electrosprayIonisation.php, **2010**.

[46] E. C. Horning, M. G. Horning, D. I. Carroll, I. Dzidic, Stillwel.Rn, *Analytical Chemistry* **1973**, *45*, 936.

[47] J. A. Syage, M. D. Evans, *Spectroscopy* **2001**, *16*, 14.

[48] M. Constapel, M. Schellentrager, O. J. Schmitz, S. Gab, K. J. Brockmann, R. Giese, T. Benter, *Rapid Communications in Mass Spectrometry* **2005**, *19*, 326.

[49] E. Hoffmann, V. Stroobant, *Mass Spectrometry Principles and Applications*, John Willey and Sons, Ltd, England, **2002**.

[50] C. Steel, M. Henchman, *Journal of Chemical Education* **1998**, *75*, 1049.

[51] R. A. Yost, C. G. Enke, D. C. McGilvery, D. Smith, J. D. Morrison, *International Journal of Mass Spectrometry and Ion Processes* **1979**, *30*, 127.

[52] J. C. Schwartz, M. W. Senko, J. E. P. Syka, *Journal of the American Society for Mass Spectrometry* **2002**, *13*, 659.

[53] Q. Z. Hu, R. J. Noll, H. Y. Li, A. Makarov, M. Hardman, R. G. Cooks, *Journal of Mass Spectrometry* **2005**, *40*, 430.

[54] http://www.textronica.com/lcline/orbitrap/orbitrap_elite_prodspec.pdf, **2011**.

2. Electrospray Mass Spectrometry for Detailed Mechanistic Studies of a Complex Organocatalyzed Triple Cascade Reaction

Redrafted from "M. Wasim Alachraf, Peni P. Handayani, Matthias R. M. Hüttl, Christoph Grondal, Dieter Enders, Wolfgang Schrader., Org. Biomol. Chem., **2011***, 9,* 1047*"*

2.1. Abstract

The development of modular combinations of organocatalytic reactions into cascades has been shown to be an effective tool despite the fact that the mechanism of such a complex organocatalytic multistep cascade reaction still remains poorly understood. Here the detailed mechanistic studies of a complex organocatalytic triple cascade reaction for the synthesis of tetra-substituted cyclohexene carbaldehydes are reported. The investigation has been carried out using a triple quadrupole mass spectrometer with electrospray ionization. Important intermediates were detected and characterized through MS/MS studies. A detailed formation pathway is presented based on these characterized intermediates, and supporting the proposed mechanism of the formation of the substituted cyclohexene carbaldehydes.

2.2. Introduction

Until a few years ago, it was generally accepted that transition metal complexes and enzymes were the two main classes of efficient asymmetric catalysts. Since the year 2000, a third approach to the catalytic production of enantiomerically pure organic compounds has emerged – *organocatalysis*. These small chiral organic molecules are metalfree, generally nontoxic, commercially available, and very often robust, in which they act as catalytically active species in the reaction.[1]

Recently, amine-catalyzed reactions are gaining importance, particularly with chiral secondary amines, which belong to a class of organocatalysts that offer the capability of promoting several types of reactions through different activation modes. They either activate aldehyde and ketone substrates via enamine formation[1] or α,β-unsaturated aldehyde substrates via iminium-ion formation.[2] Consequently, chiral secondary amines are ideally suited for organocatalytic cascade reactions.[3-6] These cascades, also known as tandem or domino reactions, are complex reactions that combine several different steps in a one-pot synthesis without purification between each step and, in general, without changes in conditions. Thus, all reactants, substrates and catalysts are present from the beginning.

Therefore, this concept for the formation of carbon-carbon bonds with the control of multiple stereocenters in a one-pot synthesis has been a challenge in asymmetric catalysis. The design and implementation of organocatalytic cascade reactions are a powerful way for the construction of complex molecules from simple precursors. Its efficiency can be judged by the number of bonds formed, the number of stereocenters generated and the increase in molecularcomplexity, as well as economy of time, labor, resource management, and waste generation. In addition, organocatalytic cascade reactions are advantageous as they proceed consecutively under the same reaction conditions.[7-9]

Although modular combinations of asymmetric organocatalytic reactions into cascades have become a fruitful concept in organic synthesis, detailed mechanistic studies of complex cascade reactions is largely unexplored due to different reasons. Multi-step organocatalytic cascade reactions consist of several different substrates and catalysts hence the reaction mixture is becoming quite complex. Consequently, isolation and characterization of reaction intermediates can be problematic and time consuming and hence contradict the effect of a cascade reaction. Additionally, the short lived intermediates, often appearing only in minor concentrations, are generally not stable enough and amenable for the isolation as they are rapidly transformed in the subsequent reactions.

For that reason, NMR and IR spectroscopy as the widely used tools to gain efficient information about structural parameters are not providing sufficient data to the mechanistic studies of complex organocatalytic cascade reactions. To date, the development of mass spectrometric ionization methods at atmospheric pressure (API) particularly electrospray ionization (ESI)[10-13] opened up the access to the investigation and the detailed mechanistic studies of chemical reactions.[14-24]

ESI-MS and its tandem version ESI-MS/MS are rapidly becoming a preferred method for solution-phase mechanistic studies in chemistry due to the ability to select one specific ion and fragment it with *collision activated dissociation* (CAD) to obtain structural information concerning the molecular mass and structure of compounds in a reaction mixture. These combinations of techniques allow studying not only reaction substrates
and products, but even short-lived reaction intermediates as they are present in solution. These data provide novel insights into the mechanisms of many reactions.

ESI-MS and CAD can be useful to face the challenge for detailed mechanistic studies of a complex cascade reaction. Especially, the occurrence of side reactions can be troubling and a powerful method is needed to differentiate between the reaction steps and to help understanding the mechanism.

Continuing the previous successful work on the mechanistic investigation of organocatalytic reactions[25], [26] by ESI-MS and ESI-MS/MS, we report here that these methods are also excellent tools for the interception and characterization of the reactive intermediates in a complex triple organocatalytic cascade reaction.

Secondary amines are capable to catalyze organocatalytic cascade reactions via both enamine and iminium ion formation. List,[4] MacMillan[5] and Jorgensen[6] have developed cascade reactions by merging first iminium and then enamine activation. On the contrary, Enders initiated a new reverse strategy using enamine activation of the first substrate to start a triple cascade. For the three-component (a linear aldehyde, a nitroalkene, an α,β-unsaturated aldehyde) cascade reaction diphenylprolinol trimethylsilyl ether as the catalyst is employed.

This cascade reaction is recognized as a powerful tool for the construction of *tetra*-substituted cyclohexene carbaldehydes with four stereogenic centers and its stereochemistry has been studied thoroughly.[27-30] Recently, in a related quadruple cascade reaction the intermediates have been charaterized by ESI-MS.

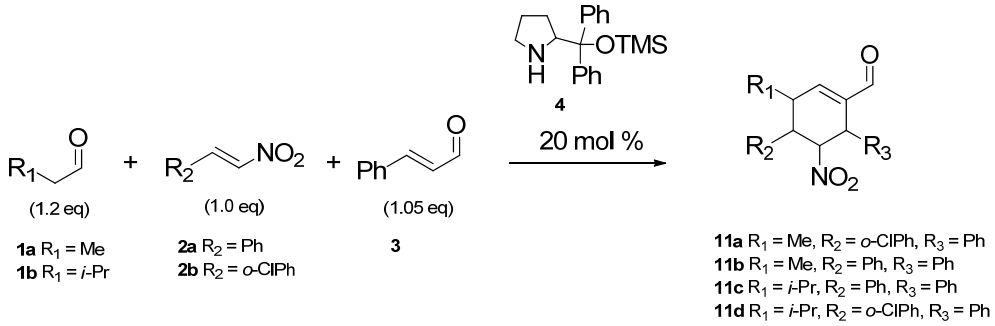

Entry	1	2	Product 11
1	1a	2b	11a
2	1a	2a	11b
3	1b	2a	11c
4	1b	2b	11d

Scheme 2.1 The experimental set up of triple cascade reaction for the synthesis of *tetra*-substituted cyclohexene carbaldehydes **11a-d**.

2.3. Experimental

The reaction mixtures were stirred between 0 °C and room temperature for 16–24 h in 1 ml of toluene. The analyte was taken directly from the reaction flask and was diluted in acetonitrile (1:100) before entry to the ESI source at a flow rate of 2 µL/min. The investigation was carried out by monitoring the reaction at specified intervals through ESI-MS. The reaction intermediates that appeared during the reaction were intercepted, detected and characterized with ESI-MS. MS/MS experiments were performed for structural confirmation using the product ion scan with the collision energy ranging from 10 to 50 eV, depending on the dissociation lability of the precursor ion. Additional data of accurate mass measurements were obtained with FT-ICR MS.

2.4. Instrumental

ESI-MS data were acquired using a Thermo TSQ Quantum Ultra AM triple quadrupole mass spectrometer equipped with an ESI source which was controlled by Xcalibur software. The spray voltages were set to 4000 V and 3000 V for positive and negative ions, respectively. The heated capillary temperature was adjusted to 270 °C. For MS/MS analysis, the collision energy was increased from 10 eV to 50 eV. The mass spectrometer was operated in the Q1 scan and product ion scan modes, with the mass width for Q1 set at 0.5 Da and for Q3 set at 0.7 Da. The collision cell, Q2, contained Argon and was adjusted to a pressure of 1.2 mTorr to induce CID. Spectra were collected by averaging 10 scans with a scan time of 1.5 sec. The Mass range was adjusted between 50 and 1500 Da. Additional data were obtained using a Bruker APEX III FT-ICR MS with a 7 T actively shielded magnet operating with an Agilent ESI source. The analyte was introduced as a solution in acetonitrile 1:1 (v/v) dilution and injected in the infusion mode with a flow rate of 2 μL/min at an electrospray voltage of 4500 V. Scans was carried out from *m/z* 100 to 2400.

2.5. Results and Discussion

The goal of this study was the investigation of an organocatalytic triple cascade reaction as has been reported by Enders.[26] For the mechanistic investigation of such a complex reaction it is necessary to observe the fast changes and the formation of small amounts of intermediate components. This was done here by using a high resolution triple quadrupole mass spectrometer with an electrospray ionization source. For a better understanding of the reaction and for studying the influence of polyfunctional cyclohexene derivatives as the substrates, four different variations of the reaction have been carried out by varying the first and the second substrates, **1** and **2**, respectively which leads to changes in the mass spectral fingerprint. The experimental set up was kept the same for all reactions. The different reactions are illustrated in Scheme 2.1.

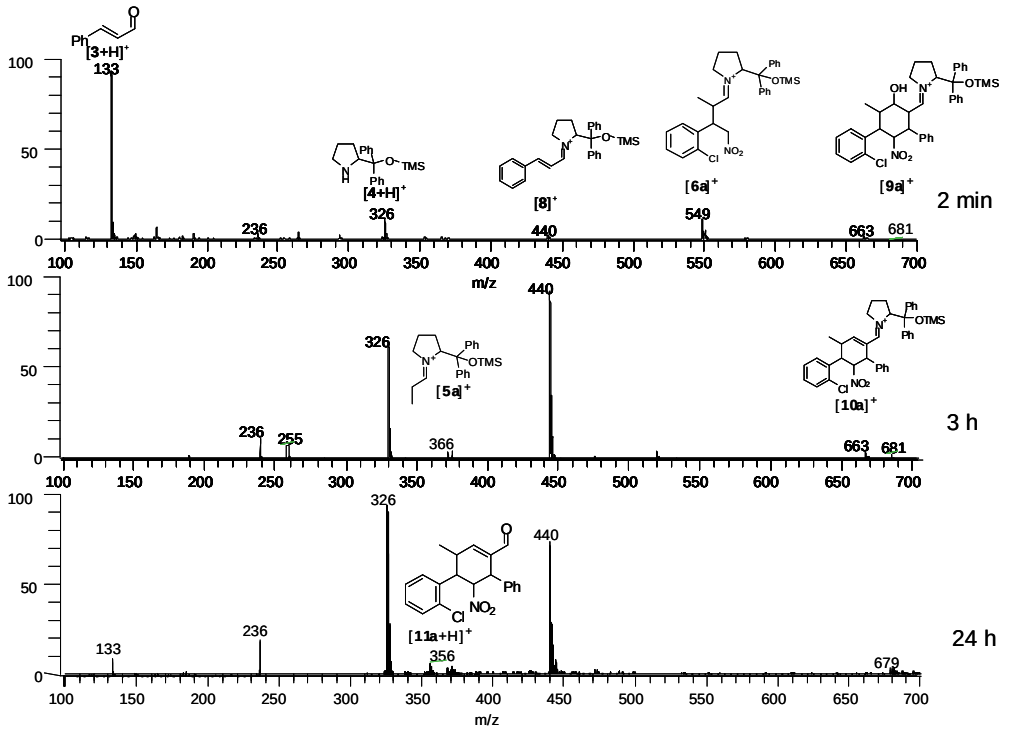

Figure 2.1 Overview of the reaction mixture of propionaldehyde **1a** and 2-chloro-β-nitrostyrene **2b** after 2 min, 3h and 24h; displayed are ESI-(+)- MS spectra.

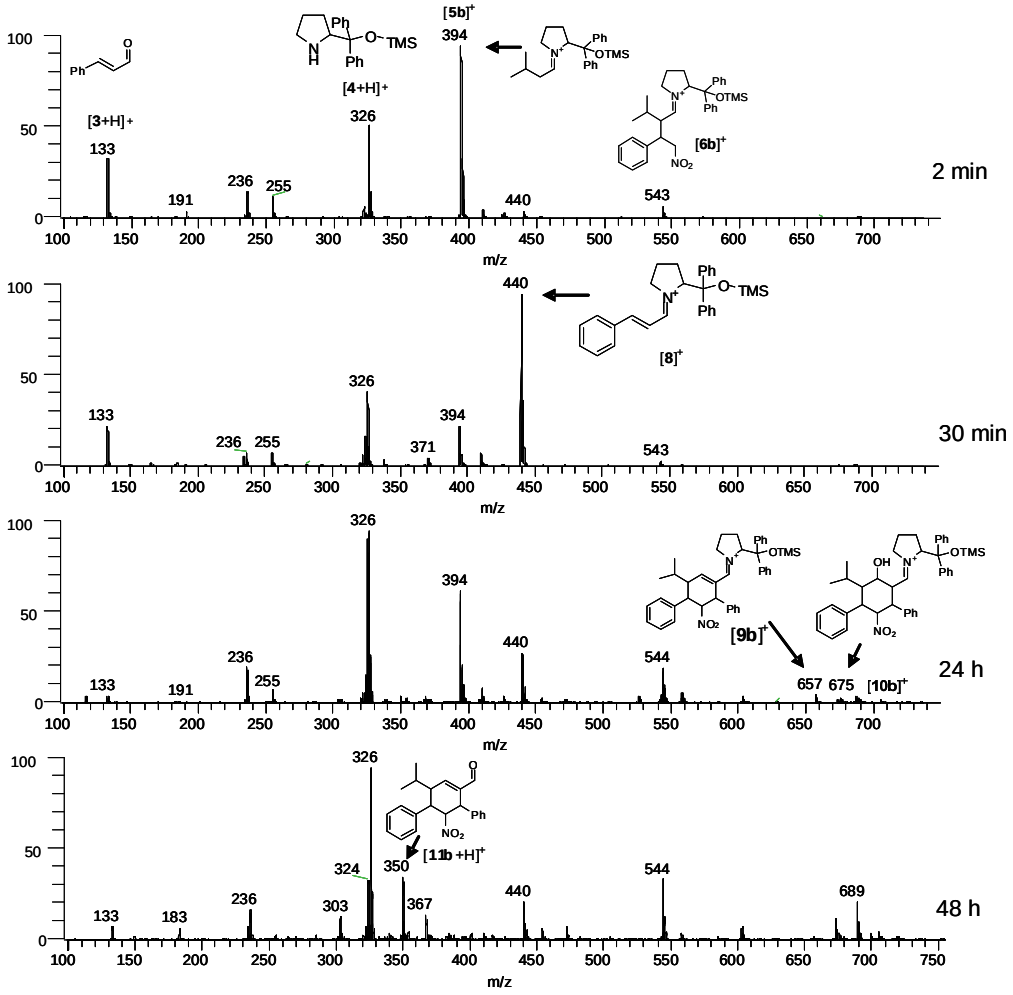

Figure 2.2 ESI(+)-MS spectrum of the reaction mixture of isovaleraldehyde **1b** and *trans*-β-nitrostyrene **2a** after 2, 30 min, 24 and 48 h.

A first experimental overview is shown in Figure 2.1 and 2.2, where spectra of reactions 1 and 3 are displayed, respectively, after different time intervals. The spectra indicate the progress of each reaction and show that the starting components make room at first for some intermediates and subsequently for the final product. In the case of reaction 3 the data showed that the reaction is much slower and some intermediates do not show the same response as in reaction 1 due to a different functional group. One of the most intense signals comes from the protonated catalyst [**4**+H]$^+$ at *m/z* 326. Other signals are also detected at *m/z* 366, 549, 440 and 681, respectively that could be assigned to the putative intermediates**.** The details of their formation will be described in the following. The mass spectra of the reaction 3 using isovaleraldehyde **1b** and *E*-β-nitrostyrene **2a** after different reaction times are illustrated in Figure2. 2. The signals at *m/z* 133 and 326 corresponding to the protonated cinnamaldehyde [**3**+H]$^+$ and catalyst [**4**+H]$^+$, respectively, being some of the most intensive peaks. Other signals at *m/z* 440, 394, 543 and 675 that could be assigned to the putative intermediates are also recognized. These data show that there is no difference in the mechanism, as the intermediates that are being formed are corresponding to the same formation pathway. In general, it has to be noted, that most compounds show a significant signal that allows a detailed characterization of the reaction pathway. Nonetheless, there are some restrictions, as the product shows a very weak signal due to a bad response during electrospray ionization or to a short live time. To account for such problems additional studies were carried out using atmospheric pressure chemical ionization (APCI) method. This ionization technique complements ESI measurements very well because APCI covers compounds that do not need to be as polar as they need to be for ESI and gives better signals for these compounds and intermediates.

Since cascade reactions are combining a set of different organocatalytic reactions in subsequent steps, it is now important to follow the details of such a reaction as it progresses. Therefore, we use the reaction of propionaldehyde **1a**, (*E*)-2-chloro-β-nitrostyrene **2b** and cinnamaldehyde **3** with (*S*)-2-(diphenyl(trimethylsilyloxy)methyl)-pyrolidine **4** as a catalyst as an example to describe the results of our mechanistic study of the investigated cascade reaction.

The reaction begins with the activation of propionaldehyde **1a** by a proline-derived catalyst **4** via enamine formation to form the first intermediate **5a** at *m/z* 366.

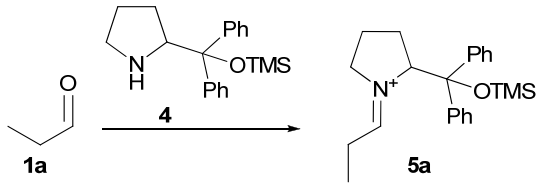

Scheme 2.2 Catalytic activation of propionaldehyde **1a**.

At this point, it was not clear how the reaction proceeds since the enamine intermediate **5a** can react in three possible ways as described in Scheme 2.3. The first probable way would be a Michael addition of enamine intermediate **5a** to *trans*-2-chloro-β-nitrostyrene **2b** to form a nitroalkane **6a** which should be detectable at *m/z* 549. The second possible way is when the enamine intermediate **5a** reacts further with an excess of propionaldehyde **1a** and forms an iminium intermediate (*m/z* 424). The third probable path could proceed via Michael addition of enamine intermediate **5a** to cinnamaldehyde **3** for the generation of an iminium intermediate *m/z* 498 (Figure 2.3).

It is well-known that nitroalkenes are reactive Michael acceptors, as the nitro group is the best-known electron-withdrawing group.[31] This fact explains that the enamine **5a** reacts faster with **2b** than with **3**. The formation of **6a** was supported by MS/MS studies of *m/z* 549 as shown in Figure 2.4 where the characteristic signals match the proposed structure ($C_{31}H_{38}N_2O_3SiCl$). Additionally, the signal from the first possibility at *m/z* 424 could not be detected during the reaction time

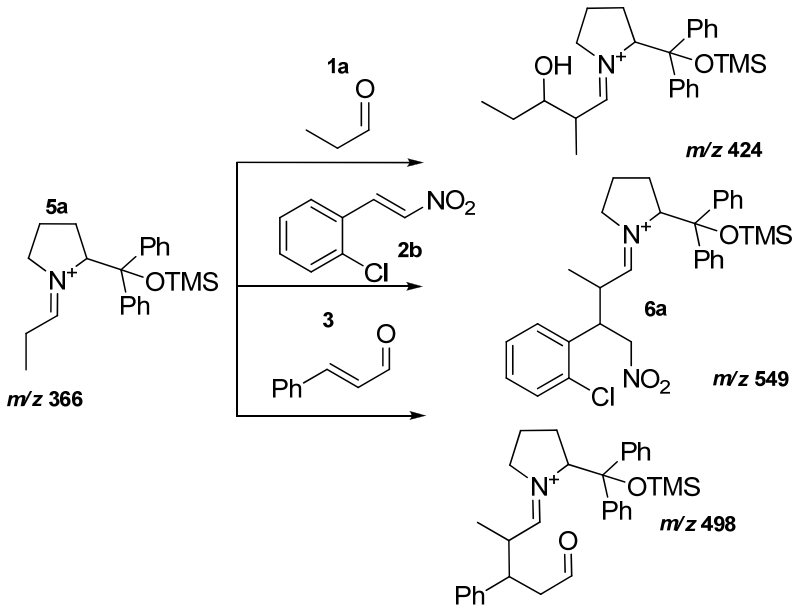

Scheme 2.3 Three possible reaction pathways for the enamine intermediate.

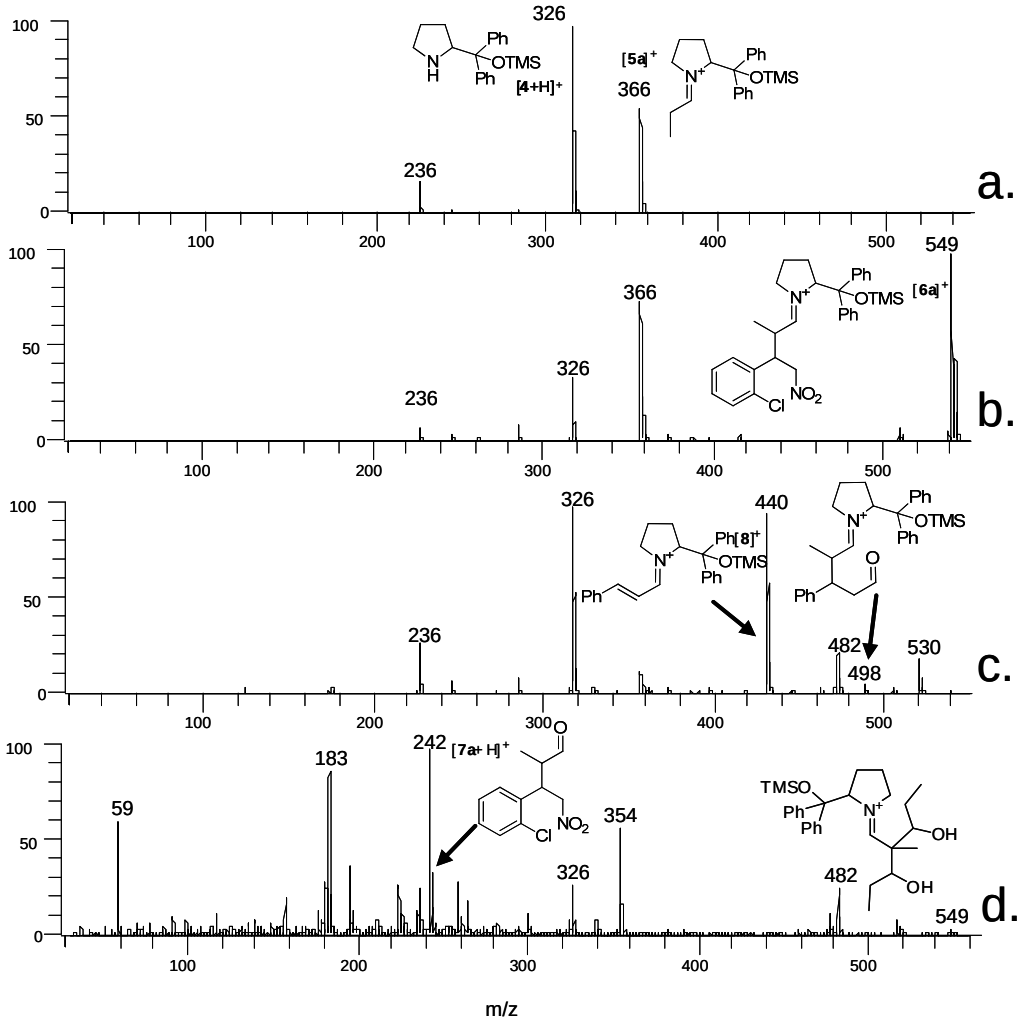

Figure 2.3 a) ESI(+)-MS spectrum of **1a** and catalyst **4** in toluene after 5 min **b)** ESI(+)-MS spectrum of **1a** and **2b** in the presence of catalyst **4** in toluene after 5 min. **c)** ESI(+)-MS spectrum of **1a** and **3** in the presence of catalyst **4** in toluene after 5 min. **d)** APCI(+)-MS spectrum of **1a** and **2b** in the presence of catalyst **4** in toluene after 24h, **7a** is clearly detectable with APCI but not with ESI.

To follow these mechanistic steps we have observed the individual steps outside of the cascade as well. The spectra are documented in Figure 2.3, where the top spectrum shows the results of a reaction of substrate **1a** with catalyst **4**, while in Figure 2.3b the results from a reaction of substrates **1a** and **2b** with catalyst **4** is shown. In Figure 2.3c the combination of **1a** and **3** with the catalyst **4** are displayed and in Figure 2.3d the overall APCI spectrum of **1a** and **2b** in the presence of catalyst **4** shows the formation of **7a** which is only detectable by this ionization method in a sufficient intensity. All together these results confirm the mechanistic findings of the cascade reaction.

During the investigation a small signal of *m/z* 498 was detected which has a fragmentation pattern that is fitting to the proposed structure in Scheme 2.3. To evaluate the conditions under which this intermediate forms different experiments were done. Especially helpful was a set of reactions where the reaction temperature was varied. An increase in temperature leads to an increase of *m/z* 498, which indicates that this intermediate is formed when the reaction temperature in higher. After recognizing this fact, the temperature during the MS studies was observed carefully but it was impossible to fully eliminate the formation of this intermediate. One additional signal appears at *m/z* 516.293 ($C_{32}H_{42}NO_3Si$, error 0.0 ppm) during later stages of the reaction. Here, MS/MS measurements and accurate mass data allowed to propose that water was added to the double bond of *m/z* 498. Other than that no signals could be assigned that follow this reaction pathway, showing that these signals belong to side products of this reaction.

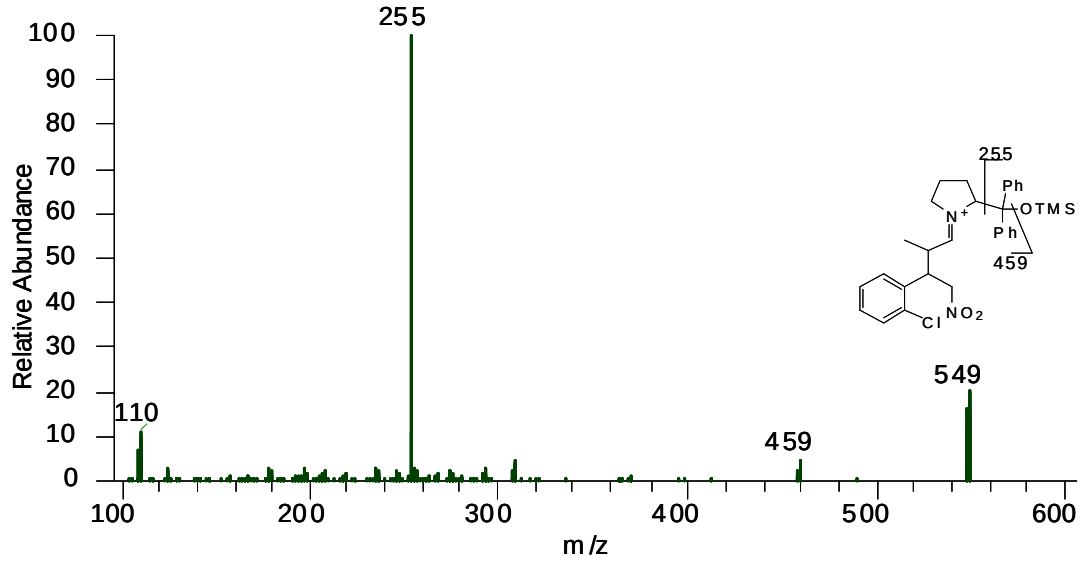

Figure 2.4 ESI(+)-MS/MS spectrum at *m/z* 549.

All these data allow to conclude that the reaction proceeds via Michael addition of enamine intermediate **5a** to *E*-2-chloro-β-nitrostyrene **2b** in order to form a nitroalkane **6a** (*m/z* 549). The iminium ion **8** (*m/z* 440.240, $C_{29}H_{34}NOSi$) is being formed early during the reaction, showing characteristic signals in the MS/MS spectrum as revealed in Figure 2.5. Once the Michael adduct **6a** was formed, the subsequent steps took place relatively fast. The first step is a hydrolysis leading to **7a** at *m/z* 242 which could not be detected directly during the reaction with ESI(+)-MS but with APCI(+)-MS (Figure 2.3d).

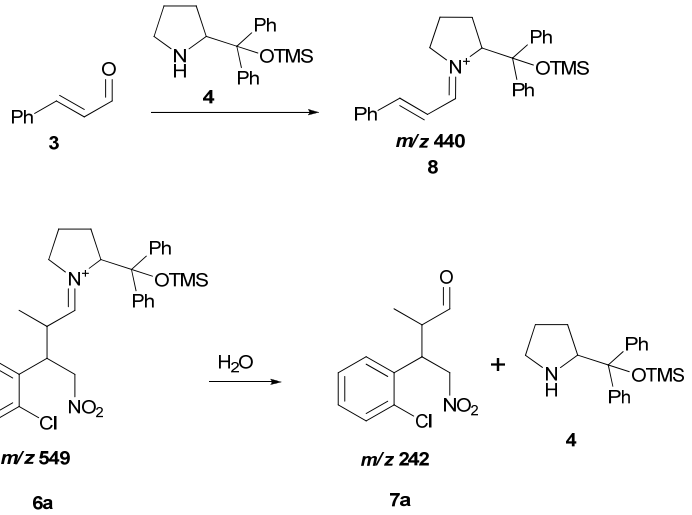

Scheme 2.4 Reaction pathways of the hydrolysis step and the activation of cinnamaldehyde **3**.

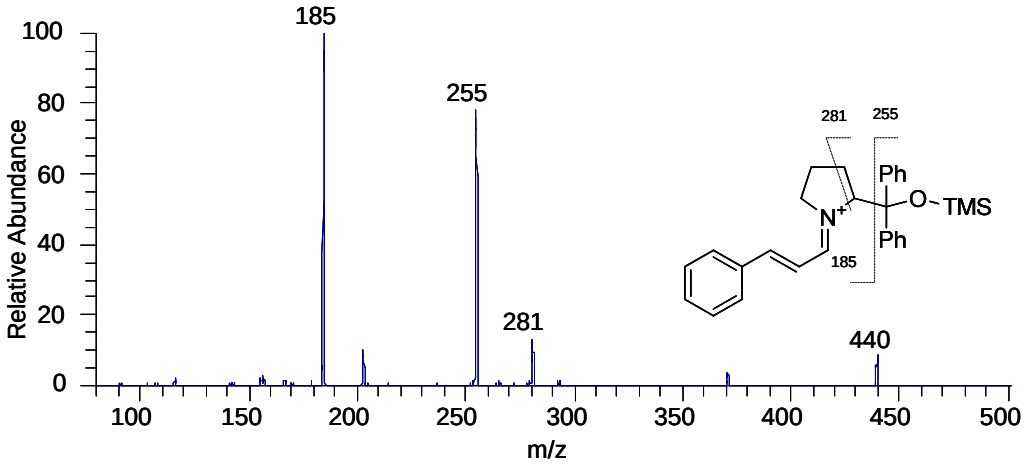

Figure 2.5 ESI(+)-MS/MS of *m/z* 440.

Afterwards, the reaction can proceed via two possible pathways. The first probable way is that the iminium ion intermediate **8** is attacked by nitroalkane **7a** in a Michael addition to yield an intermediate **9a** (*m/z* 681).

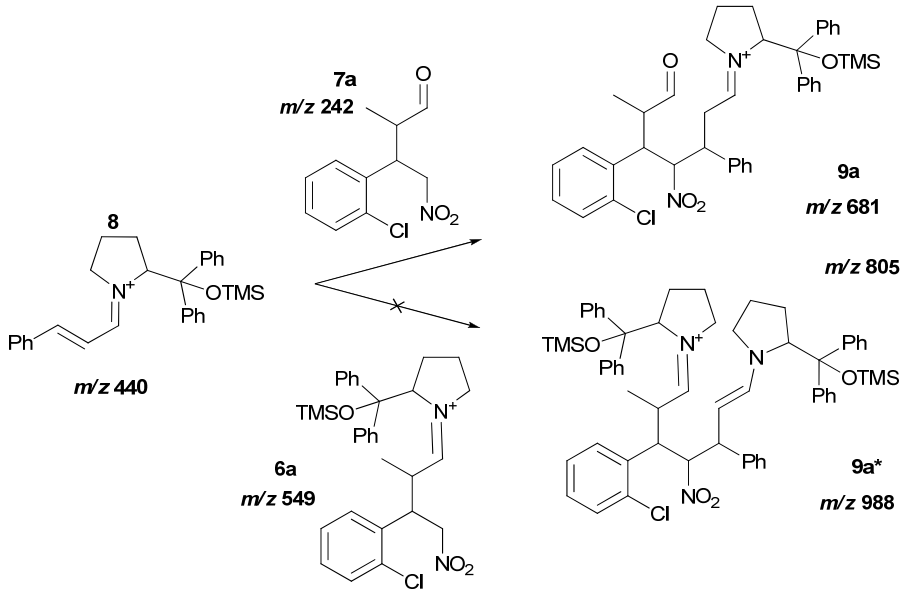

Scheme 2.5 Reaction pathways of the second Michael addition.

Another potential path would be that the iminium ion **8** reacts further with the intermediate **6a** to form an intermediate at *m/z* 988 as illustrated in Scheme 2.5. During the reaction time, the protonated ion at *m/z* 988 could not be detected. However the presence of protonated ion **9a** (*m/z* 681.292, $C_{40}H_{46}N_2O_4SiCl$) indicates that the reaction proceeded via the nitroalkane Michael addition. A posing question now is if the signal at *m/z* 681 is corresponding with the open iminium ion or with an iminium ion after ring closure according to Scheme 2.6. This is a difficult question to answer from mass spectrometric data. To try to get an answer to this question MS/MS measurments with increasing collision energies were undertaken.

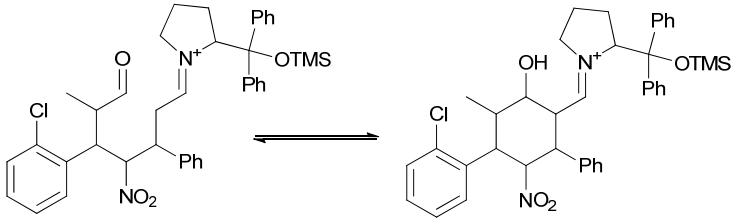

Scheme 2.6 Intramolecular aldol reaction of *m/z* 681.

The MS/MS spectrum as shown in Figure 2.6 shows that even at higher collision energies only a few fragments can be detected, indicating that the structure is stable towards the collision activation. Spectra in the data base from similar aliphatic structures show that defined fragments would be expected along the chain while a cyclic structure shows less fragments due to a higher stability. Here the fragments are very few, and although this is just an indirect indication, it seems that the signal at *m/z* 681 corresponds with the finished ringstructure.

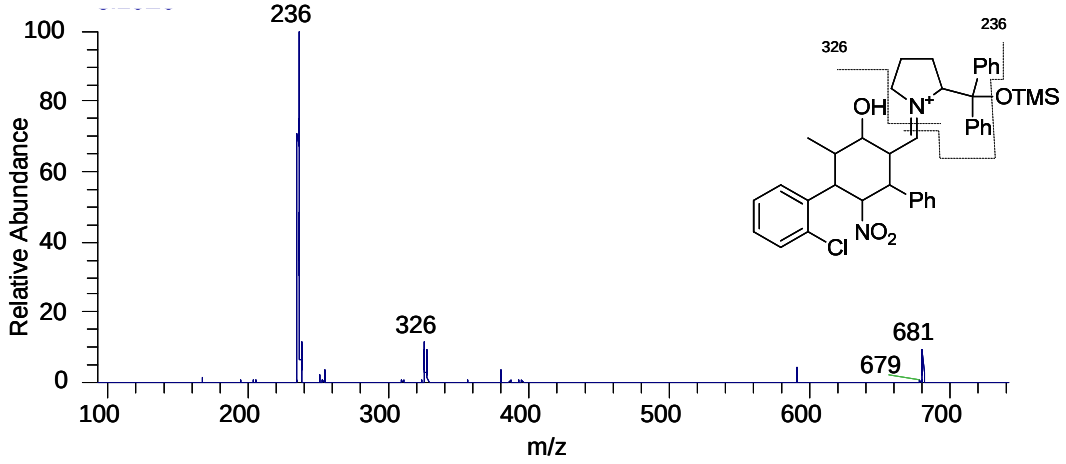

Figure 2.6 ESI(+)-MS/MS of *m/z* 681.

In the subsequent step, dehydration leads to **10a** (*m/z* 663.280, $C_{40}H_{44}N_2O_3SiCl$). Afterwards, the catalyst is released via hydrolysis step and the *tetra*-substituted cyclohexene carbaldehydes **11a** as the desired product is formed, as illustrated in Scheme 2.7.

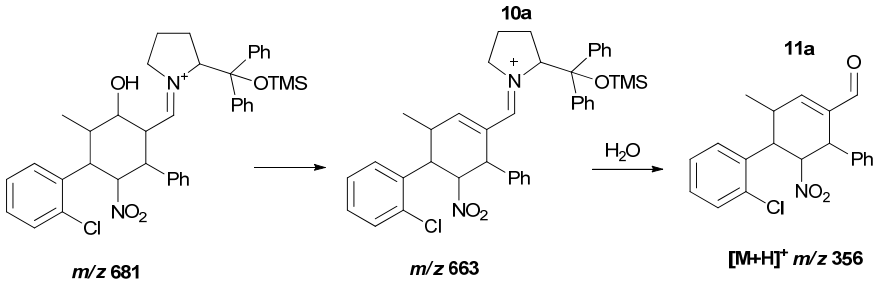

Scheme 2.7 The hydrolysis process to form cyclohexene carbaldehyde product **11a**.

For a better understanding and especially to characterize the unknown components of the reactions, all ions were also analyzed accurately for the calculation of elemental composition using FT-ICR MS. The data obtained from the reaction mixture 1 using propionaldehyde **1a** and 2-chloro-β-nitrostyrene **2b** after a reaction time of five minutes show the signal of the catalyst at *m/z* 326.194 which matches to formula $C_{20}H_{28}NOSi$ (error 1.0 ppm). The ions of other signals are revealed at *m/z* 366.225, 440.241, 549.234 and 681.291, corresponding to formulas $C_{23}H_{32}NOSi$ (error 0.5 ppm), $C_{29}H_{34}NOSi$ (error 0.3 ppm), $C_{31}H_{38}N_2O_3SiCl$ (error 0.2 ppm), $C_{40}H_{46}N_2O_4SiCl$ (error 0.6 ppm), respectively. All the data fit well with the proposed intermediates.

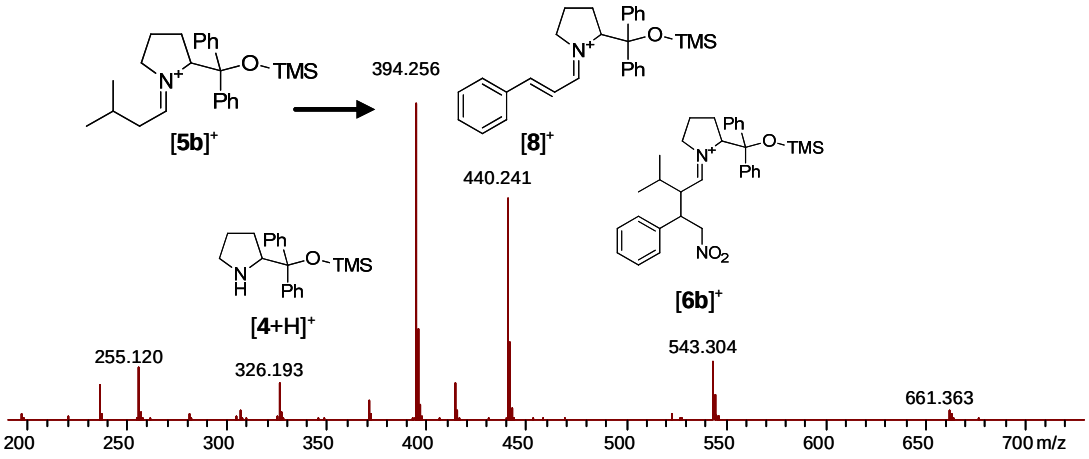

Figure 2.7 ESI(+)-MS spectrum from FT-ICR with the accurate mass data of the reaction mixture 3 of isovaleraldehyde **1b** and *E*-β-nitrostyrene **2a** after 5 min. (Note: Numbers are the same as with the components of reaction 1 to indicate the mechanism).

In addition the same results can be obained from the other reactions, as an example is given in Figure 2.7 that shows the mass spectrum from the reaction 1 using isovaleraldehyde **1b** and *E*-β-nitrostyrene **2a** after a reaction time of five minutes using FT-ICR MS. The spectrum shows the most important signals with their accurate masses and structural assignments from the catalyst at *m/z* 326.193 ($C_{20}H_{28}NOSi$) and from the putative intermediates at *m/z* 394.256 ($C_{25}H_{36}NOSi$), 440.241 ($C_{29}H_{34}NOSi$) and 543.304 ($C_{33}H_{43}N_2O_3Si$).

Table 2.1 Accurate mass data from reaction 1, showing the results from most significant signals present

Species	Formular	Mass	Error [ppm]
[**4**+H]$^+$	$C_{20}H_{28}NOSi$	326.194	0.1
[**5a**]$^+$	$C_{23}H_{32}NOSi$	366.225	0.4
[**8**]$^+$	$C_{29}H_{34}NOSi$	440.241	0.0
[**6a**]$^+$	$C_{31}H_{38}N_2O_3SiCl$	549.234	0.3
[**10a**]$^+$	$C_{40}H_{44}N_2O_3SiCl$	663.280	0.8
[**9a**]$^+$	$C_{40}H_{46}N_2O_4SiCl$	681.292	1.6

All the obtained results from ESI-MS and MS/MS experiments were supported with the data from accurate mass measurement by FT-ICR MS and the results from reaction 1 are summarized in Table 2.1.

2.6. Conclusions

Taking all the results into account, a complex triple organocatalytic cascade reaction for the stereoselective synthesis of *tetra*-substituted cyclohexene carbaldehydes has been successfully studied. The intermediates of an enamine-iminium-enamine activated triple cascade reaction have been intercepted through ESI-MS monitoring. Structural assignments were aided by using the accurate mass data from FT-ICR MS. ESI-MS, its tandem version MS/MS and the accurate mass determination are powerful methods to investigate complex organocatalyzed reactions by the interception, isolation, detection and structurally characterization of important intermediates from the reaction, thus providing significant information to the proposed catalytic cycle of the reactions. Furthermore, the ability to isolate ions directly from crude reaction mixtures for further characterization of active species, reactive intermediates, and products without previous purification is an advantage.

The cascade starts with the activation of an aldehyde **1** by enamine formation thus allowing its addition to a nitroalkene **2** via a Michael reaction. The liberated catalyst from the hydrolysis process forms an iminium ion of an α,β-unsaturated aldehyde **3** to accomplish the conjugate Michael addition with the nitroalkane **7**. In subsequent steps, the enamine **9** leads to an intramolecular aldol condensation via **10**. The final product tetra-substituted cyclohexene carbaldehyde **11** is obtained after hydrolysis. The complete reaction cycle of the organocatalytic triple cascade reaction is displayed in Scheme 2.8. Further research concerning method development of mass spectrometry for the investigation of organocatalytic reactions is being pursued in our laboratory.

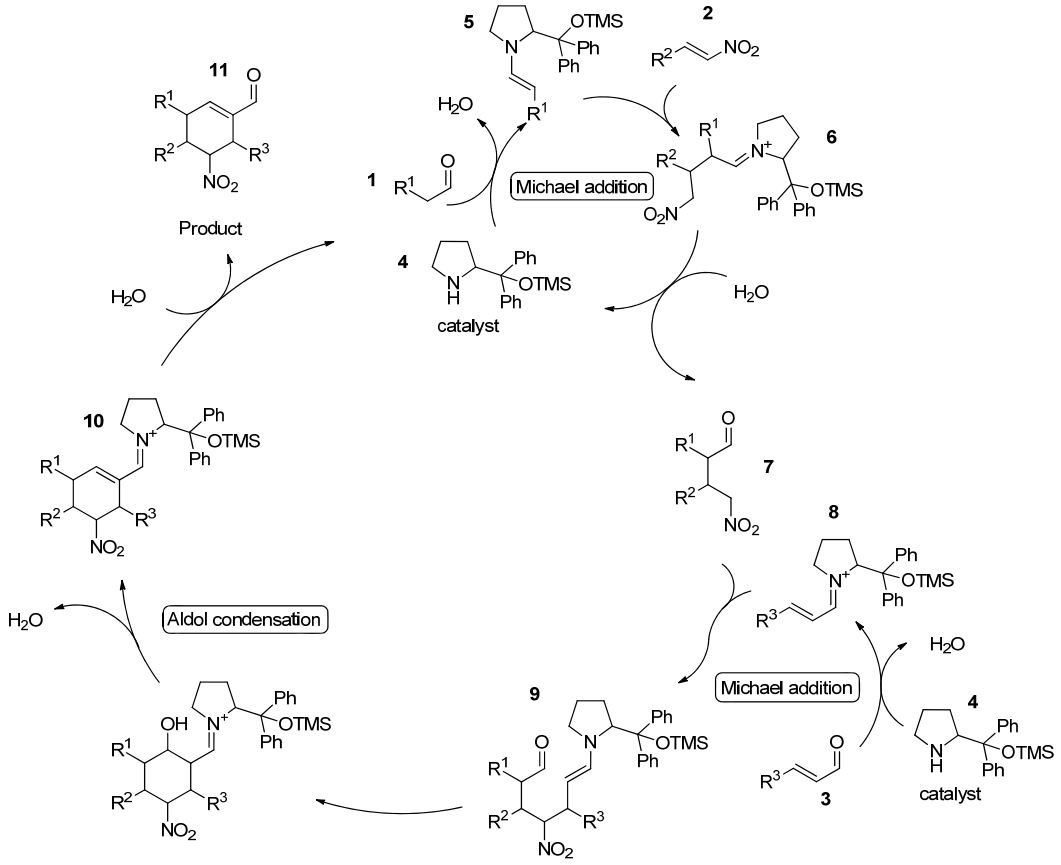

Scheme 2.8 The proposed catalytic cycle for the complex organocatalyzed triple cascade reaction.

References

[1] B. List, *Chemical Communications* **2006**.

[2] K. A. Ahrendt, C. J. Borths, D. W. C. MacMillan, *Journal of the American Chemical Society* **2000**, *122*, 4243.

[3] T. Bui, C. F. Barbas, *Tetrahedron Letters* **2000**, *41*, 6951.

[4] M. T. H. Fonseca, J. W. Yang, B. List, *Journal of the American Chemical Society* **2005**, *127*, 15036.

[5] Y. Huang, A. M. Walji, C. H. Larsen, D. W. C. MacMillan, *Journal of the American Chemical Society* **2005**, *127*, 15051.

[6] M. Marigo, T. Schulte, J. Franzen, K. A. Jorgensen, *Journal of the American Chemical Society* **2005**, *127*, 15710.

[7] D. Enders, C. Grondal, M. R. M. Huettl, *Angewandte Chemie-International Edition* **2007**, *46*, 1570.

[8] K. C. Nicolaou, D. J. Edmonds, P. G. Bulger, *Angewandte Chemie-International Edition* **2006**, *45*, 7134.

[9] J. C. Wasilke, S. J. Obrey, R. T. Baker, G. C. Bazan, *Chem. Rev.* **2005**, *105*, 1001.

[10] M. Yamashita, J. B. Fenn, *The Journal of Physical Chemistry* **1984**, *88*, 4451.

[11] C. M. Whitehouse, R. N. Dreyer, M. Yamashita, J. B. Fenn, *Analytical Chemistry* **1985**, *57*, 675.

[12] J. B. Fenn, M. Mann, C. K. Meng, S. F. Wong, C. M. Whitehouse, *Science* **1989**, *246*, 64.

[13] J. B. Fenn, *Journal of the American Society for Mass Spectrometry* **1993**, *4*, 524.

[14] A. O. Aliprantis, J. W. Canary, *Journal of the American Chemical Society* **1994**, *116*, 6985.

[15] C. Adlhart, C. Hinderling, H. Baumann, P. Chen, *Journal of the American Chemical Society* **2000**, *122*, 8204.

[16] J. Griep-Raming, S. Meyer, T. Bruhn, J. O. Metzger, *Angewandte Chemie-International Edition* **2002**, *41*, 2738.

[17] S. Meyer, R. Koch, J. O. Metzger, *Angewandte Chemie-International Edition* **2003**, *42*, 4700.

[18] L. S. Santos, C. H. Pavam, W. P. Almeida, F. Coelho, M. N. Eberlin, *Angewandte Chemie-International Edition* **2004**, *43*, 4330.

[19] A. A. Sabino, A. H. L. Machado, C. R. D. Correia, M. N. Eberlin, *Angewandte Chemie-International Edition* **2004**, *43*, 2514.

[20] J. O. Metzger, L. S. Santos, L. Knaack, *International Journal of Mass Spectrometry.* **2005**, *246*, 84.

[21] C. Marquez, J. O. Metzger, *Chemical Communications* **2006**, 1539.

[22] C. A. Marquez, F. Fabbretti, J. O. Metzger, *Angewandte Chemie-International Edition* **2007**, *46*, 6915.

[23] C. D. F. Milagre, H. M. S. Milagre, L. S. Santos, M. L. A. Lopes, P. J. S. Moran, M. N. Eberlin, J. Augusto, R. Rodrigues, *Journal of Mass Spectrometry* **2007**, *42*, 1287.

[24] L. S. Santos, *European Journal of Organic Chemistry* **2008**, *2008*, 235.

[25] W. Schrader, P. P. Handayani, C. Burstein, F. Glorius, *Chemical Communications* **2007**, 716.

[26] W. Schrader, P. P. Handayani, J. Zhou, B. List, *Angewandte Chemie-International Edition* **2009**, *48*, 1463.

[27] D. Enders, M. R. M. Huettl, C. Grondal, G. Raabe, *Nature* **2006**, *441*, 861.

[28] D. Enders, M. R. M. Huettl, J. Runsink, R. G., B. Wendt, *Angewandte Chemie-International Edition* **2007**, *46*, 467.

[29] D. Enders, M. R. M. Huettl, G. Raabe, J. W. Batsb, *Advanced Synthesis & Catalysis* **2007**, Review.

[30] C. B. Shinisha, R. B. Sunoj, *Organic & Biomolecular Chemistry* **2008**, *6*, 3921.

[31] O. M. Berner, L. Tedeschi, D. Enders, *European Journal of Organic Chemistry* **2002**, 1877.

3. Mechanistic studies of a multicatalyst promoted cascade reaction by electrospray mass spectrometry

Redrafted from "*M. Wasim Alachraf, Raffael C. Wende, Sören M. M. Schuler, Peter R. Schreiner, Wolfgang Schrader (will be submitted to Org. Lett.)*"

3.1. Abstract

A new multifunctional organocatalysis developed by Schreiner has been studied fully using electrospray mass spectrometry (ESI-MS). This reaction consists of two steps, enatioselective monoacylation of cyclohexanediol and oxidation of the second hydroxyl group to the corresponding ketone. A side-product is noticed when the reaction achieved at room temperature, but at lower temperature the yield of side-reaction is minimized. The reactive intermediates and product as well as side-product were successfully characterized and the effect of temperature in regard of side-reaction is well understood.

3.2. Introduction

Enantioselective organocatalysis is considered as one of the fastest growing fields in synthetic chemistry. Organocatalysis. One emphasis in developing new reactions has been that they are environment-friendly and a new field of green chemistry has become more important in regard to saving energy, chemicals and time.[1] One major development in this direction has been the use of cascade or multicomponent reactions which are designed in a manner that multiple chemical transformations are combined in a one-pot setup.[2] thus minimizing time, solvents, and waste generation. Many reports are published in the last years focusing on organocatalyzed cascade reactions.[3-5] The difficulty of this approach is that for a cascade with up to three or four transformations the reactive components are present all the time and the differerent steps need to be adjusted accordingly to avoind cross reactivities. Schreiner and co-workers developed a very innovative method where different catalytic moieties are combined in one catalyst conneced to an oligopeptide backbone[1, 6-9] which acts similar like an assembly line where each catalytic moiety performs a certain function to give the desired transfomration. That imitates many biological processes such as protein biosynthesis. The assemply line approach has the advantage that each catalytic moiety needs to be activated indicidually before it is needed. To understand the effects of this approach detailed mechanistic studies are an important way to allow optimization of the reaction conditions and to understand the transformation of reaction components in detail. It is very challenging to achieve a mechanistic study of such reactions that the concentrations of the used catalysts as well as the reactive intermediates are very low in the reaction solution.

While NMR and IR spectroscopy are excellent methods to follow structural changes of organic compounds, the limitations are lying in the fact that the intermediates that need to be intercepted for following such a reaction in detail are present only in short time frames and usually in low concentrations thus making the use of both NMR and IR less suitable. ESI-MS has developed into a method of choice for the analysis of rapid and complex catalytic reactions.[10-12] The main advantage of this technique is its ability to transfer starting materials, intermediates and products softly, selectively and very sensitively from reaction solution to the gas phase in ionic form in order to measure their masses and to illustrate their structure using tandem-MS methods even in very low concentrations.[11, 12] A lot of mechanistic studies in chemistry have been carried out in the last few years using ESI-MS to investigate chemical reactions in the gas phase[13, 14] or in the solution.[15-18]

The aim of this study is the investigation of a one-pot cascade reaction (desymmetrization/oxidation) of (±) 1,2 cyclohexanediol catalyzed with a peptide-based multi catalyst as reported by Schreiner and coworkers[19] (Scheme 3.1). The reaction involves two reaction steps, the enatioselective monoacetylation of 1,2-cyclohedandiole **1** to monoester **2** using a N-methyimidazol as catalytic moiety **A** followed by an oxidation of the hydroxyl group of **2** to the corresponding ketone **3** imploying the catalytic moiety (2,2,6,6-Tetramethylpiperidin-1-yl)oxyl (TEMPO) **B**.

ESI-MS(/MS) was employed for the sudies of this reaction and for the influence on the big catalyst molecule high resolution mass spectrometry was necessary because it can provide substantial information about the structural changes in the molecule.

To follow the transformation reactive reaction markers need to be indentified that usually are intermediates formed during the conversions.

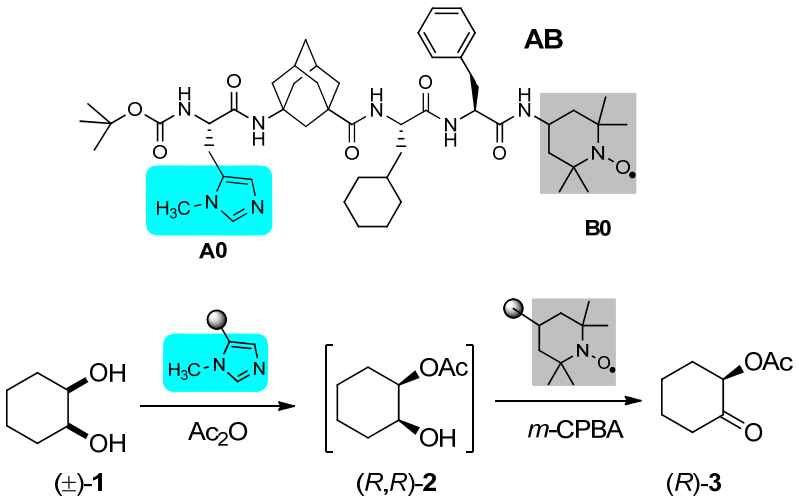

Scheme 3.1 A multicatalyst **AB** in the organocatalytic sequence of **1** to **3**.

3.3. Experimental

3.3.1. Reaction procedure

Catalyst **AB** (2.3 mg, 0.0025 mmol, 5 mol%) and 1,2-cyclohedandiole **1** (6.0 mg, 0.05 mmol) were dissolved in 10 mL of dry toluene under argon atmosphere. The reaction mixture was cooled to 0 °C and 25 µL (0.26mmol, 5.3 equivalents) Ac_2O were added. The mixture was stirred for 6 h. For the oxidation of the non-acylated OH-group 1 mg Bu_4NBr (0.0025 mmol, 5 mol%) and 37 mg of *m*-CPBA (70%) (0.15 mmol, 3 equivalents) were added and the

reaction mixture was stirred at 0 °C for 1 h. Samples of the reaction mixture have been taken over time and diluted with dichloromethane 1:200 (v/v) and measured with ESI(+)MS(/MS).

Catalyst **CAT-A** (1.9 mg, 0.0025 mmol, 5 mol%) and 1,2-cyclohedandiole **1** (6.0 mg, 0.05 mmol) were dissolved in 10 mL of dry toluene under argon atmosphere. The reaction mixture was cooled to 0 °C and 25 µL (0.26mmol, 5.3 equivalents) Ac_2O were added. The mixture was stirred for 6 h. Samples of the reaction mixture have been taken over time and diluted with dichloromethane 1:200 (v/v) and measured with ESI(+)MS(/MS).

3.3.2. Mass spectrometry

MS and MS/MS experiments were performed using a Thermo TSQ Quantum Ultra AM triple quadrupole mass spectrometer (Thermo Scientific, Dreieich, Germany) equipped with an ESI source which was controlled by Xcalibur software. The ESI spray voltages were set to 4000 V and 3000 V for positive and negative ions, respectively. The heated capillary temperature was adjusted to 270◦C. For MS/MS analysis, the collision energy was increased from 10 eV to 50 eV. The mass spectrometer was operated in the Q1 scan and product ion scan modes, with the mass width for Q1 set at 0.5 Da and for Q3 set at 0.7 Da. The collision cell Q2 contained argon and was adjusted to a pressure of 1.5 mTorr to induce CID. Spectra were collected by averaging 10 scans with a scan time of 1 sec. The Mass range was adjusted between 50 and 1500 Da.

High resolution MS data were acquired using an LTQ-Orbitrap Elite mass spectrometer (Thermo Scientific, Bremen, Germany). All experimental parameters were the same as for the triple quadruple experiments, except that MS/MS measurements were carried out with an isolation window of 1 Da and different collision energies (30 eV).

3.4. Results and discussion

The first reaction step is the enanitoselective acetylation of 1,2-cyclohexanediol to cyclohexanediol-monoacetateester using an imidazole catalytic moiety **A** within the multicatalyst **AB**. To activate this moiety acetic acid anhydride is added. While the transformation is a straightforward reaction leading to the desired product the activation of the catalytic moiety was not leading only to the desired acetyl-imidazol catalyst but an additional signal could be detected at *m/z* 985, which indicates a second acetylation (Figure 3.1). The details of this second acetylation will be discussed later in the text.

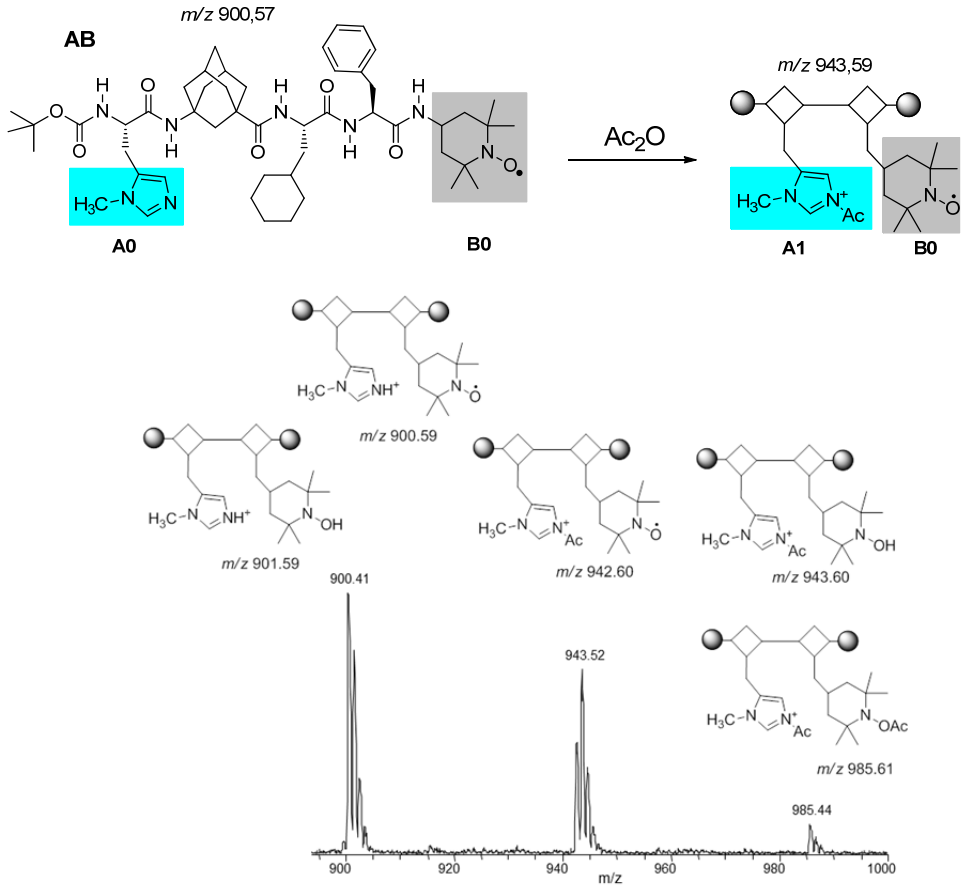

Figure 3.1 Reaction sequence of first transformation and corresponding mass spectrum of activated catalyst **AB** and its reactive intermediates.

To confirm these results an additional reaction was carried out, using the peptide backbone of the multicatalyst **AB** but with only catalytic moiety **A** attached. The activation of this moiety from **A0** to **A1** leads to just one signal in the spectrum and shows only the activation of this moiety as depicted in Figure 3.2.

The catalyst **CAT-A** was detected at *m/z* 761 and the intermediate of the catalyst with an acetylated N-methylimidazole moiety **CAT-A1** at *m/z* 803 (Figure 3.2). Unfortunately, it was not possible to intercept the adduct intermediate between the acetylated catalyst **CAT-A1** and the precursor 1,2 cyclohexandiol **1** due to the weak hydrogen bonds in this adduct intermediate, which is not stable in the measurement condition that the transfer capillary temperature in MS is about 270 °C.

ESI(+)-MS/MS was applied on *m/z* 803 to illustrate the structural information of the intermediate **CAT-A1** (Figure 3.3).

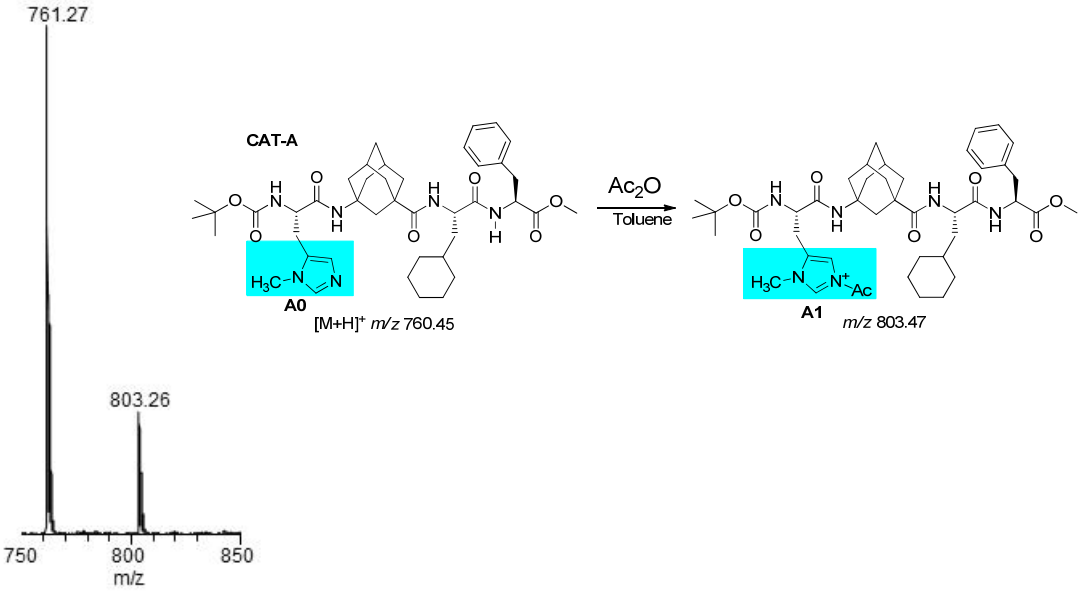

Figure 3.2 Mass spectrum of **CAT-A** in the presence of **1** and acetic acid anhydride. The protonated **CAT-A** at *m/z* 761, activated form **CAT-A1** at *m/z* 803.

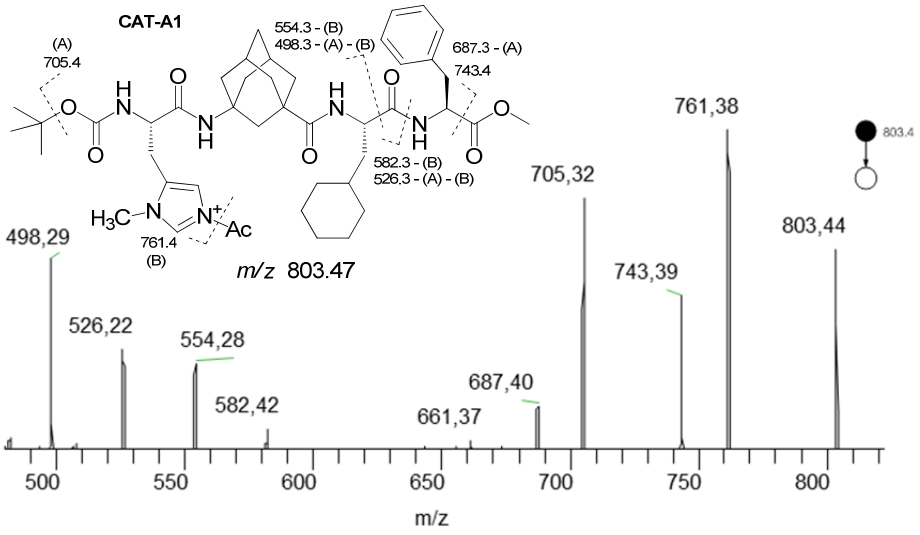

Figure 3.3 ESI(+)MS/MS spectrum of **CAT-A1** at *m/z* 803.

Figure 3.3 shows the fragmentation pattern of **CAT-A1** (parent peak *m/z* 803). The fragment at *m/z* 761 is the acetate elimination ion which has a high signal intensity indicating a weak bond between acetate and the imidazole moiety. The typical elimination fragments for such analytes is the cleavage of methyl acetate and *t*-Bu group at *m/z* 743 and *m/z* 705, respectively. The structural elucidation of **CAT-A1** was successfully achieved and the activation position of the acetate group on the imidazole moiety was characterized.

The esterification of moiety **B** has been also confirmed when TEMPO compound **4** was treated with Ac_2O and measured by high resolution ESI(+)-MS. The different oxidation states of TEMPO at *m/z* 156.1388, *m/z* 157.1467 and *m/z* 158.1539 were assigned as oxidized, radical and reduced form, respectively. The intensity of the reduced form at *m/z* 158.1539 was very weak. This can be explained by its consumption in the reaction with acetic acid anhydride to form the corresponding ester **5** at *m/z* 200.1645 (Figure 3.4).

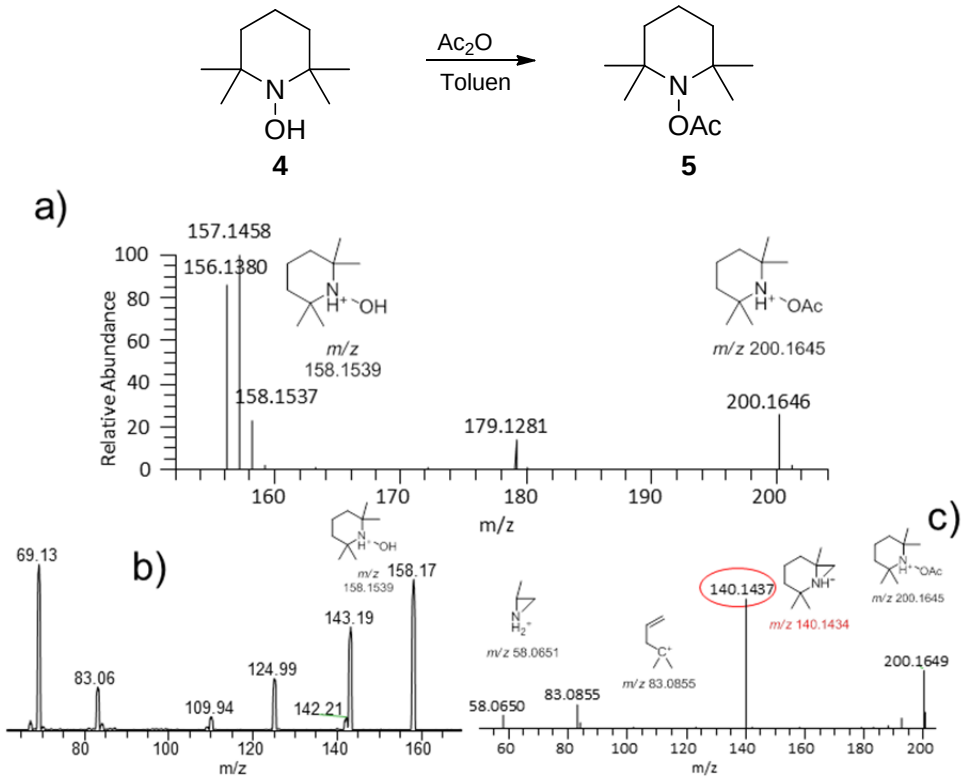

Figure 3.4 a) High resolution ESI(+)-MS spectrum of TEMPO **4** with acetic acid anhydride. **b)** ESI(+)-MS/MS spectrum of TEMPO (reduced form) **4** at *m/z* 158. **c)** High resolution ESI(+)-MS/MS spectrum of TEMPO acetate ester **5** at *m/z* 200.

To elucidate the structure of **5**, ESI(+)-MS/MS experiment was used for the parent peak, *m/z* 200.1645. The base-peak of the fragmentation spectrum was *m/z* 140.1437 which correspond to the elimination of acetic acid molecule (Figure 3.4c). On the other hand, this

loss of acetic acid was not observed in the case of fragmentation of **4** at *m/z* 158.1539 (Figure. 3.4b). Therefore the [60 Da]-loss in the tandem-MS experiments can be considered as a diagnostic indicator for the presence of TEMPO acetate ester. As a result, this experiment confirmed two things: First the possibility of building the ester between TEMPO and acetic acid anhydride, and second gave a characterized fragment for such esters in the form of acetic acid elimination. Accordingly an accurate ESI(+)-MS/MS was performed for **A1B**3 at *m/z* 985.81. In analogy to the previous experiment, acetic acid molecule elimination fragment at *m/z* 925.5915 was detected in the fragmentation spectrum which gives an evidence of the acetate esterification on the TEMPO-moiety of the catalyst **AB** (Figure 3.5).

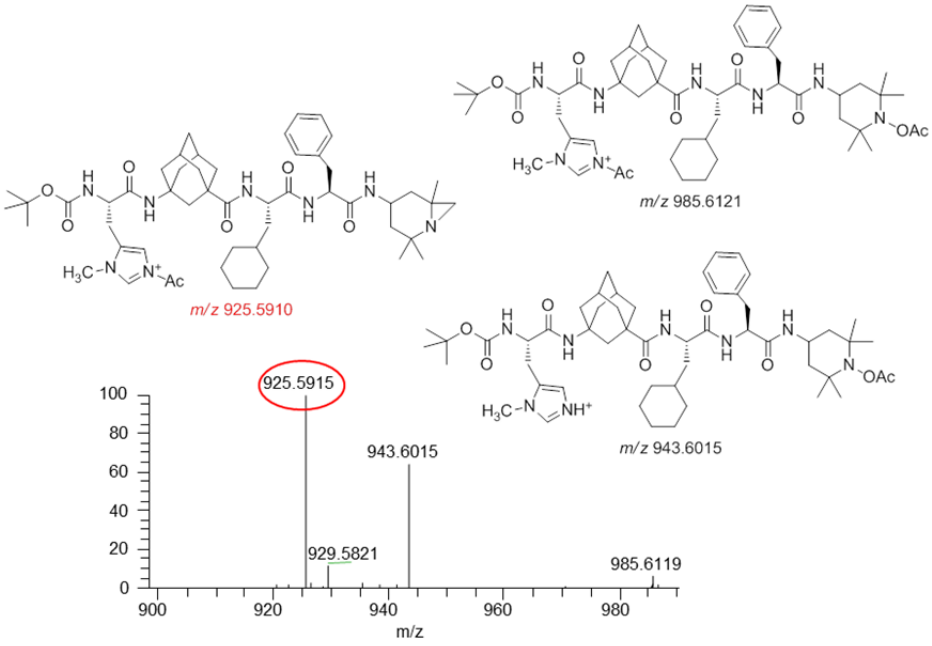

Figure 3.5 Accurate ESI(+)MS/MS spectrum at *m/z* 985.6.

The second step of the cascade reaction was the oxidation of the monohydroxyl group of the first step product (2-hydroxycyclohexyl acetate) **2** to the corresponding ketone (2-oxocyclohexyl acetate) **3** by means of the activated TEMPO-moiety **B2** of the catalyst **AB**. The oxidation reaction begins with activation of the TEMPO-moiety via the oxidant *m*-CPBA, which converts TEMPO-moiety from the radical form **B0** to activated oxidized form **B2**. Figure 3.6 shows the MS-spectrum of catalyst **AB** with all oxidation forms: a) without oxidant, b) in the presence of *m*-CPBA. Here we can notice the increasing of the intensity of the oxidized form of **A0B2** at *m/z* 450.2915 after the addition of the oxidant. The analytes appeared as doubly charged, one from the protonation of imidazole-moiety due to its high basicity and the other charge comes from the TEMPO-moiety.

The activated TEMPO-moiety **B2** oxidizes the Hydroxyl group of the precursor **2** to the corresponding ketone **3**. This oxidation is restricted to the presence of the catalyst since no oxidation reaction was noticed when *m*-CPBA was mixed with **2** in absence of **AB**.

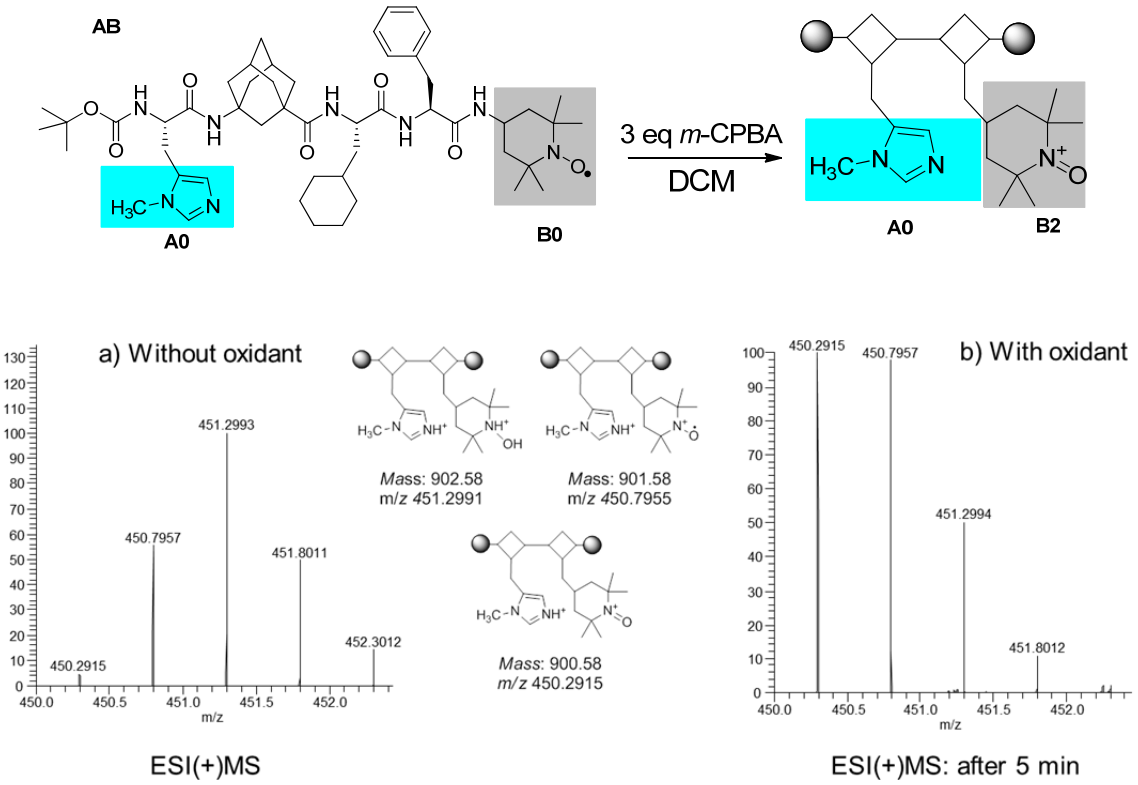

Figure 3.6 a) ESI(+)-MS spectrum of **AB** as doubly charged with all oxidation states before adding *m*-CPBA. **b)** after adding *m*-CPBA (5 min reaction time).

In addition to the final product **3** an additional new side product **6** was detected that occurs when product **3** is further oxidized with *m*-CPBA.[20] Detailed structural analysis using MS/MS studies of this side product (Figure 3.7) allowed characterizing it as a corresponding lactone according to a Baeyer-Villinger oxidation.

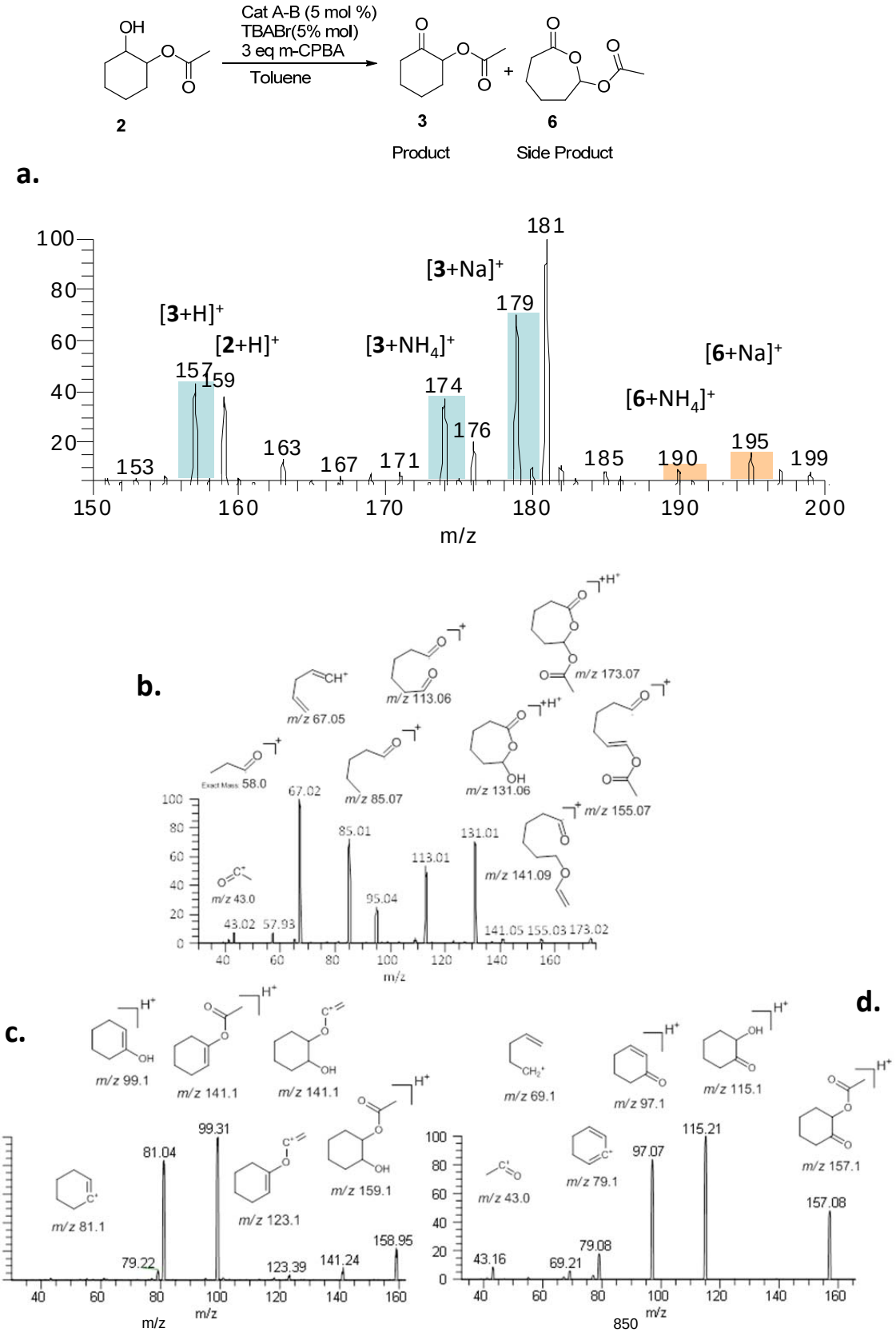

Figure 3.7 a) ESI(+)-MS spectrum of oxidation reaction of **2** to **3** (blue) and side-product **6** (red) catalyzed by **AB** at 0°C, reaction time 30 min. **b)** ESI(+)-MS/MS spectrum of the side-product **6. c)** ESI(+)-MS/MS spectrum of the product **2**. **d)** ESI(+)-MS/MS spectrum of the product **3**.

To study the effect of temperature on the oxidation reaction as well as the side-reaction route, the reaction has been monitored using ESI(+)-MS at different temperatures.

Figure 3.8a illustrates the absolute intensity of Baeyer villager side-product [**6**+Na]$^+$ at *m/z* 195 in the course of time at room temperature and 0 °C. It was clear that the concentration of side-product **6** at room temperature increases faster than the reaction at 0 °C. On other hand the desired product **3** shows a higher yield at 0 °C in the comparison to the reaction at room temperature (Figure 3.8b) that product **3** was consumed further to produce **6** at this temperature. The low temperature 0 °C suppressed the side-reaction distinctly but not the desired reaction.

No significant changes on the N-methylimidazole moiety has been observed under this oxidation conditions.

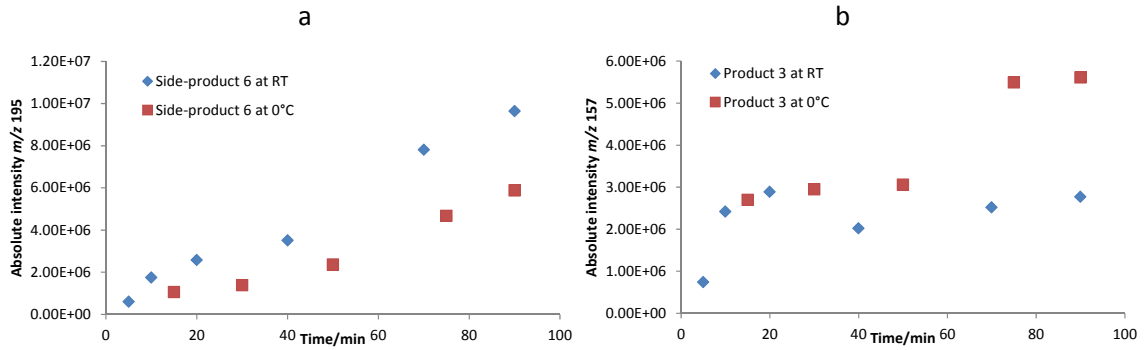

Figure 3.8 a) Absolute intensity of side-product [**6**+Na]$^+$ *m/z* 195 at 0 °C, at room temperature in course of time by ESI(+)-MS. **b)** Absolute intensity of product [**3**]$^+$ *m/z* 157 at 0 °C, at room temperature in course of time by ESI(+)-MS.

According to a previous study[7] the catalyst **AB** shows a high activity in the second reaction step (oxidation of hydroxyl group of **2**). Nevertheless according to our observation a side-reaction on TEMPO-moiety as esterification takes place after adding acetic acid anhydride in the first step as mentioned previously. This did not affect the effectively of TEMPO-moiety which can be attributed to a possible reversibility of the esterification reaction of the TEMPO-moiety in the presence of the N-methylimidazole-moiety. The latter catalyzes the esterification reaction as well as the de-esterification reaction of TEMPO-moiety. This equilibrium can be shifted to the back-direction by adding the oxidant *m*-CPBA where reduced form of TEMPO-moiety **B1** (the precursor of the esterification reaction) can be consumed to the oxidized one **B2**. The TEMPO-moiety ester in the catalyst **A1B3** can be liberated from the acetate group and catalyzes the second step of the cascade reaction with full activity.

To simulate this hypothesis different experiments have been performed. TEMPO compound *m/z* 158 was treated with acetic acid anhydride in the presence and absence of N-methyl imidazole for 30 min at room temperature. *m*-CPBA was added to both reactions and mixed at room temperature for another 30 min. Samples are taken from reaction solutions, diluted with dichloromethane and measured by ESI(+)MS.

The ester formation **5** at *m/z* 200 was detected in the reaction of TEMPO with acetic acid anhydride in the presence of N-methylimidazole (Figure 3.9a) and without (Figure 3.4a). After adding the oxidant *m*-CPBA the ester **5** was drastically eliminated only in the reaction solution with N-methylimidazole (Figure 3.9c). The signal at *m/z* 172 in Figure 3.9b, c belongs to a side product from the reaction between a decomposed TEMPO compound at *m/z* 142 and the oxidant *m*-CPBA.

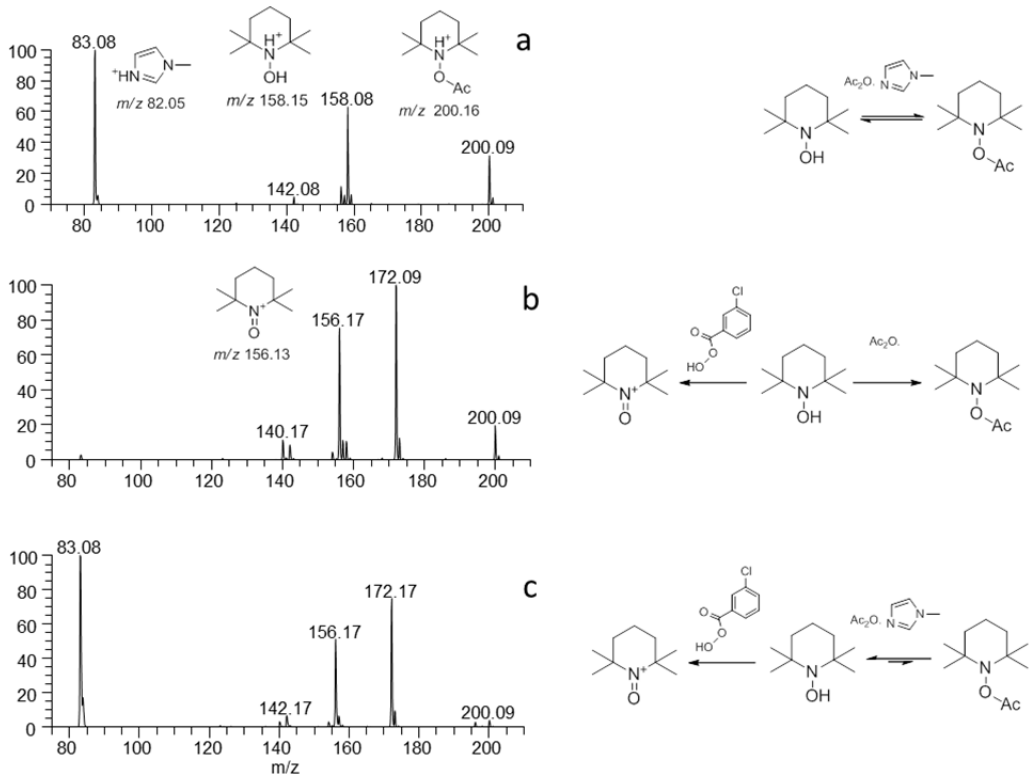

Figure 3.9 a) ESI(+)-MS spectrum of reaction mixture of TEMPO **4** *m/z* 158 (reduced form) with acetic acid anhydride in the presence of N-methylimidazole *m/z* 83 after 30min. **b)** ESI(+)-MS spectrum of TEMPO with acetic acid anhydride in the presence of oxidant *m*-CPBA (not detectable in positive modus) after 1h reaction time. **c)** ESI(+)-MS spectrum of TEMPO with acetic acid anhydride in the presence of N-methylimidazole and oxidant *m*-CPBA after 1h reaction time.

ESI-MS spectra of catalyst **AB** in the reaction solution with acetic acid anhydride before and after treatment with oxidant *m*-CBPA were compared to see any difference in the intensity of TEMPO-ester signal after adding the oxidant.

The decrease of the intensity of **A1B3** at *m/z* 985 was considerable after addition of the oxidant in the second step confirming the hypothesis of the liberation of TEMPO-moiety from the acetate group because of the effect of N-methylimidazole and *m*-CBPA, leading to the conclusion that the activity of TEMPO-moiety for the second reaction step is not affected (Figure 3.10).

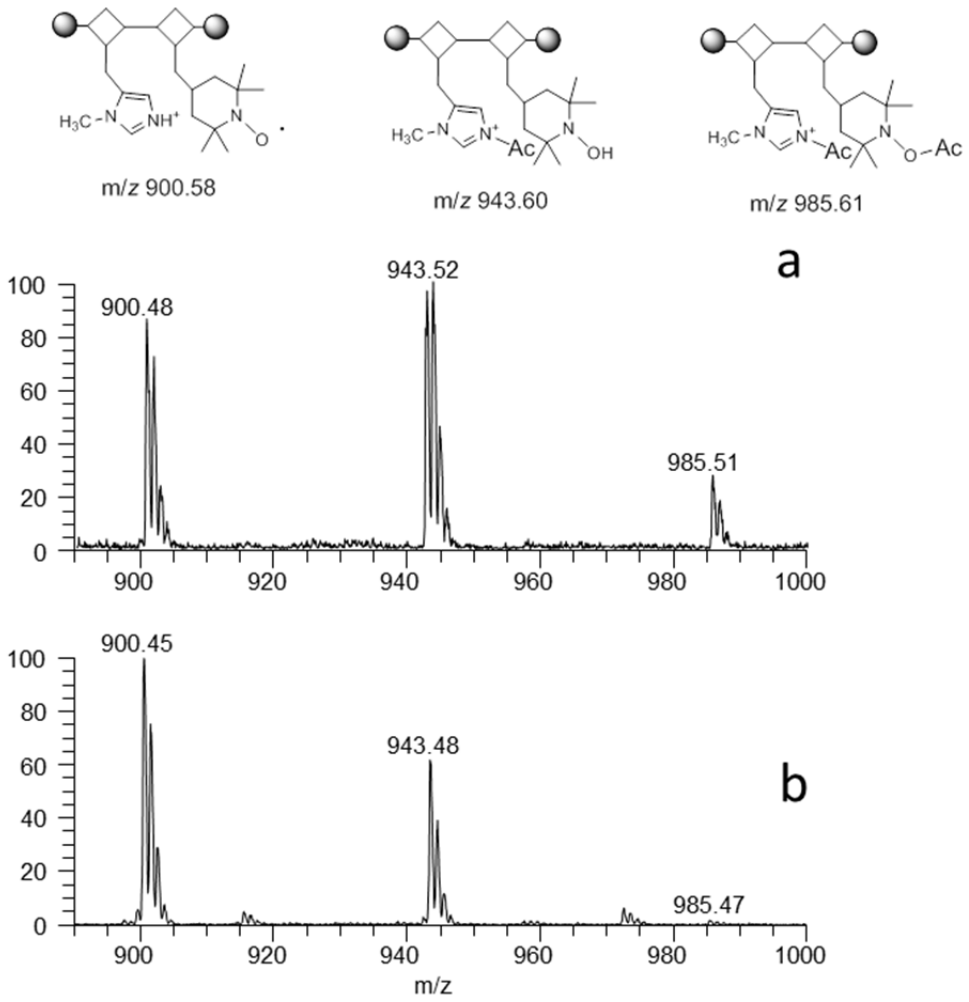

Figure 3.10 a) ESI(+)-MS spectrum of **AB** after adding acetic acid anhydride. **b)** MS-spectrum of **AB** after adding acetic acid anhydride and *m*-CPBA.

3.5. Conclusion

In this study it was possible to investigate the mechanism of a one pot cascade reaction of enantio-selective monoesterification followed by oxidation of the reminder hydroxyl group of (±) 1,2 cyclohexanediol catalyzed with a multicatalyst with two catalytic moieties by ESI-MS and MS/MS.

Detailed MS studies have shown that an additional side product is formed that reduces the yield of the main product. Reduced reaction temperature can lead to a better yield because the side product is suppressed under these conditions. An additional acetylation of the second catalytic moiety does not have any effects on the transformation since it is removed during the activation of the second catalytic moiety. All things considered a detailed study of this reaction was performed leading to the full understanding of each reaction step that can be combined in a catalytic cycle as shown in Scheme 3.2.

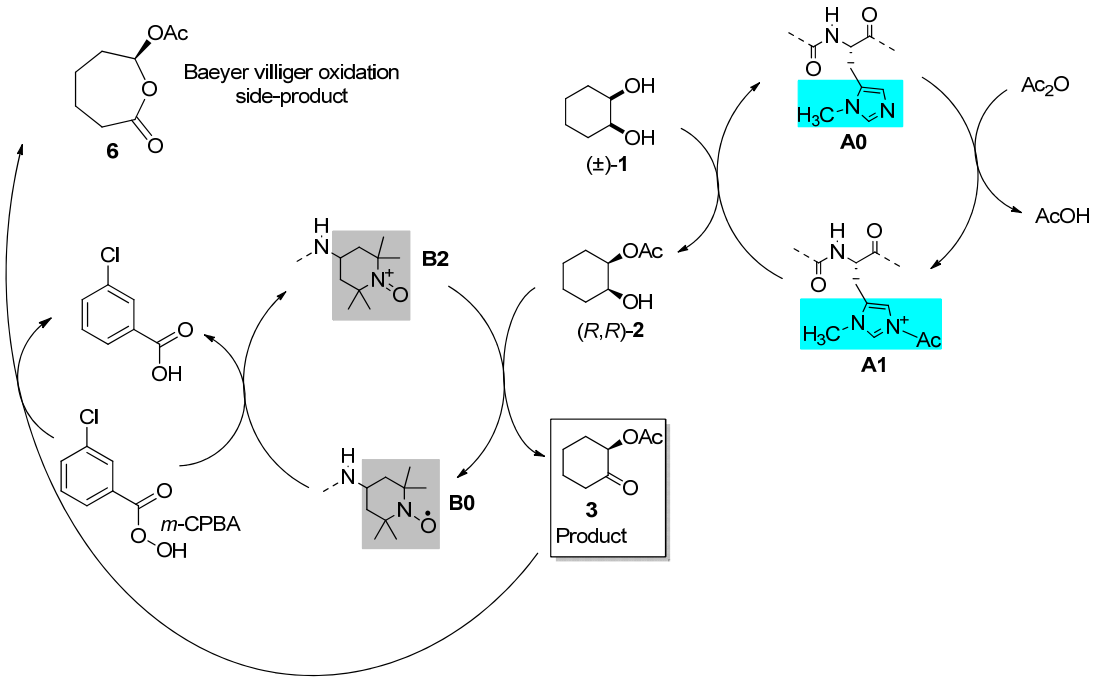

Scheme 3.2 The proposed catalytic cycle for the reaction and the side-reaction.

References

[1] R. C. Wende, P. R. Schreiner, *Green Chemistry* **2012**, *14*, 1821.

[2] K. C. Nicolaou, D. J. Edmonds, P. G. Bulger, *Angewandte Chemie-International Edition* **2006**, *45*, 7134.

[3] X. Zhang, X. Song, H. Li, S. Zhang, X. Chen, X. Yu, W. Wang, *Angewandte Chemie International Edition* **2012**, *51*, 7282.

[4] D. Enders, M. R. Huettl, G. Raabe, J. W. Bats, *Advanced Synthesis & Catalysis* **2008**, *350*, 267.

[5] B. Tan, Z. Shi, P. J. Chua, G. Zhong, *Organic letters* **2008**, *10*, 3425.

[6] C. E. Muller, L. Wanka, K. Jewell, P. R. Schreiner, *Angewandte Chemie-International Edition* **2008**, *47*, 6180.

[7] C. E. Muller, R. Hrdina, R. C. Wende, P. R. Schreiner, *Chemistry-a European Journal* **2011**, *17*, 6309.

[8] R. Hrdina, C. E. Muller, R. C. Wende, L. Wanka, P. R. Schreiner, *Chemical Communications* **2012**, *48*, 2498.

[9] C. E. Mueller, D. Zell, P. R. Schreiner, *Chemistry-a European Journal* **2009**, *15*, 9647.

[10] J. B. Fenn, M. Mann, C. K. Meng, S. F. Wong, C. M. Whitehouse, *Science* **1989**, *246*, 64.

[11] C. M. Whitehouse, R. N. Dreyer, M. Yamashita, J. B. Fenn, *Analytical Chemistry* **1985**, *57*, 675.

[12] C. Trage, D. Schroder, H. Schwarz, *Chemistry-a European Journal* **2005**, *11*, 619.

[13] D. Schroeder, *European Journal of Mass Spectrometry* **2012**, *18*, 139.

[14] S. M. Polyakova, R. A. Kunetskiy, D. Schroeder, *International Journal of Mass Spectrometry* **2012**, *314*, 13.

[15] W. Schrader, P. P. Handayani, J. Zhou, B. List, *Angewandte Chemie-International Edition* **2009**, *48*, 1463.

[16] C. Marquez, J. O. Metzger, *Chemical Communications* **2006**, 1539.

[17] L. S. Santos, L. Knaack, J. O. Metzger, *International Journal of Mass Spectrometry* **2005**, *246*, 84.

[18] T. D. Fernandes, B. G. Vaz, M. N. Eberlin, A. J. M. da Silva, P. R. R. Costa, *Journal of Organic Chemistry* **2010**, *75*, 7085.

[19] K. Zumbansen, A. Doehring, B. List, *Advanced Synthesis & Catalysis* **2010**, *352*, 1135.

[20] G. R. Krow, *Organic Reactions* **1993**.

4. Functionality, effectiveness, and mechanistic evaluation of a multicatalyst–promoted reaction sequence by electrospray mass spectrometry

Redrafted from "*M. Wasim Alachraf, Raffael C. Wende, Sören M. M. Schuler, Peter R. Schreiner, Wolfgang Schrader (submitted to Angew. Chem. Int. Ed.)*"

4.1. Abstract

A new asymmetric triple cascade reaction has been studied thoroughly using mass spectrometry. The epoxidation, hydrolysis and enantioselective monoacylation of cyclohexene have been carried out in a one-pot reaction using a chiral multifunctional organocatalyst. All reaction steps are fully studied by ESI-MS(/MS) as well as high resolution MS for more structural elucidation. The most interesting part of this reaction was the activation process of each catalytic moiety. Because of the hard oxidation condition in the first reaction step the catalytically moieties N-methylimidazole of the acylation reaction in the second step suffered under oxidation side-reaction. This has been characterized and the results explain the low efficiency of the catalyst in this step. All reactive intermediates of the reaction steps and the side reactions as well as product can be monitored and the mechanistic cycle of the reaction is presented.

4.2. Introduction and discussion

Various synthetic methods have been developed for using small organic molecules as organocatalysts.[1-6] One especially intriguing development has been the use of cascade or tandem reactions[7-18] where in a one-pot synthetic scheme the reaction components are put together and different reactions are subsequently carried out without intermediate isolation. These types of reactions are promise higher efficiency while minimizing resource and energy requirements.

The elucidation of the reaction mechanisms of such complex reactions is rather challenging because many intermediates are short-lived and occur often only in minor quantities. Methods that allow the characterization of structural changes typically are nuclear magnetic resonance (NMR)[19-23] and, to a minor extend, infrared (IR)-spectroscopy.[23-26]

A powerful tool for the investigation of complex organocatalytic reactions is mass spectrometry (MS) due to its advantages to detect components at low concentrations within short time frames. Examples have shown that even some structural data can be determined when using MS/MS experiments.[27-29] The fragmentation of individual intermediates can be utilized for the characterization of catalytic reactions.[30-36]

Typical cascade or tandem reactions combine the reactants from the beginning in a one-pot synthetic approach,[7-18] often giving rise to a broad variety of side reactions. One very innovative concept of a cascade reaction is when the catalyst carries multiple catalytic moieties, separated by a spacer molecule, a so-called multicatalyst.[18, 37, 38] This methodology is reminiscent of an assembly line where a new molecule is assembled consecutively in a manner that at the correct time each catalytic moiety is selectively activated.[37, 38] Due to the novelty of this approach no mechanistic studies have been carried out yet. Here, we report a detailed mechanistic investigation concerning the catalytic epoxidation of olefins followed by hydrolysis and a catalytic kinetic resolution through acylation.[39] Each individual step can be defined by a special reaction marker that can be detected by electrospray mass spectrometry (ESI-MS).

The multicatalyst used in this study consists of a chiral peptide backbone[40, 41] with an adamantane spacer[37, 38, 42-44] that separates two catalytically active components. One is a dicarboxylic function **A** that is responsible for the first step of the reaction, an epoxidation,[40] and an imidazole moiety **B** that catalyzes the terminal acylation.[38] The major difference between standard cascade reactions and reactions with a multicatalyst is that each catalytic moiety needs to be activated individually before use allowing the optimization of the reaction conditions that are needed for each individual reaction. Various catalysts have been developed

where the catalytically active moieties where placed at different positions[38] within the peptide backbone and for this study the most effective one was used. The overall reaction is presented in Scheme 4.1.

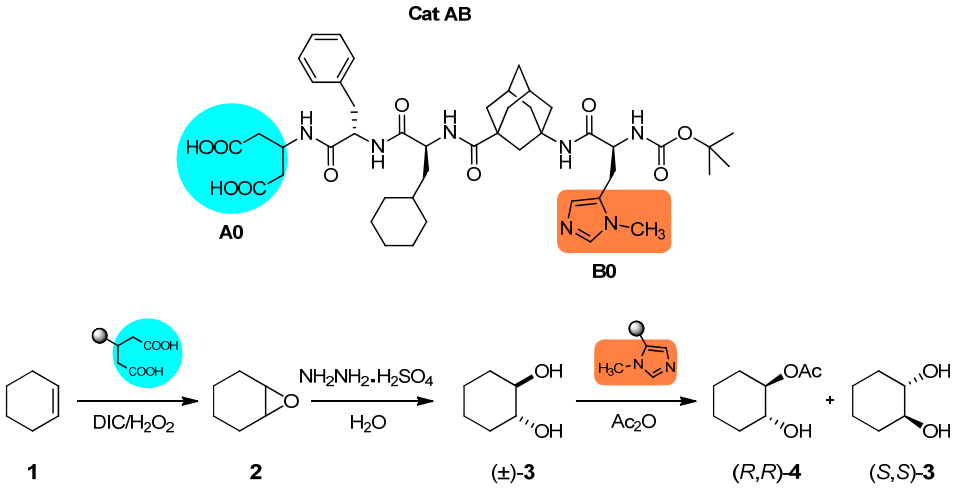

Scheme 4.1 Reaction scheme describing the reaction and a multicatalyst with two catalytic moieties: **A0** a dicarboxylic function and **B0** an imidazole group, both in their inactivated states.

The first step in the mechanistic evaluation of a catalytic reaction is the determination and characterization of reaction markers that allow an unequivocal assignment of the reaction intermediates. Here, the first step of the reaction is the epoxidation of an olefin, with cyclohexene being used in this example. While the reaction itself is straightforward, the role of the catalytic moieties is a much more interesting and important part of this work. The activation of the catalytic moiety **A0** involves the formation of anhydride **A2** using diisopropyl carbodiimide (DIC), which is subsequently converted to the corresponding peracid **A3** using hydrogen peroxide. This activated catalyst oxidizes the olefin to the corresponding epoxide (Scheme 4.2; the corresponding accurate MS/MS spectra of the dicarboxylic acid, the intermediate with the DIC reagent and the anhydride are presented in Figure A4.1).

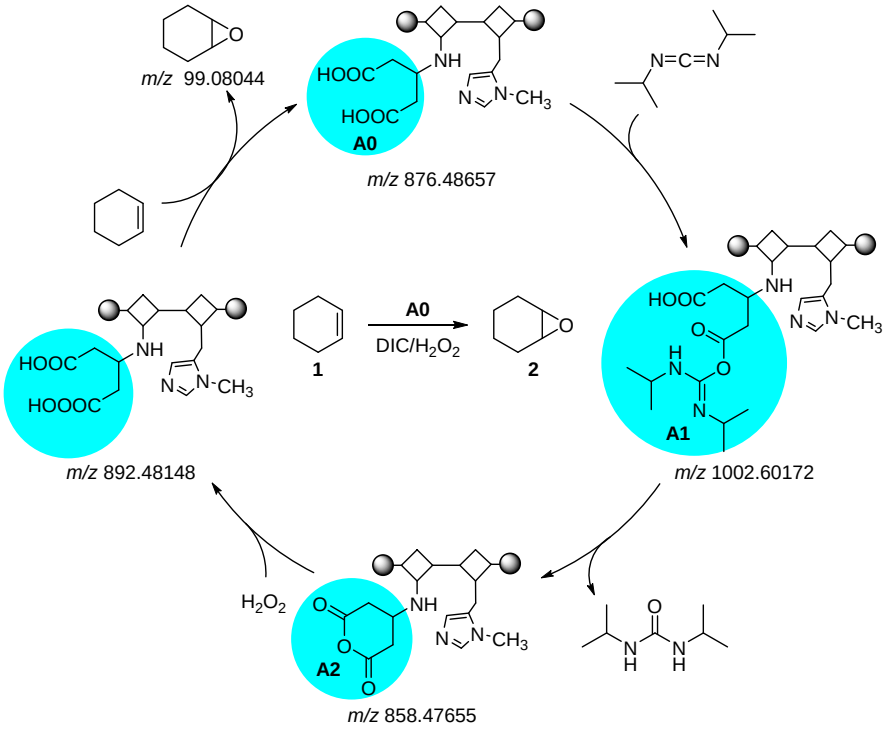

Scheme 4.2 Activation of the di- carboxylic acid catalytic moiety for the epoxidation step.

For the activation of the catalytic moiety **A0** DIC is added to the carboxylic group forming the *O*-acylisourea **A1**, which, after cleavage, removes a water molecule from the catalyst to give the corresponding anhydride **A2**. This further reacts with hydrogen peroxide to form the peracid, which is the activated catalytic moiety **A3**. One potential side reaction was reported by Montalbetti et al.[45] for such compounds, namely the rearrangement from an *O*-acylisourea to an *N*-acylurea attached to the peptide (Scheme3. 3). We also observed this side reaction but the molecular ion is almost not detectable implying that it does not affect the catalytic step (for details of the accurate MS/MS spectrum see also Figure A4.1).

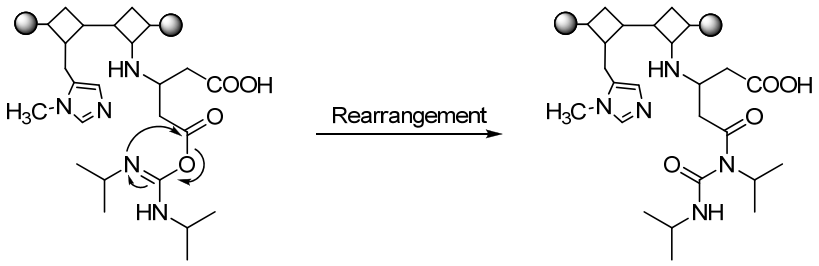

Scheme 4.3 Rearrangement reaction of *O*-acylisourea to *N*-acylurea.

After formation of the activated catalytic peracid **A3** the catalyst reacts with olefin **1** to form the corresponding epoxide **2**. For the hydrolysis of the epoxide to the diol additionally water

and hydrazine sulfate needs to be added. The MS/MS spectrum detailing this is shown in Figure A4.2.

As recent studies found that the catalyst converts about 57% (±)-**3** (2 mol% catalyst loading, 3 h) when used alone but only 37% of the monoacetylated product **4** (5 mol% catalyst loading, 17 h) are obtained when the reaction is performed under multicatalysis conditions,[38] we set out to determine the reasons for this somewhat reduced effectiveness of the multicatalyst.

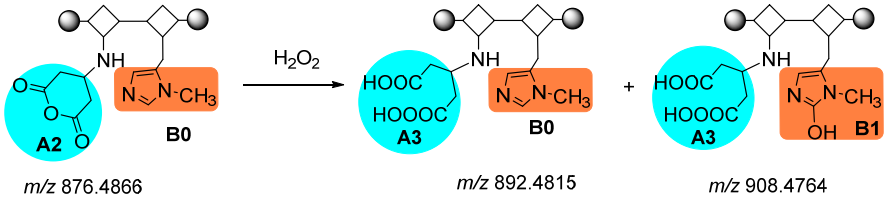

Scheme 4.4 Oxidation of moiety **B0** to form hydantoin derivative **B1**.

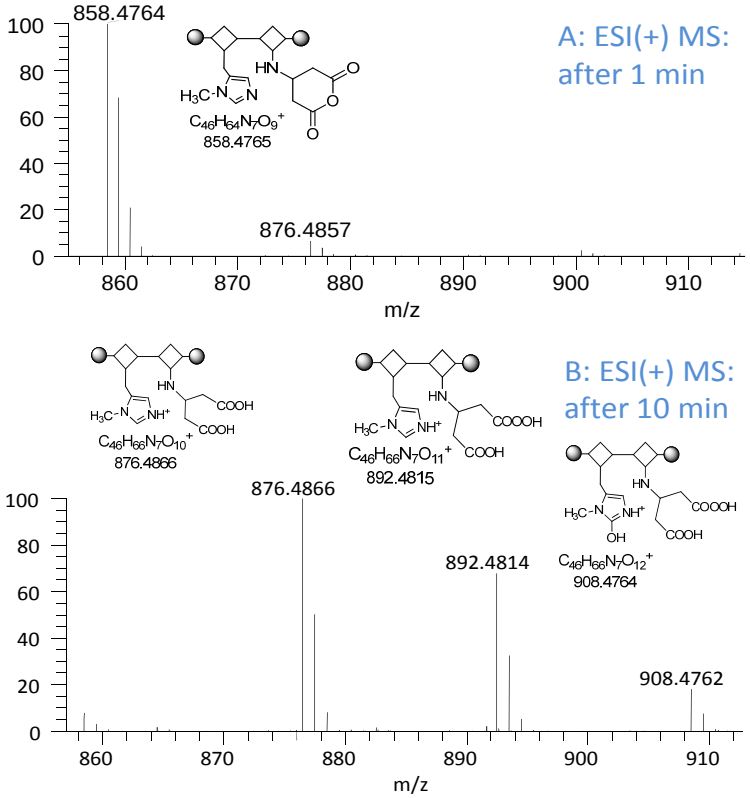

Figure 4.1 MS spectra of the activation of the catalytic moiety **A**: above spectrum A shows the anhydride moiety **A2** after adding DIC while below spectrum B shows the moiety **A3** after adding DIC and H_2O_2. Additional signals are characterized as shown.

During the studies of this reaction and especially the formation of the **A3** moiety, we found that another reaction occurs that could have direct impact on the effectiveness of the imidazole group **B0** that is responsible for the second catalytic step, the acylation. During the

formation of peracid **A3** an additional signal was found at *m/z* 908 (Figure 4.1). The difference of 16 Da indicates oxidation within the molecule, which was confirmed by accurate mass data. The position of the oxidation was studied thoroughly by using highly accurate MS/MS and MS^n experiments, where the molecule was fragmented and the structural differences were analyzed. We determined the oxidation of the imidazole group: activation of the **A** moiety also leads to oxidation of the **B** moiety, resulting in the formation of hydantoin derivative **B1** (Scheme3. 4; for accurate MS/MS spectra see Figure A4.3). The oxidation of the imidazole moiety leads to a reduced effectiveness of the catalyst and explains the reduced activity of this catalytic moiety when used as a multicatalyst.

The second catalytic step in this reaction sequence is the stereo-selective monoacylation of the diol. The activation of the catalytic moiety **B0** is accomplished by adding acetic acid anhydride to the reaction mixture after completion of the preceding reactions. The resulting active moiety is acetylated imidazole **B2** (Scheme3. 5).

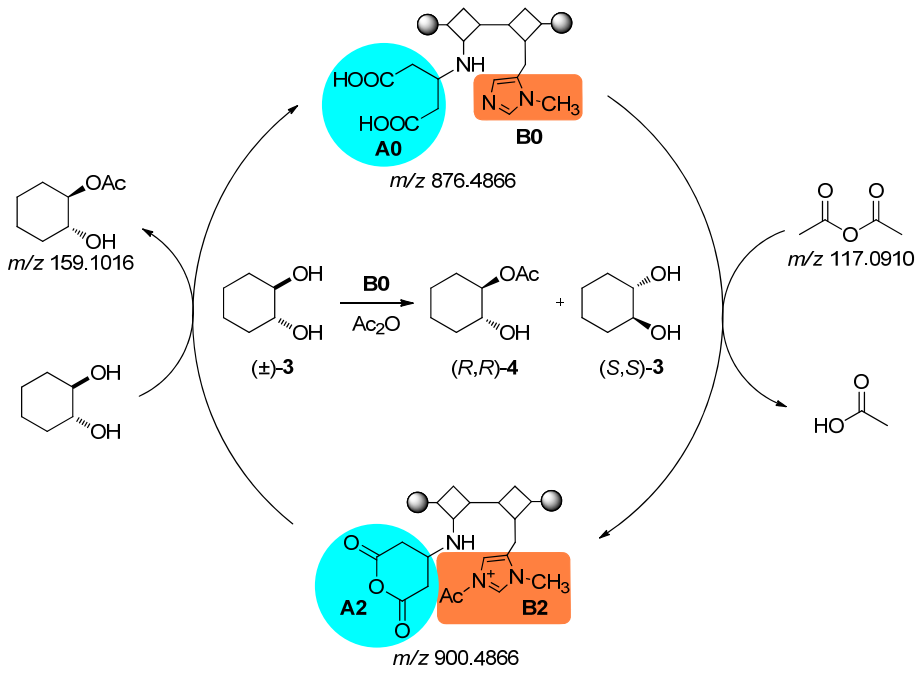

Scheme 4.5 Activation of the catalytic moiety **B0**.

The characterization of the activation of the catalyst is shown in the MS spectra in Figure A4.4. After activation of the catalyst monoacylation of the diol follows (Figure 4.2).

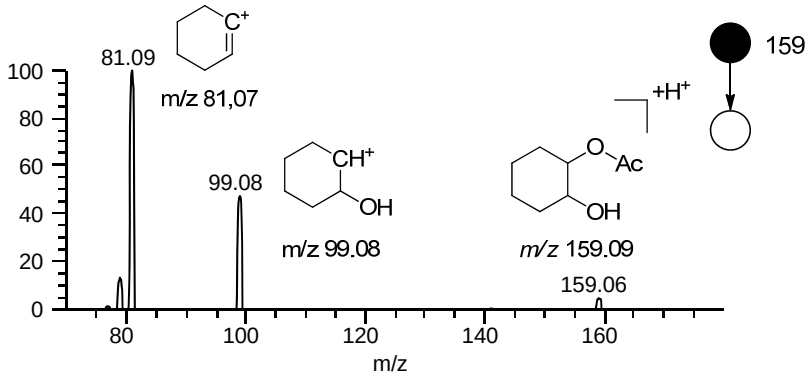

Figure 4.2 MS/MS spectrum of the product cyclohexane diol monoacetate.

At the beginning of the second catalytic step the multicatalyst is in the state **A0B0**, which means both catalytic sites are inactive. When acetic acid anhydride is utilized to activate the second moiety the **B** moiety is converted to the acetylated imidazolium **B2**. These results also indicate that during this step not only the **B** moiety was activated by acetic acid anhydride but also the **A** moiety as **A0** was directly converted to anhydride **A2** (Scheme 4.5). The corresponding MS spectrum is shown in Figure 4.3. In a subsequent step **A2B2** is oxidized to **A3B2** by hydrogen peroxide. Figure A4.4 shows the MS/MS spectrum of **A3B2** while Figure A4.5 presents additional MS^3 spectra with the detailed fragmentation pattern of each catalytic moiety.

All things considered, the detailed mass spectrometric study of a multicatalyst allows the meticulous and individual characterization of both catalytic reactions. The activation of each catalytic moiety can be explained in detail. The somewhat lower yield of the second catalytic moiety is likely due to an oxidative side reaction that occurs during the activation of the first step. This is a prime example how detailed mechanistic studies using highly accurate MS and MS^n data can help in understanding complex organocatalytic reactions.

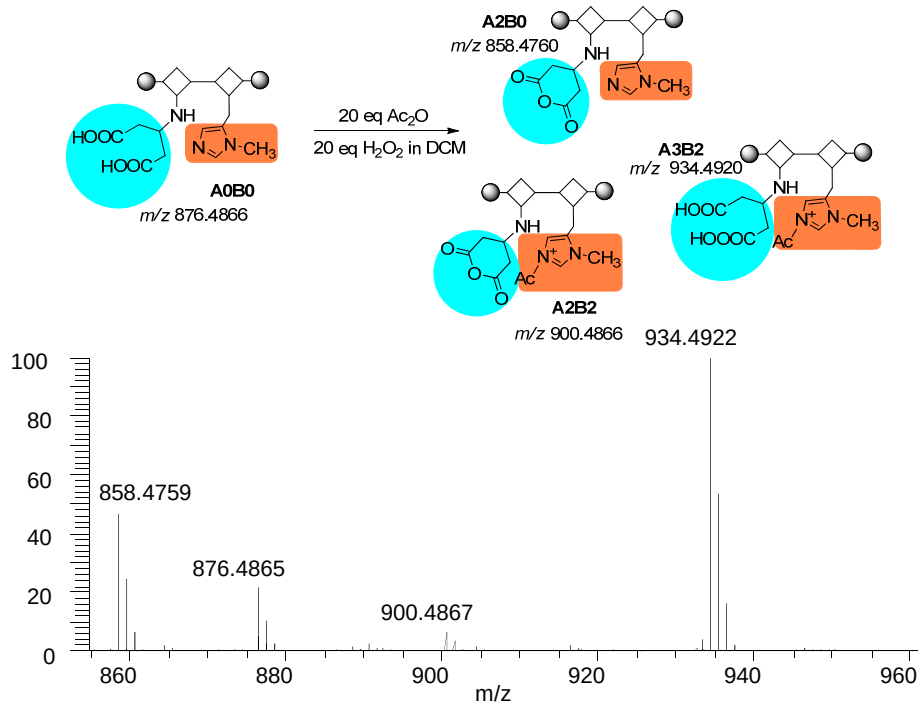

Figure 4.3 MS spectrum of the catalyst **A2B2** and the oxidation product **A3B2** after activation.

4.3. Experimental

4.3.1. Reaction procedure

Catalyst (0.05 mmol, 21.9 mg, 5 mol%), cyclohexene (1 mmol, 101 µL, 1 eq) and DIC (1.2 mmol, 185 µL, 1.2 eq) were dissolved in 2 mL DCM. To this mixture 30% hydrogen peroxide (130 µL, 1.2 eq) was added and the resulting reaction mixture was stirred at room temperature for 24 h. After this time the addition of DIC (1.2 mmol, 185 µL, 1.2 eq) and 30% hydrogen peroxide (130 µL, 1.2 eq) was repeated and the reaction was stirred under the same conditions for additional 24 h. Then toluene (6 mL) was added, followed by the addition of H_2O (10 mmol, 180 µL, 10 eq) and hydrazine sulfate (0.1 mmol, 13 mg, 0.1 eq) and the reaction was stirred at room temperature for 18 h. In the next step toluene (180 mL) and $^{i}Pr_2EtN$ (5.3 mmol, 901 µL, 5.3 eq) were added and the reaction was cooled to 0 °C. Ac_2O (5.3 mmol, 501 µL, 5.3 eq) was added at last and the kinetic resolution was monitored by chiral GC. After 17 h the reaction was quenched by adding methanol (10 mL), the solvents were evaporated under reduced pressure and the column chromatography on silicagel in hexane/EtOAc 1:1 provided 56 mg (35%) of 1-acetoxy-2-cyclohexane alcohol (60% yield).

4.3.2. Mass spectrometry

MS and MS/MS experiments were done using a Thermo TSQ Quantum Ultra AM triple quadrupole mass spectrometer (Thermo Scientific, Dreieich, Germany) equipped with an ESI source which was controlled by Xcalibur software. The ESI spray voltages were set to 4000 V and 3000 V for positive and negative ions, respectively. The heated capillary temperature was adjusted to 270 °C. For MS/MS analysis, the collision energy was increased from 10 eV to 50 eV. The mass spectrometer was operated in the Q1 scan and product ion scan modes, with the mass width for Q1 set at 0.5 Da and for Q3 set at 0.7 Da. The collision cell, Q2, contained argon and was adjusted to a pressure of 1.5 mTorr to induce CID. Spectra were collected by averaging 10 scans with a scan time of 1 s. The mass range was adjusted between 50 and 1500 Da.

High resolution MS data were aqcuirred using an LTQ-Orbitrap Elite mass spectrometer (Thermo Scientific, Bremen, Germany). All experimental parameters were the same as for the triple quadrupole experiments, except that MS/MS measurements were carried out with an isolation window of 1 Da and different collision energies.

References

[1] A. Berkessel, H. Gröger, *Asymmetric Organocatalysis: From Biomimetic Concepts to Applications in Asymmetric Synthesis*, Wiley-VCH, Weinheim, **2005**.

[2] P. I. Dalko, *Enantioselective Organocatalysis: Reactions and Experimental Procedures*, Wiley-VCH, Weinheim, **2007**.

[3] A. Dondoni, A. Massi, *Angewandte Chemie-International Edition* **2008**, *47*, 4638.

[4] D. W. C. MacMillan, *Nature* **2008**, *455*, 304.

[5] A. Moyano, R. Rios, *Chemical Reviews* **2011**, *111*, 4703.

[6] F. Giacalone, M. Gruttadauria, P. Agrigento, R. Noto, *Chemical Society Reviews* **2012**, *41*, 2406.

[7] D. E. Fogg, E. N. dos Santos, *Coordination Chemistry Reviews* **2004**, *248*, 2365.

[8] J.-C. Wasilke, S. J. Obrey, R. T. Baker, G. C. Bazan, *Chemical Reviews* **2005**, *105*, 1001.

[9] H. C. Guo, J. A. Ma, *Angewandte Chemie-International Edition* **2006**, *45*, 354.

[10] C. J. Chapman, C. G. Frost, *Synthesis-Stuttgart* **2007**, 1.

[11] D. Enders, C. Grondal, M. R. M. Hüttl, *Angewandte Chemie-International Edition* **2007**, *46*, 1570.

[12] A. M. Walji, D. W. C. MacMillan, *Synlett* **2007**, 1477.

[13] X. Yu, W. Wang, *Organic & Biomolecular Chemistry* **2008**, *6*, 2037.

[14] A.-N. Alba, X. Companyó, M. Viciano, R. Rios, *Current Organic Chemistry* **2009**, *13*, 1432.

[15] C. Grondal, M. Jeanty, D. Enders, *Nature Chemistry* **2010**, *2*, 167.

[16] B. Westermann, M. Ayaz, S. S. van Berkel, *Angewandte Chemie-International Edition* **2010**, *49*, 846.

[17] H. Pellissier, *Advanced Synthesis & Catalysis* **2012**, *354*, 237.

[18] R. C. Wende, P. R. Schreiner, *Green Chemistry* **2012**, *14*, 1821.

[19] M. B. Schmid, K. Zeitler, R. M. Gschwind, *Angewandte Chemie-International Edition* **2010**, *49*, 4997.

[20] M. B. Schmid, K. Zeitler, R. M. Gschwind, *Journal of the American Chemical Society* **2011**, *133*, 7065.

[21] M. B. Schmid, K. Zeitler, R. M. Gschwind, *Journal of Organic Chemistry* **2011**, *76*, 3005.

[22] Z. Zhang, K. M. Lippert, H. Hausmann, M. Kotke, P. R. Schreiner, *The Journal of Organic Chemistry* **2011**, *76*, 9764.

[23] K. M. Lippert, K. Hof, D. Gerbig, D. Ley, H. Hausmann, S. Guenther, P. R. Schreiner, *European Journal of Organic Chemistry* **2012**, *2012*, 5919.

[24] A. T. Messmer, K. M. Lippert, S. Steinwand, E.-B. W. Lerch, K. Hof, D. Ley, D. Gerbig, H. Hausmann, P. R. Schreiner, J. Bredenbeck, *Chemistry – A European Journal* **2012**, *18*, 14989.

[25] A. T. Messmer, S. Steinwand, K. M. Lippert, P. R. Schreiner, J. Bredenbeck, *The Journal of Organic Chemistry* **2012**, *77*, 11091.

[26] A. T. Messmer, K. M. Lippert, P. R. Schreiner, J. Bredenbeck, *Physical Chemistry Chemical Physics* **2013**, *15*, 1509.

[27] J. Griep-Raming, S. Meyer, T. Bruhn, J. O. Metzger, *Angewandte Chemie-International Edition* **2002**, *41*, 2738.

[28] L. S. Santos, J. O. Metzger, *Angewandte Chemie-International Edition* **2006**, *45*, 977.

[29] W. Schrader, P. P. Handayani, C. Burstein, F. Glorius, *Chemical Communications* **2007**, 716.

[30] J. B. Domingos, E. Longhinotti, T. A. S. Brandao, C. A. Bunton, L. S. Santos, M. N. Eberlin, F. Nome, *Journal of Organic Chemistry* **2004**, *69*, 6024.

[31] L. S. Santos, C. H. Pavam, W. P. Almeida, F. Coelho, M. N. Eberlin, *Angewandte Chemie-International Edition* **2004**, *43*, 4330.

[32] C. A. Marquez, F. Fabbretti, J. O. Metzger, *Angewandte Chemie-International Edition* **2007**, *46*, 6915.

[33] C. D. F. Milagre, H. M. S. Milagre, L. S. Santos, M. L. A. Lopes, P. J. S. Moran, M. N. Eberlin, J. A. R. Rodrigues, *Journal of Mass Spectrometry* **2007**, *42*, 1287.

[34] W. Schrader, P. P. Handayani, J. Zhou, B. List, *Angewandte Chemie-International Edition* **2009**, *48*, 1463.

[35] G. W. Amarante, M. Benassi, H. M. S. Milagre, A. A. C. Braga, F. Maseras, M. N. Eberlin, F. Coelho, *Chemistry – A European Journal* **2009**, *15*, 12460.

[36] M. W. Alachraf, P. P. Handayani, M. R. M. Huettl, C. Grondal, D. Enders, W. Schrader, *Organic & Biomolecular Chemistry* **2011**, *9*, 1047.

[37] C. E. Müller, R. Hrdina, R. C. Wende, P. R. Schreiner, *Chemistry – A European Journal* **2011**, *17*, 6309.

[38] R. Hrdina, C. E. Müller, R. C. Wende, L. Wanka, P. R. Schreiner, *Chemical Communications* **2012**, *48*, 2498.

[39] C. E. Müller, P. R. Schreiner, *Angewandte Chemie International Edition* **2011**, *50*, 6012.

[40] G. Peris, C. E. Jakobsche, S. J. Miller, *Journal of the American Chemical Society* **2007**, *129*, 8710.

[41] H. Wennemers, *Chemical Communications* **2011**, *47*, 12036.

[42] C. E. Müller, L. Wanka, K. Jewell, P. R. Schreiner, *Angewandte Chemie-International Edition* **2008**, *47*, 6180.

[43] C. E. Müller, D. Zell, P. R. Schreiner, *Chemistry-a European Journal* **2009**, *15*, 9647.

[44] R. Hrdina, C. E. Müller, P. R. Schreiner, *Chemical Communications* **2010**, *46*, 2689.

Appendix

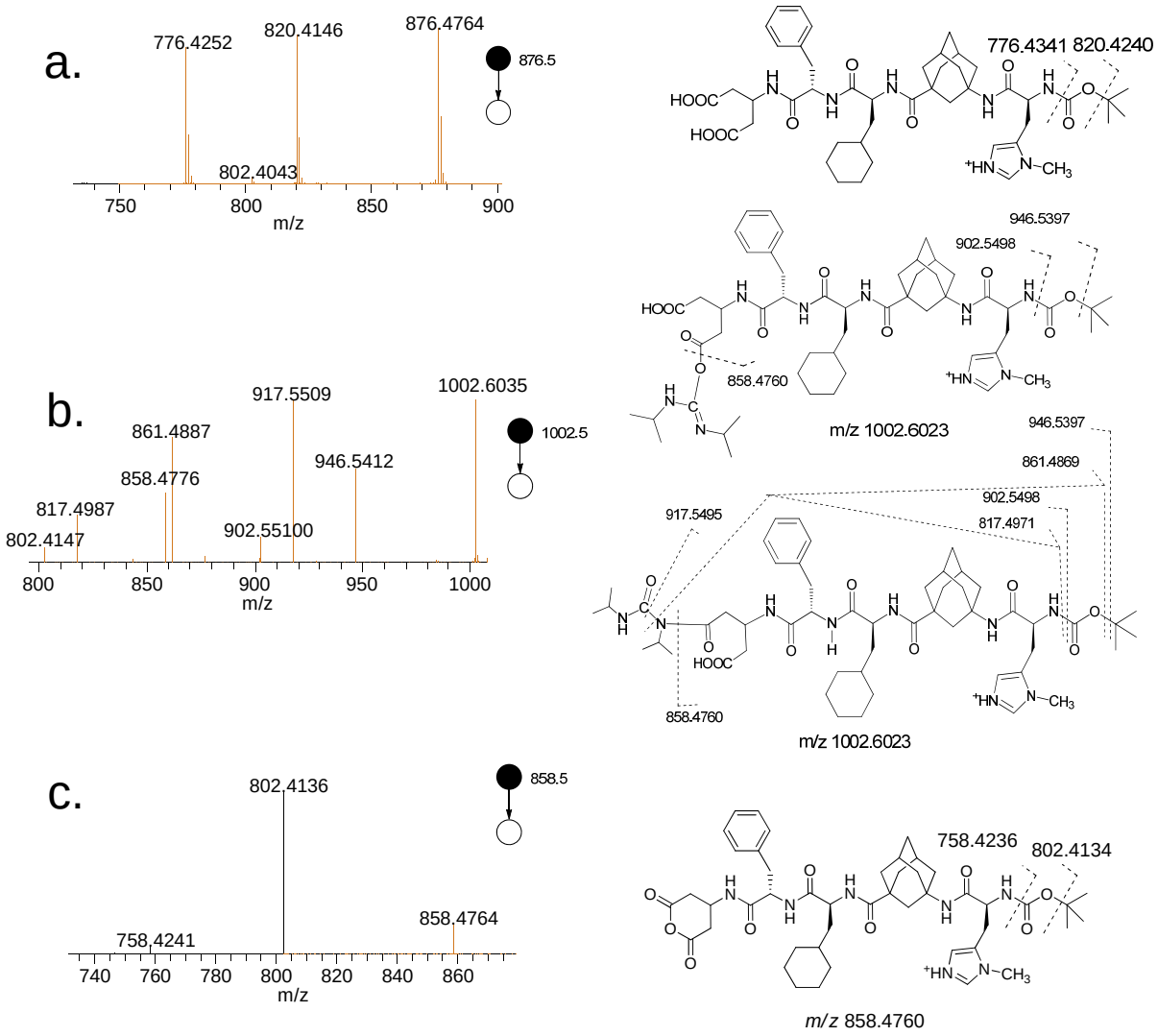

Figure A 4.1 MS/MS spectra of a. catalyst **A0B0,** b. **A1B0** after addition of DIC, and c. **A2B0.** The spectrum of intermediate **A1B0** in b was obtained by using a micro-reactor set-up after 10 min of reaction time.

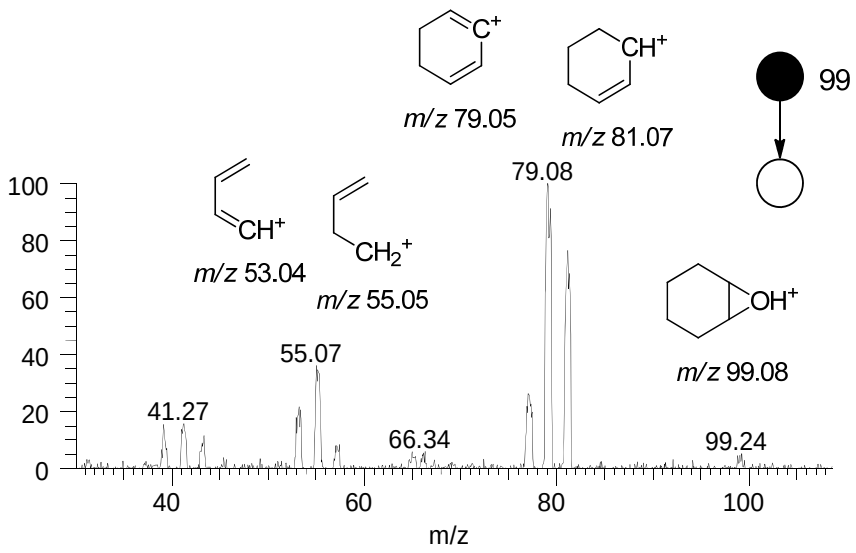

Figure A 4.2 MS/MS spectrum of the formed epoxide **2**.

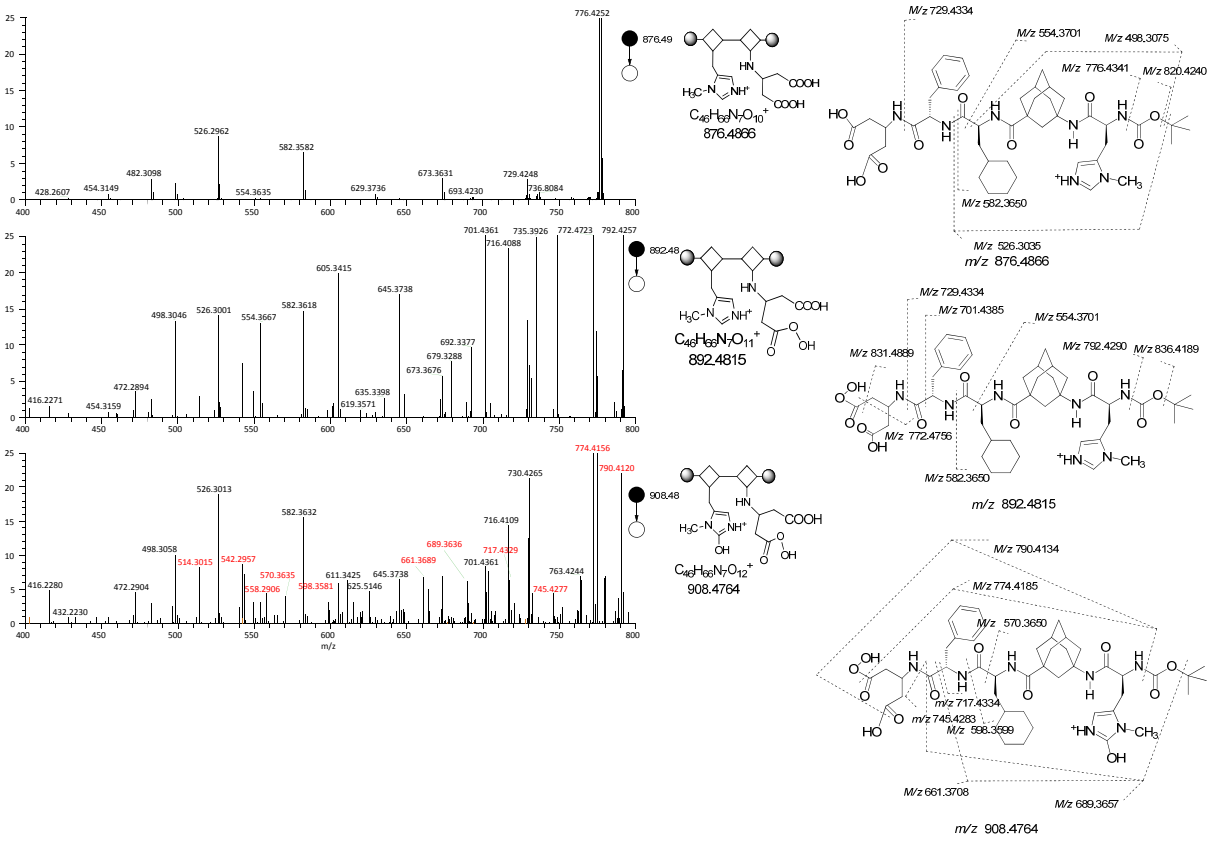

Figure A 4.3 MS/MS spectra of *m/z* 876 (**A0B0**), 892 (**A3B0**), and 908 (**A3B1**), respectively, and their corresponding fragmentation scheme; red numbers indicate the fragments of the oxidized functionality.

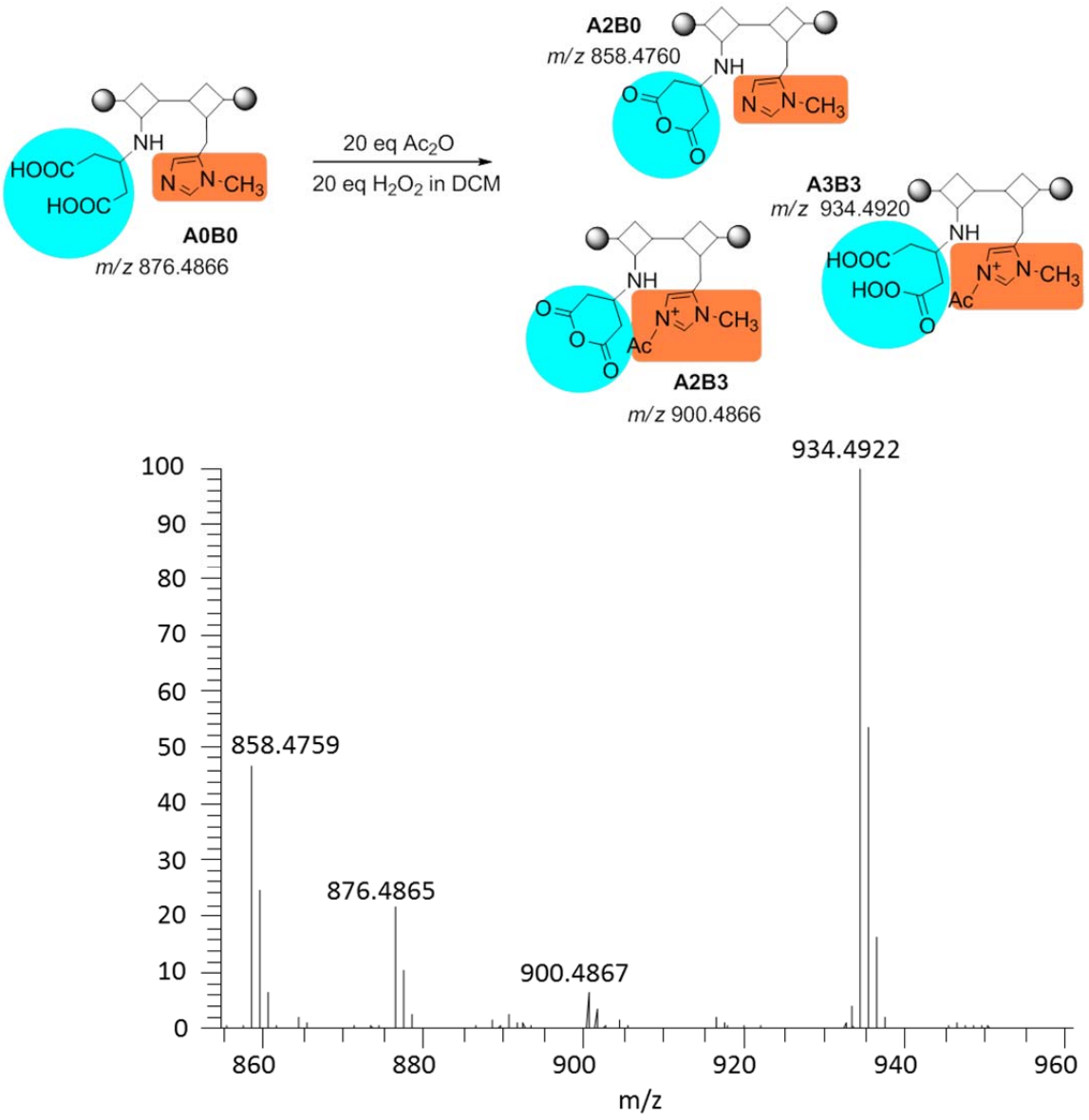

Figure A 4.4 MS spectrum of the catalyst after activation of catalyst **A3B2**.

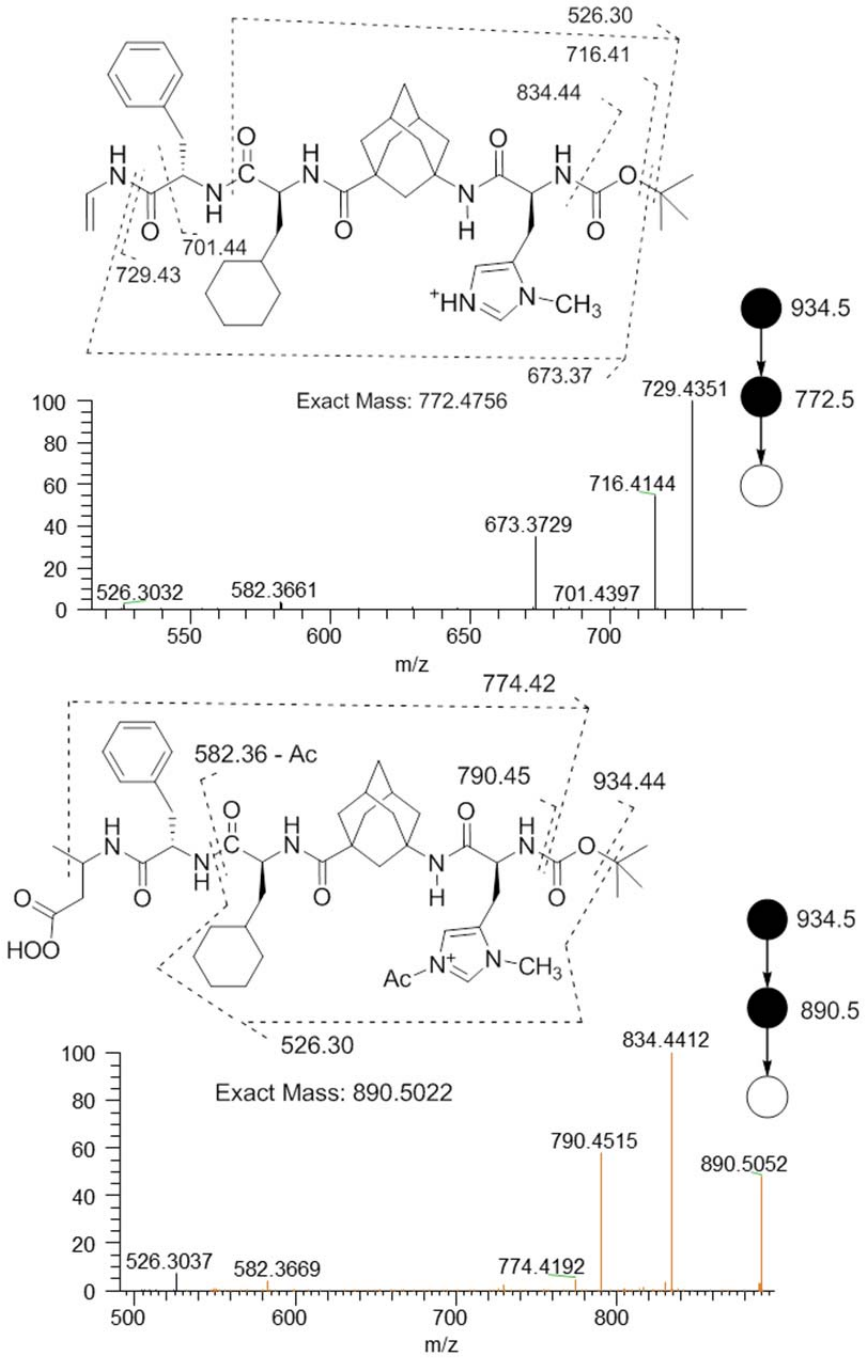

Figure A 4.5 MS^3 spectra of catalyst **A3B2** detailing the fragments that allow a detailed structural characterization of both catalytic moieties.

Micro reactor procedure

Due to the short life time of some intermediates it was not possible to determine them from the reaction mixture alone. Therefore, some additional studies were carried out using an online micro-flow reactor as shown in Figure A4.6. In these experiments two different syringes were filled with different reaction solutions. The reaction takes place after the two flows are combined in a mixing-T. The reaction time depends on the length of the capillary after the mixing-T and can be adjusted to the time frame of interest. This allows studying very reactive and short-lived intermediates. Due to the continuous formation of the same components it is possible to study them in detail by MS and MS/MS methods. One example that could only be investigated by the micro-reactor experiment is the intermediate **A2B0**. For this experiment syringe **I** was filled with catalyst (0.005 mmol, 4.5 mg) in 1 ml DCM, syringe **II** with reagent diisopropyl carbodiimide (DIC) 0.12 mmol (15 mg, 18.7 µL) in 1 ml DCM. The reaction takes place in PEEK (polyetherether ketone) capillary after combining reactants from syringe **I**, **II** in the mixing chamber. Syringe pumps for **I** and **II** have been adjusted to flow rates of 5 µL/min and connected directly to the ion source. It was not just possible to determine the intermediate itself, but also the rearrangement product of this intermediate as fragments at *m/z* 917.54, 861.48 and 817.49, respectively, using tandem MS.

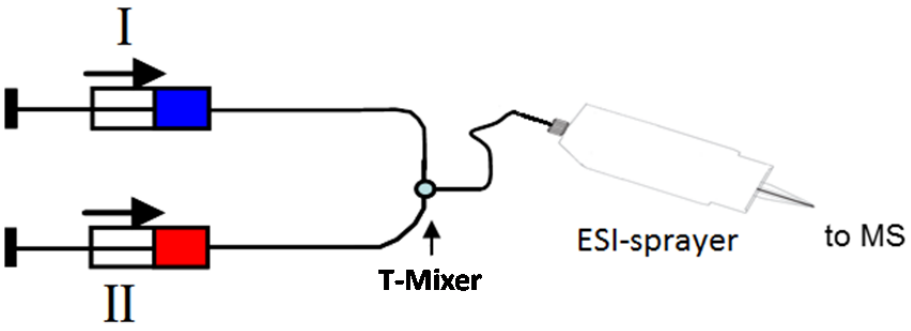

Figure A4.6 Experimental set-up of the micro-flow reactor.

5. Mechanistic characterization of the proline catalyzed aldol reaction: solving a long debate

Redrafted from "*M. Wasim Alachraf, Kristina Zmbansin, Benjamin List, Wolfgang Schrader (will be submitted to J. Am. Chem. Soc.)*"

5.1. Abstract

This work presents a mechanistic investigation of the aldol addition reaction catalyzed by L-proline. The aim of this study was to understand and follow all chemical transformations of this reaction. Additionally to standard ESI-MS(/MS) techniques other more specific techniques such as isotopic labeling, ion/molecule reaction in the collision cell of the MS triple quadrupole analyzer for characterization of the reactive reaction intermediates and the determination of the reaction pathways of the product and side product were applied.

5.2. Introduction and discussion

L-proline catalyzed asymmetric aldol addition reaction is one of the first and typical organocatalytic reactions.[1, 2] This reaction has been discussed for more than 10 years, [3-5] and still some questions are not solved regarding the mechanism of this reaction. The major point is that in addition to the chiral aldol product a condensation product as side-product is formed with relatively high yields thus disturbing the reaction.[6] The formation mechanism of this undesired product is not yet fully understood. For a better understanding of the different reactions it is imminent to characterize the mechanistic relations. The best way to understand mechanisms during such reactions is to follow the formation of intermediates. Here, different methods allow a clean understanding of the reaction pathways although the isolation and characterization of reaction intermediates is not an easy task. Even well-established analytical techniques, such as NMR and IR, experience difficulties due to the low concentrations and short life times exhibited by reaction intermediates. Mass spectrometry, especially when it is connected to soft-ionization methods, like electrospray (ESI-MS),[7,8] is an analytical technique that has rapidly grown in previous years as an important tool in molecular analysis and was successfully applied for the investigation of reaction mechanisms.[9-19] ESI-MS has its strength in the detection of low concentrated components and is able to provide structural information of intermediates by using MS/MS methods, especially when polar components are present. One advantage of ESI-MS for such tasks is the flexibility which also allows for simple combining with additional accessories i.e. time resolved measurement and using a micro reactor for online monitoring.[20-22]

In order to develop a proline-catalyzed direct asymmetric aldol reaction with aliphatic aldehydes, it is necessary to study the mechanisms involved. As a model reaction, the proline catalyzed aldol reaction of acetone with hexanal (Scheme 5.1) was studied. The use of acetone as a solvent suppresses the formation of aldehyde self-aldolization.[23]

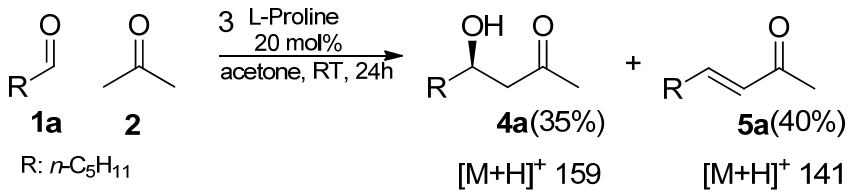

Scheme 5.1 Proline catalyzed aldol reaction of acetone with hexanal.

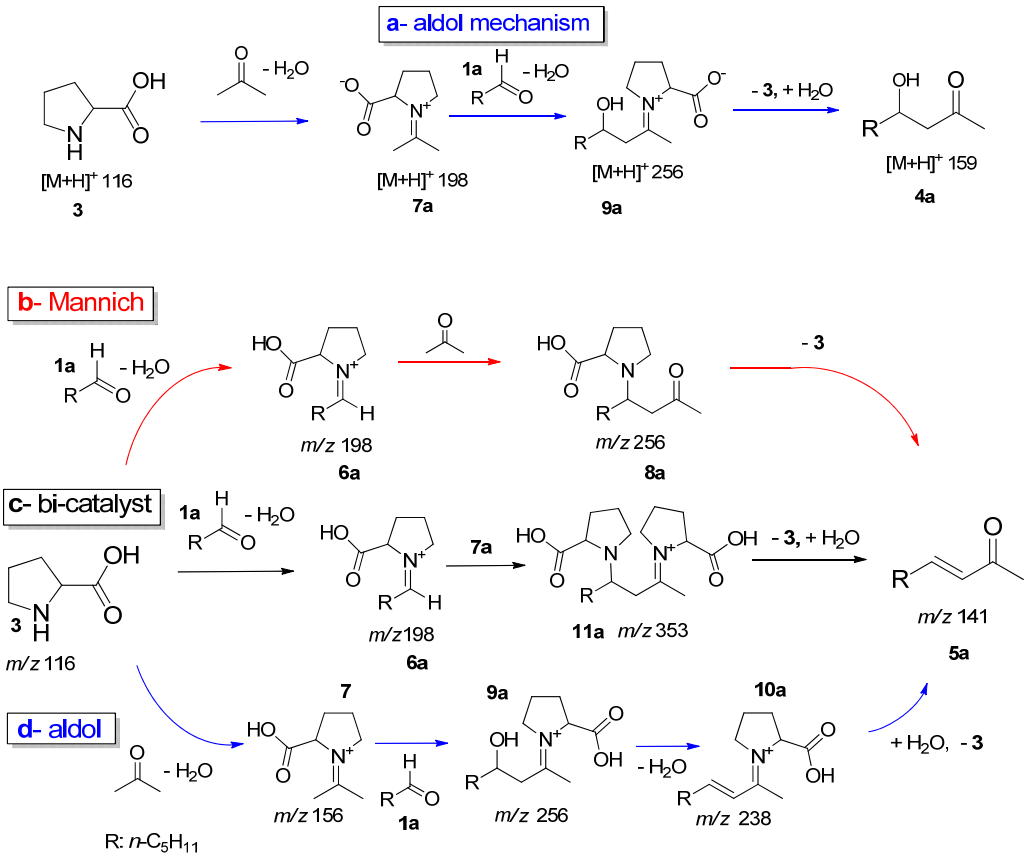

Scheme 5.2 Potential mechanisms for the formation of the product and byproduct.

The major problem of this reaction is long debated as a significant amount of a side product is being formed which mechanistic pathways are not yet fully understood. Even detailed mass spectrometric studies[16] of this reaction only covered the formation of the major product, while the formation of the side product was omitted. Avoiding this condensation product **5a** would allow further developing this reaction. For this understanding of the mechanisms it is essential to understand the formation of intermediates. While the formation of the main product is going through an aldol mechanism the chemical reactivities allow for different pathways to form the condensation product (see Scheme 5.2) with a Mannich and an aldol mechanism the most plausible ones. Additionally, a combination of both mechanisms is a viable chemical alternative and needs to be considered during these studies.

The first experimental approach is to determine the correct reaction markers that allow following the mechanistic formation of the different components. ESI and APCI (atmospheric pressure chemical ionization) were investigated as ionization methods. The results show that ESI is the better method for studying the more polar intermediates, while APCI shows stronger signals from the product ions. Therefore, ESI was primarily used as investigation tool and a typical spectrum obtained after 1.5 h is shown in Figure 5.1a. The high resolution

spectrum shows the major signals of all expected components. In this case the major reaction markers were identified as the protonated Mannich intermediate **8a** and the aldol intermediate **9a** and a very small **10a**.

The spectrum in Figure 5.1a clearly allows concluding that a combination mechanism of both the aldol and the Mannich reaction shown in Scheme 5.2c cannot be observed because a potential intermediate (**11a** at *m/z* 353) is absent.

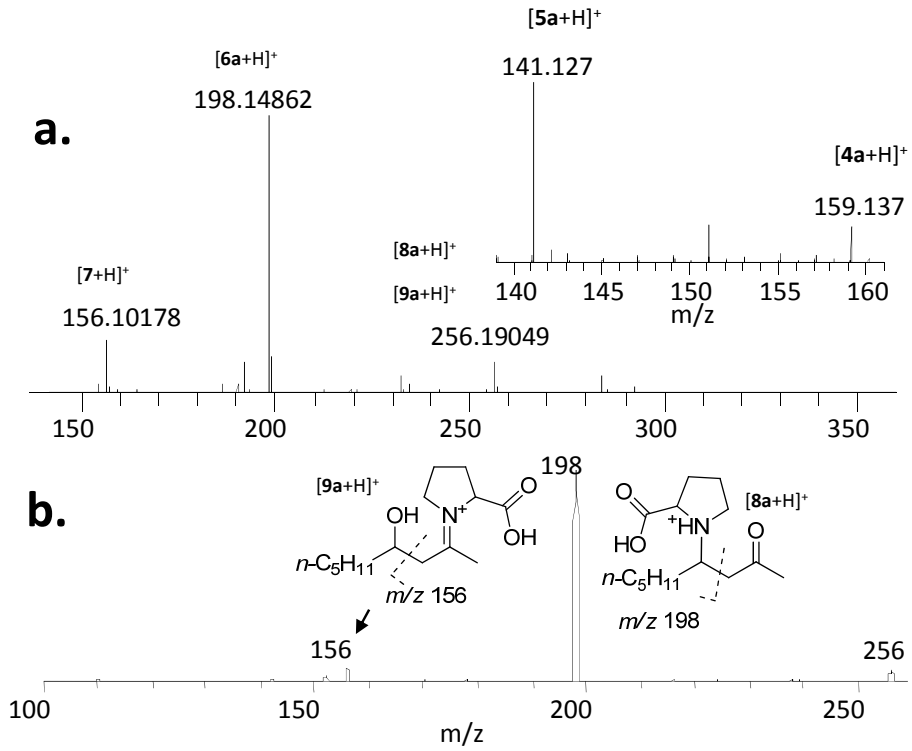

Figure 5.1 a) High resolution ESI(+)-MS spectrum of the proline catalyzed aldol reaction of acetone with hexanal, 1.5 h after the start of the reaction at RT; insert shows the products obtained by using high resolution APCI-MS. **b)** ESI(+)-MS/MS of *m/z* 256 to characterize the intermediates **8a** and **9a** which have the same mass.

This is not the case for the other different intermediates. Unfortunately though, both **8a** and **9a** have the same mass at *m/z* 256. The best way to solve this dilemma is to use ESI-MS/MS to gain structural information about the different intermediates. Figure 5.1b illustrates that the fragmentation of *m/z* 256 yields fragments from both the Mannich and the aldol components. A diagnostic fragment at *m/z* 198 represents the Mannich and a fragment at *m/z* 156 an aldol intermediate, both fragments are being formed after McLafferty rearrangement (for details see Scheme A5.1 in appendix). This example shows that the MS/MS experiment allow differentiating different structural entities that even have the same mass. We know that intermediate **8a** leads only to the side product, now we must further eliminate whether intermediate **9a** can also leads to the side-product **5a** or just to the desired product **4a**.

The intermediate **10a** which is produced from a water elimination of **9a** can be observed at *m/z* 238 albeit in small intensity. The low intensity of this intermediate can have multiple reasons. First of all, the signal can have a small response although this should not be the case due to the fact that the intermediated is present in ionic form and should give a strong signal. Second, this pathway that leads to the formation of **10a** is not a major reaction pathway and therefore the intermediate is just not formed in larger quantities. The third possibility is that the next hydrolysis step that follows the formation of **10a** is a fast and reactive step that quickly consumes **10a** from the reaction solution.

We tried to gain the intermediate **10a** with higher concentration for more investigation. The hydrolysis pathway of **10a** can be reversible, thus, we treated **5a** with L-proline in acetone as solvent (same conditions of the direct reaction) but no significant signals of any intermediates were seen. In opposite we found that using methanol as solvent for the retro-reaction of **5a** with L-proline a high MS signal has been observed of **10a** at *m/z* 238.

As a result, deuterated methanol was used as solvent for the retro-reaction of **5a** with L-proline **3** to identify the hydrolysis rate of the intermediate **10a** by MS**.** This intermediate suffers deuterium exchange and will later be mirrored in the condensation production as Scheme 5.3 illustrates.

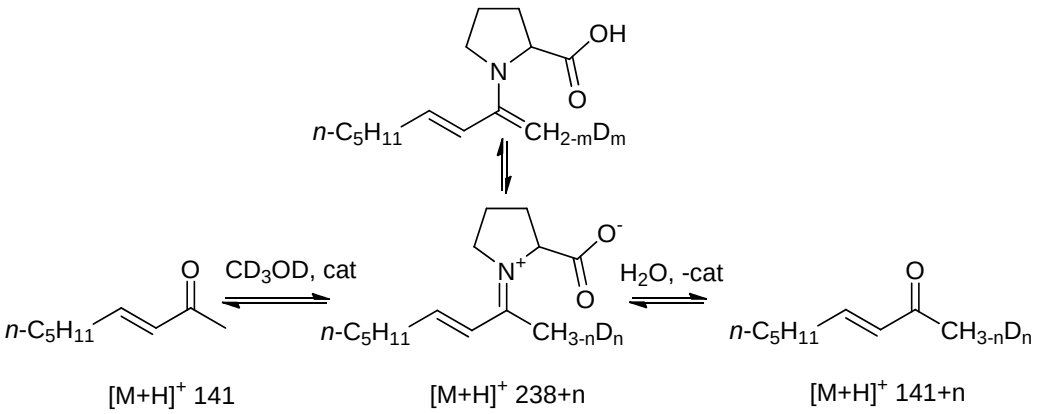

Scheme 5.3 Deuterium exchange reaction via retro-reaction of condensation product **5a** with L-proline **3** in deuterated methanol.

As it is shown in Figure 5.2, the deuterium exchange rate of condensation product **5a** (*m/z* 141 to *m/z* 144) in the retro-reaction using deuterated methanol is very slow, that after 23h less than 20 % has been converted. That means that the hydrolysis rate of **10a** is very low, thus **10a** is not capable of being an intermediate for the aldol condensation product **5a**.

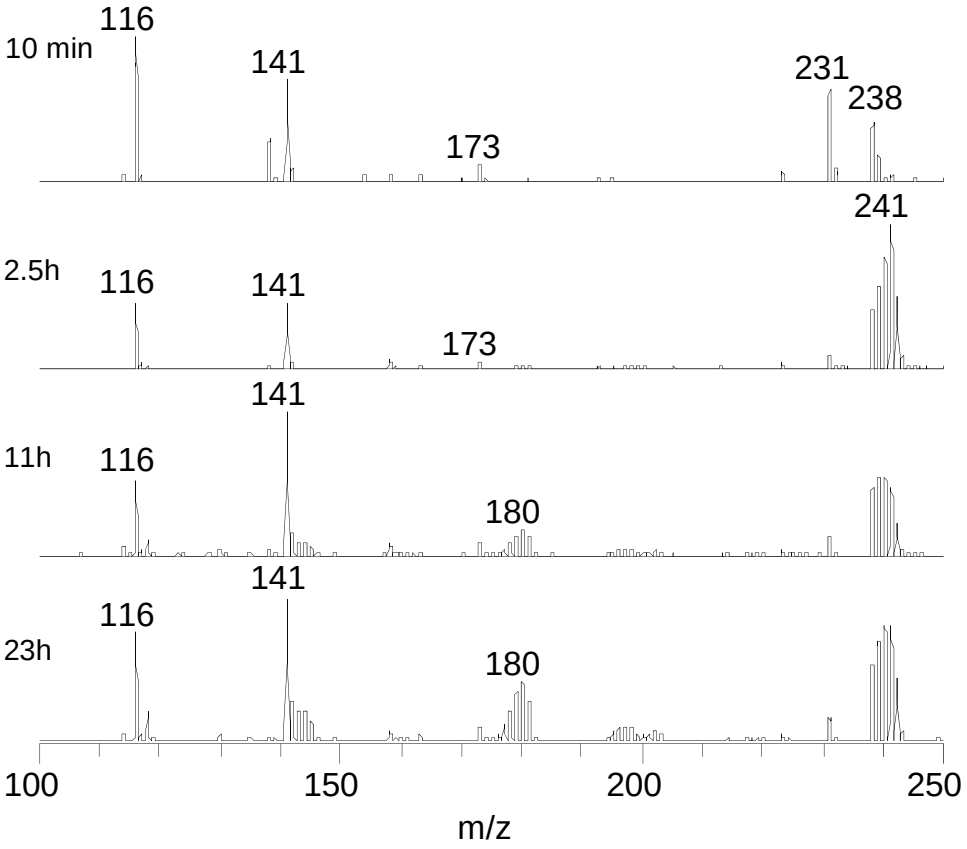

Figure 5.2 ESI(+)-MS spectrum of the retro-reaction of **5a** with L-proline **3** in deuterated methanol in course of time. The deuterium exchange rate of **5a** (*m/z* 141) indicates the activity of intermediate **10a** (*m/z* 238).

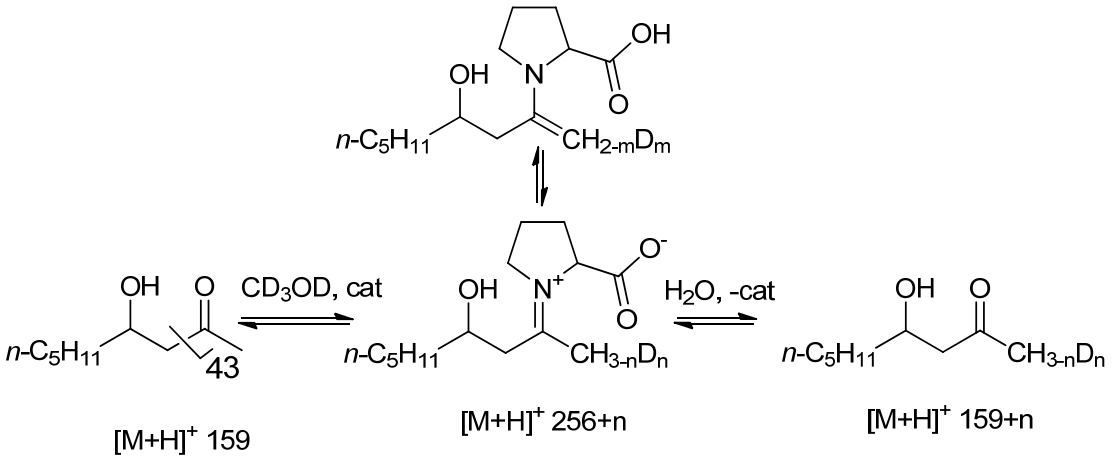

Scheme 5.4 Deuterium exchange reaction via retro-reaction of condensation product **5a** with L-proline **3** in deuterated methanol.

The same reaction was repeated using **4a** as starting material in deuterated methanol. The results show that the deuterium exchange rate was faster than in the previous reaction as 50% had been converted after 11h, confirming the high reactivity of intermediate **9a** in regard to forming **4a** (Figure 5.3). (See Figure A5.1 in appendix for the ESI(+)-MS/MS of the deuterium exchanged addition product **4a** confirming the position of the deuterium exchange

from the alpha methyl group to the carbonyl group) . It has to be noted that in this experiment the intermediate **10a** *m/z* at 238 and condensation product **5a** at *m/z* 141 are detectable with their corresponding deuterium exchanged derivatives. We think that this occurs because of the water elimination in the gas phase of **9a** and **4a** during the MS measurement. NMR experiment was completed for the same aldol addition product **4a** with L-proline and deuterated methanol, showing no significant changes occur over time (Figure 5.4). This confirms that the **10a** and **5a** signals in Figure 5.3 are no more than gas phase water elimination during the MS measurement.

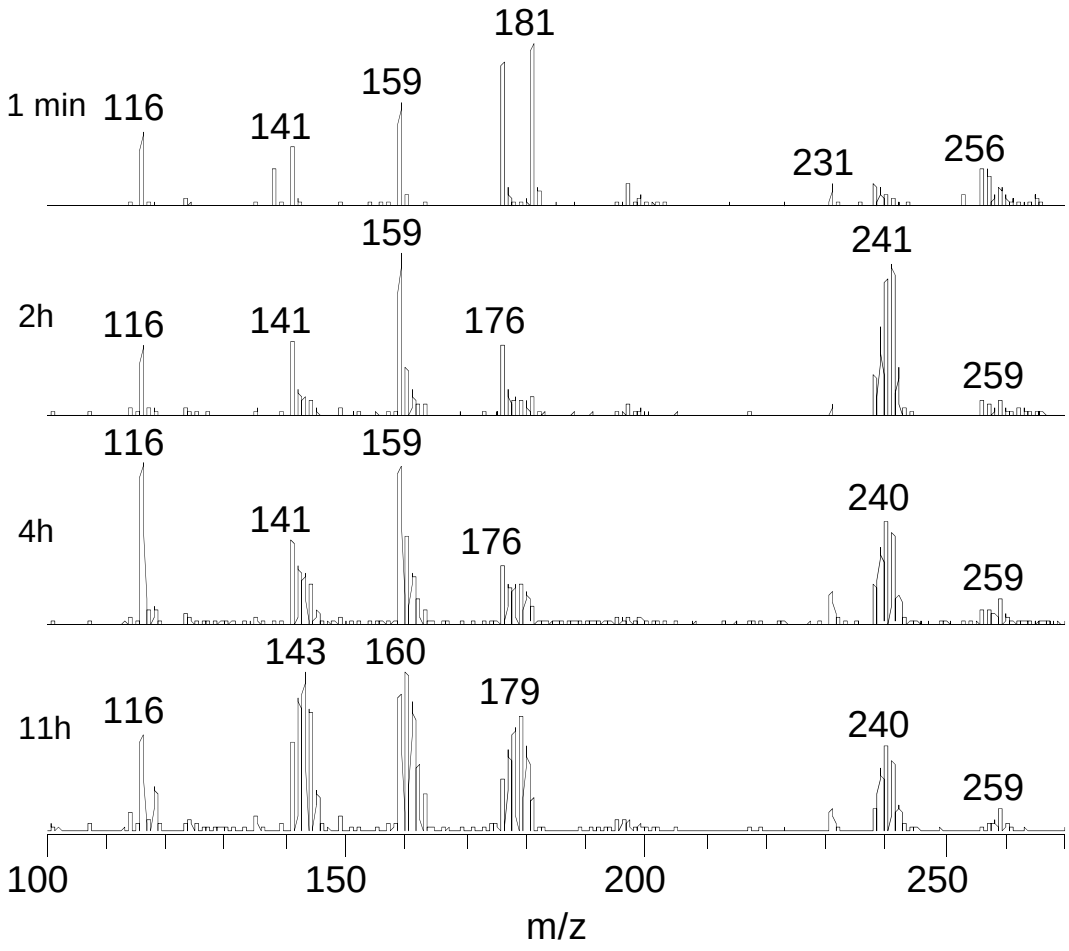

Figure 5.3 ESI(+)-MS spectrum of the retro-reaction of **4a** with L-proline in deuterated methanol in course of time.

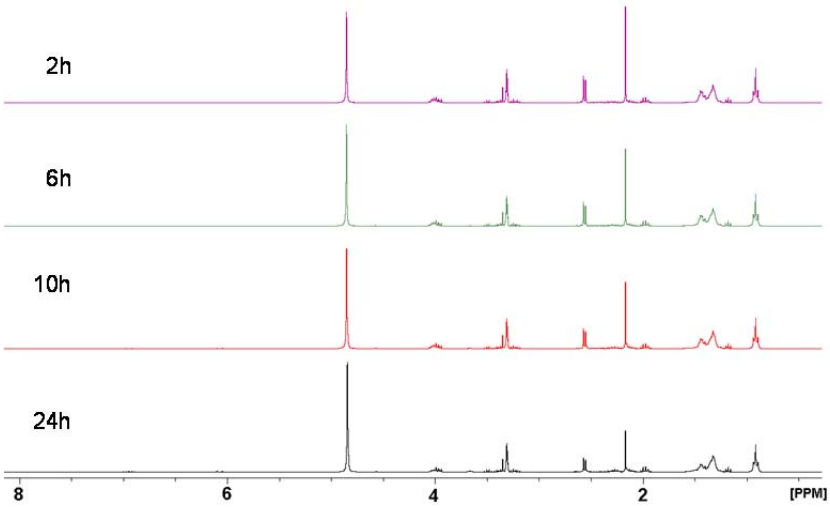

Figure 5.4 NMR spectra of retro-reaction of **4a** with L-proline **3** in deuterated methanol at 2, 6, 10 and 24h.

In the end this means that the Mannich mechanism leads to the formation pathway of the condensation product **5a** through intermediates **6a**, **8a**. On the other hand aldol pathway leads to the desired product **4a** by intermediates **7** and **9a** (Scheme5.5).

In conclusion, we have successfully detected all potential intermediates of the proline catalyze aldol reaction, characterized the important reaction markers responsible for the formation of both products and were able to determinate the mechanistic pathways for the aldol reaction of beta-hydroxycompounds. The formation of both the addition and the condensation product is being characterized and the direct pathways were defined. Additionally, the relative rates of the defining steps were identified and the catalytic cycle is shown in Scheme 5.6.

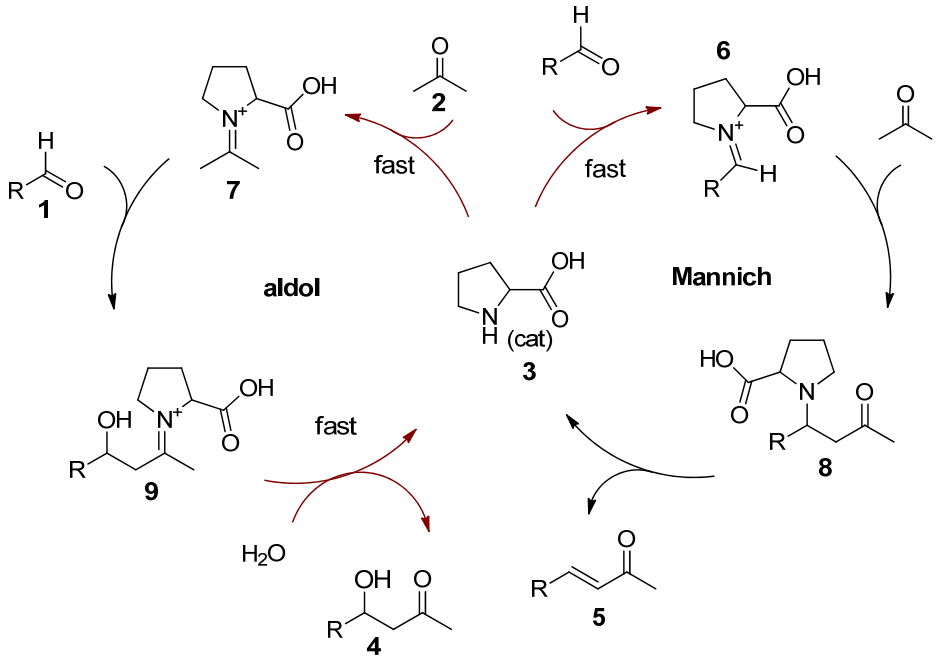

Scheme 5.5 The proposed catalytic cycle for the L-Proline catalyzed aldol reaction of acetone with hexanal.

References

[1] Z. G. Hajos, D. R. Parrish, *Journal of Organic Chemistry* **1974**, *39*, 1615.

[2] U. Eder, G. Sauer, R. Weichert, *Angewandte Chemie-International Edition* **1971**, *10*, 496.

[3] B. List, L. Hoang, H. J. Martin, *Proceedings of the National Academy of Sciences of the United States of America* **2004**, *101*, 5839.

[4] M. B. Schmid, K. Zeitler, R. M. Gschwind, *Journal of the American Chemical Society* **2011**, *133*, 7065.

[5] M. B. Schmid, K. Zeitler, R. M. Gschwind, *Angewandte Chemie International Edition* **2010**, *49*, 4997.

[6] G. Szöllősi, G. London, L. Baláspiri, C. Somlai, M. Bartók, *Chirality* **2003**, *15*, S90.

[7] J. B. Fenn, M. Mann, C. K. Meng, S. F. Wong, C. M. Whitehouse, *Science* **1989**, *246*, 64.

[8] C. M. Whitehouse, R. N. Dreyer, M. Yamashita, J. B. Fenn, *Analytical Chemistry* **1985**, *57*, 675.

[9] A. O. Aliprantis, J. W. Canary, *Journal of the American Chemical Society* **1994**, *116*, 6985.

[10] C. Adlhart, C. Hinderling, H. Baumann, P. Chen, *Journal of the American Chemical Society* **2000**, *122*, 8204.

[11] J. Griep-Raming, S. Meyer, T. Bruhn, J. O. Metzger, *Angewandte Chemie-International Edition* **2002**, *41*, 2738.

[12] S. Meyer, R. Koch, J. O. Metzger, *Angewandte Chemie-International Edition* **2003**, *42*, 4700.

[13] L. S. Santos, C. H. Pavam, W. P. Almeida, F. Coelho, M. N. Eberlin, *Angewandte Chemie-International Edition* **2004**, *43*, 4330.

[14] A. A. Sabino, A. H. L. Machado, C. R. D. Correia, M. N. Eberlin, *Angewandte Chemie-International Edition* **2004**, *43*, 2514.

[15] L. S. Santos, L. Knaack, J. O. Metzger, *International Journal of Mass Spectrometry* **2005**, *246*, 84.

[16] C. Marquez, J. O. Metzger, *Chemical Communications* **2006**, 1539.

[17] C. A. Marquez, F. Fabbretti, J. O. Metzger, *Angewandte Chemie-International Edition* **2007**, *46*, 6915.

[18] C. D. F. Milagre, H. M. S. Milagre, L. S. Santos, M. L. A. Lopes, P. J. S. Moran, M. N. Eberlin, J. A. R. Rodrigues, *Journal of Mass Spectrometry* **2007**, *42*, 1287.

[19] L. S. Santos, *European Journal of Organic Chemistry* **2008**, 235.

[20] M. W. Alachraf, P. P. Handayani, M. R. M. Huettl, C. Grondal, D. Enders, W. Schrader, *Organic & Biomolecular Chemistry* **2011**, *9*, 1047.

[21] W. Schrader, P. P. Handayani, C. Burstein, F. Glorius, *Chemical Communications* **2007**, 716.

[22] W. Schrader, P. P. Handayani, J. Zhou, B. List, *Angewandte Chemie-International Edition* **2009**, *48*, 1463.

[23] B. List, P. Pojarliev, C. Castello, *Organic Letters* **2001**, *3*, 573.

[24] G. Szöllősi, G. London, L. Baláspiri, C. Somlai, M. Bartók, *Chirality* **2003**, *15*, S90.

Appendix

Instrumental

ESI-MS and APCI-MS data were acquired using a Thermo TSQ Quantum Ultra AM triple quadrupole mass spectrometer (Thero Scientific, Dreieich, Germany) equipped with an APCI and an ESI source which were controlled by Xcalibur software. The ESI spray voltages were set to 4000 V and 3000 V for positive and negative ions, respectively. The heated capillary temperature was adjusted to 270°C. For MS/MS analysis, the collision energy was increased from 10 eV to 50 eV. The mass spectrometer was operated in the Q1 scan and product ion scan modes, with the mass width for Q1 set at 0.5 Da and for Q3 set at 0.7 Da. The collision cell, Q2, contained argon and was adjusted to a pressure of 1.5 mTorr to induce CID. Spectra were collected by averaging 10 scans with a scan time of 1 s. The Mass range was adjusted between 50 and 1500 Da. APCI-MS measurement were acquired with vaporizer temp set at 50 °C. Although usually higher temperature is used for APCI measurements, in this case a decrease in intensity of **4a** due to water elimination in the gas phase made it necessary to reduce the temperature. Source current was set to 4 μA.
High resolution MS data were aqcuirred using an LTQ-Orbitrap Elite mass spectrometer (Thero Scientific, Bremen, Germany). All experimental parameters were the same as for the triple quadrupole experiments, except that MS/MS measurements were carried out with an isolation window of 1 Da and different collision energies.

Synthesis

0.05 mmol (20 mol%) L-proline were added to a mixture of 0.25 mmol hexanal in 2.5 mL acetone. The reaction mixtures were stirred at room temperature for 16–24 h. The analyte was taken directly from the reaction flask and was diluted in methanol (1 : 100) before entry to the ESI source at a flow rate of 10 μL min^{-1}.The investigation was carried out by monitoring the reaction at specified intervals through ESI-MS. The reaction intermediates that appeared during the reaction were intercepted, detected and characterized with ESI-MS. MS/MS experiments were performed for structural confirmation using the product ion scan with the collision energy ranging from 10 to 50 eV, depending on the dissociation lability of the precursor ion.

Retro-reactions

0.05 mmol (20 mol%) L-proline was added to a mixture of 0.25 mmol **4a**, **5a** respectively in 2.5 mL 4d-methanol and stirred at room temperature. 5 µL of reaction mixture are diluted in 1 mL of dichloromethane for ESI-MS measurement. Samples were taken and measured in course of time.

Fragmentation

To deterime the position of the deuterium exchange in product **4a** MS/MS measurements were carried out for each isotopic signal from *m/z* 159-162 (**4a**+nD).

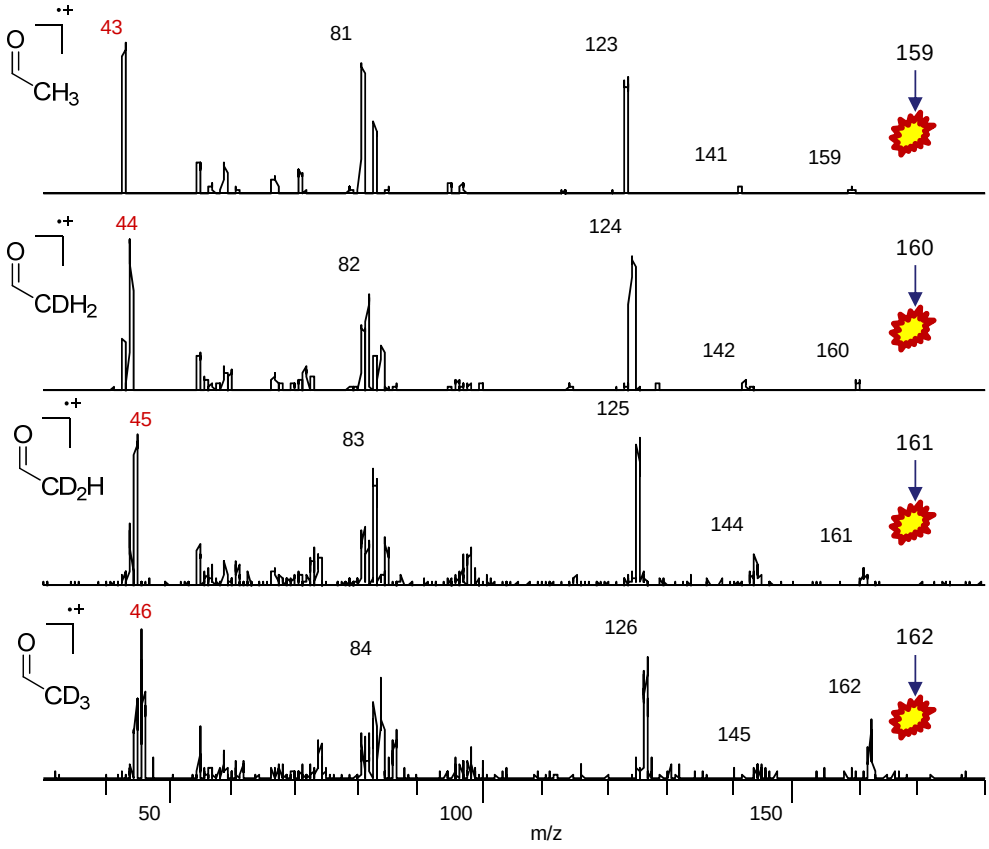

Figure A 5.1 ESI(+)-MS/MS spectrum of the deuterium exchanged derivatives of addition product **4a** to determine the position of deuterium exchange.

The isotopic signals (**4a**+nD) were isolated isopically clean with isolation windows of 1 Da which excludes the neighboring isotopic signal. The CID energy of fragmentation was the same for all signals 25 eV.

According to the fragmentation shown in Scheme 5.4 the acetyl-fragment is a major fragment of **4a**. When now the deuteration takes place the *m/z* value is increasing due to H/D exchange. Figure A5.1 illustrates the shift of the acetyl-fragment from *m/z* 43 to *m/z* 44 and above for

each different isotopic precursor ion when this is shifted from *m/z* 159 up to *m/z* 162 indicating that the deuterium exchange occurs at the acetyl side chain of **4a**.

McLafferty rearrangement

As described in the text, the intermediate **8a** and **9a** undergo a McLafferty rearrangement during fragmentation experiments. The mechanism for this is shown in Scheme A5.1.

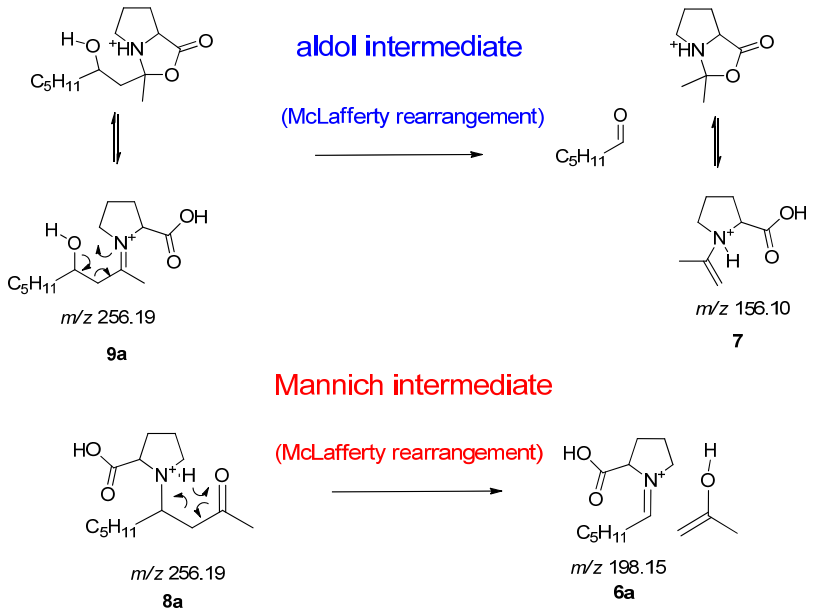

Scheme A 5.1 Proposed fragmentation of intermediates **8a** and **9a** by McLafferty rearrangement.

Additional reactions

In addition to the standard reaction describe in the main text, different reactions were carried out to fully investigate the reaction.

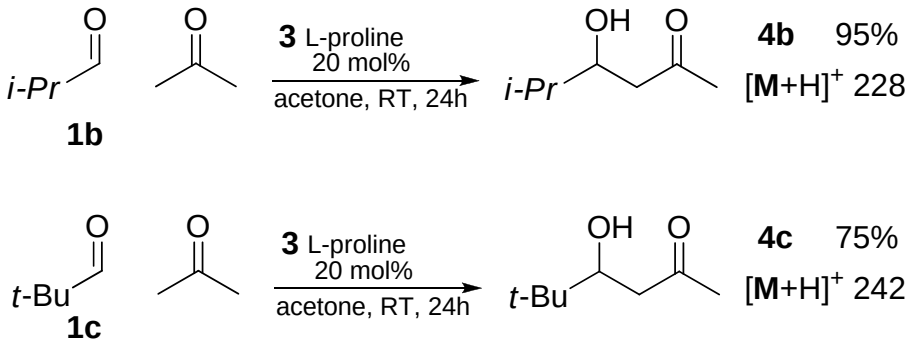

Scheme A 5.2 Proline catalyzed aldol reaction of acetone with isobutyraldehyde **1b** or pivalaldehyde **1c.**

When isobutyraldehyde **1b** or pivalaldehyde **1c** were used instead of hexanal **1a,** as shown in Scheme A5.2**,** a higher selectivity of the corresponding addition product **4b, 4c** was found**.**[24] In fact, a yield of 95% for **1b** and 75% for **1c** were found as opposed for a yield of 35% when using **1a**. While the diagnostic fragments indicating the aldol reactions at *m/z* 156, the corresponding fragment for the Mannich reaction appears at *m/z* 170 and 184 for the reactions 2 and 3, respectively. As expected, a higher ratio of the diagnostic fragment of aldol intermediate **9b, 9c** at *m/z* 156 for the Mannich intermediate fragment **8b** at *m/z* 170 and **8c** with *m/z* 184 was found using ESI(+)MS/MS, when compared to that of the hexanal reaction (Figure A5.3). This confirms the results described in the main text, that the Mannich intermediate is responsible for the condensation product and the aldol intermediate is responsible for the addition product.

Figure A5.3 shows the relative intensities of the parent ion obtained by ESI(+)-MS at *m/z* 256 and its fragments obtained via ESI(+)MS/MS at *m/z* 156 and 198 at CID 20 eV at various reaction times.

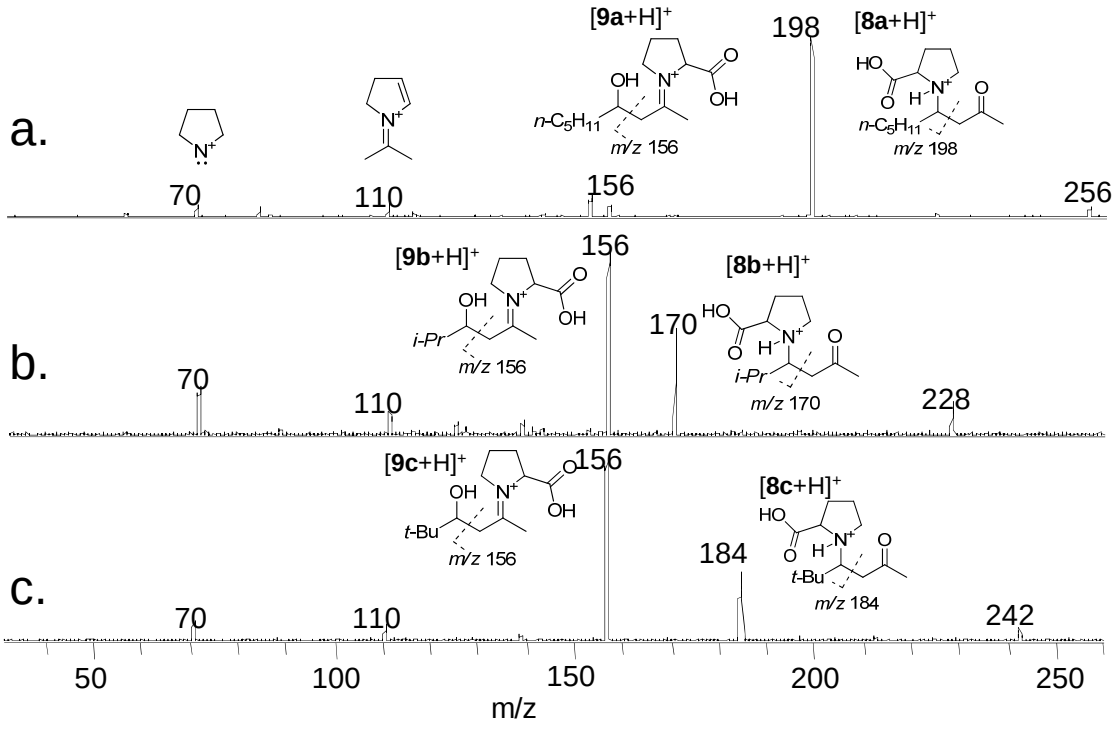

Figure A 5.2 a) ESI(+)-MS/MS of *m/z* 256 of proline catalyzed aldol reaction of acetone with hexanal **1a. b)** ESI(+)-MS/MS of *m/z* 228 of proline catalyzed aldol reaction of acetone with isobutyraldehyde **1b. c)** ESI(+)-MS/MS of *m/z* 242 of proline catalyzed aldol reaction of acetone with pivalaldehyde **1c**. (CID 20 eV for both).

Time dependent studies of intermediates 8a and 9a

Time dependent studies about the formation behavior of both intermediates **8a** and **9a** show that the increase of the parent ion at *m/z* 256 is due to an increase of **8a** which corresponds to the formation of the Mannich intermediates while the aldol intermediate remains constant (see Figure A5.2).

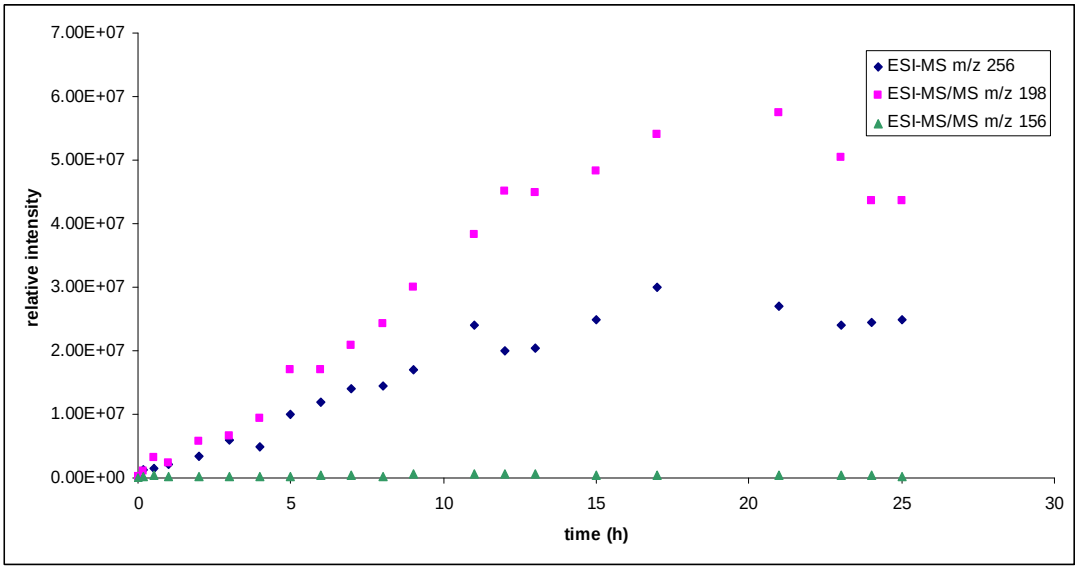

Figure A 5.3 The relative intensities of the parent ion obtained via ESI(+)-MS at *m/z* 256 and its fragments obtained via ESI(+)MS/MS at *m/z* 156 and *m/z* 198 at CID 20 eV at different reaction Times.

Exclusion of gas phase activities

Because the Mannich intermediates **8a** is the addition of **6a** with acetone that could also have happened in the gas-phase instead of the liquid phase, an additional experiment was carried out to exclude the gas phase adduct building of Mannich intermediate **8a**.

Scheme A5.3. Investigation of adduct formation in the gas-phase by adding ^{18}O-labeled acetone to the diluted measurement sample

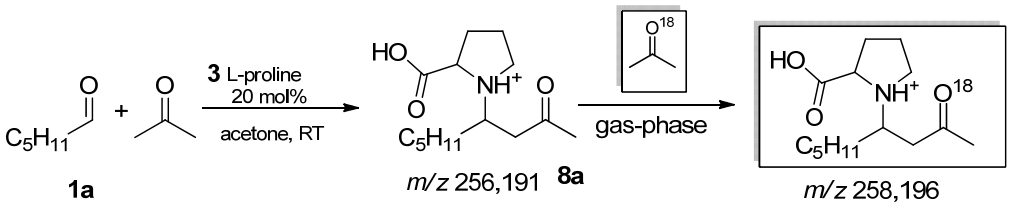

Scheme A 5.3 Investigation of adduct formation of intermediate **8a** in the gas-phase by adding ^{18}O-labeled acetone to the diluted measured sample.

A sample of 5 µL of the reaction mixture was diluted with 1 mL dichloromethane and mixed with 5 µL ^{18}O-labeled acetone and measured with ESI-MS. No signal found at *m/z* 258 which mean the Mannich intermediate **8a** not formd in the gas phase but is in the reaction mixture Figure A5.4.

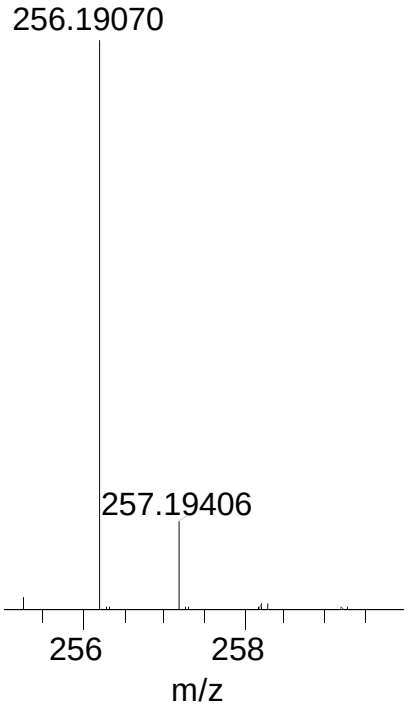

Figure A 5.4 High resolution ESI(+)-MS spectrum of reaction solution investigating potential gas-phase reactivities; signal at *m/z* 256 indicates that no ^{18}O was involved, indicating that no gas-phase reactivities were found.

6. Mass spectrometric studies of an organocatalyzed bi-mechanistic aldol condensation reaction

Redrafted from "*M. Wasim Alachraf, Kristina Zmbansin, Benjamin List, Wolfgang Schrader (will be submitted to J. Mass Spectrom.*)"

6.1. Abstract

A unique organocatalyic aldol reaction was studied in detail using different mass spectrometric techniques to analyze the mechanism and the formation pathways. In this aldol condensation reaction acetone reacts with different aromatic aldehydes catalyzed by a new organcatalyst, morpholinium-trifluoroacetate. It was possible to determine the reaction markers for this reaction by ESI(+)-MS and ESI(+)-MS/MS. Different techniques have been used, such as online, offline monitoring and isotopic labeling with regard to detailed investigation of the catalytic mechanism, as well as the activity of the major intermediates. The results indicate that the reaction pathway can allow two different routes. This is an example of a reaction that in the end depending on the reaction condition is following two different pathways, therefore it is a bi-mechanistic reaction.

6.2. Introduction

In the last few years, organocatalysis has emerged as a new catalytic method based on metal-free organic molecules for the synthesis of chiral compounds.[1-4] Despite the first research reported of this type of reaction in the form of a proline catalyzed interamolecular asymetic aldol reaction in the early 1970s,[5, 6] the real breakthrough of this method began in the late 1990s with the work from List and Barbas who opened a concept for a number of related transformations such as the enantioselective intermolecular cross-aldol reactions, as well as Mannich, Michael and Diels–Alder-type transformations, and the application of these transformations in multistep (domino) reactions.[7, 8]
These catalysts have many advantages, such as low price, non-toxicity and the ability to work under mild conditions compared to the classical asymmetric catalysis such as metal-containing complexes or enzymes.[9, 10]

Organocatalysis is one of the fastest growing fields in synthetic chemistry and important discoveries have been made. Not all of them are yet fully understood, because mechanistic information is still lacking. Here, studies implementing different mass spectrometric methods have been carried out to help define formation pathways of a complex and difficult organocatalytic reaction.
In the last years electrospray ionisation mass spectrometry (ESI-MS) has developed into the method of choice for the analysis of rapid and complex catalytic reactions.[11-13] The main advantage of this technique is its ability to transfer starting materials, intermediates and products softly, selectively and very sensitively from reaction solution to the gas phase in ionic form. In order to measure their masses and illustrate their structure MS/MS and MS^n techniques are important tools because they allow to gain information about structural changes in chemical reactions. A lot of mechanistic studies in chemistry have been carried out in the last few years using ESI-MS to investigate chemical reactions in the gas phase[14, 15] or in the solution[16-19]. In principle, there are two different methods to study a reaction using atmospheric pressure ionization MS (API-MS): offline and online screenings. For offline screening, the reaction reagents are mixed to produce the different intermediates, products and by-products which determined overtime as the reactants are progressively transformed into products.[20] The limitation of this technique is that it requires intermediates to have a reasonable concentration and enough life-time before degradation can be detected. In online-monitoring, it is possible to study the kinetic and mechanistic information about the reactions

in solution by using reactors coupled to the ion source.[21] The main advantage of this technique is the ability to detect reaction intermediates which have very short life-times, by using a mixing -T, which combines the different solutions of the reactants continuously and direct them to the ion source.[22] The reactivity of the reaction markers can be further investigated using ESI-MS/MS experiments via gas phase ion/ molecule reaction in the collision cell.[22]

The formation of C-C bonds is of vital importance in organic synthesis because it allows construction of large molecules from smaller ones. Aldol condensation reaction is a classical reaction that allows two carbonyl compounds to form new carbon-carbon double bonds.[23] The mechanism of this kind of reactions catalyzed with secondary amine-based organocatalysts has been widely studied.[24-26] The usual accepted mechanism is the aldol pathway where the ketone reacts with the catalyst to form an enamine intermediate which reacts further with the aldehyde to from a second adduct intermediate and in the end the product. Another mechanistic pathway has been investigated for similar reactions. Millagre et al[27] reported a study of the mechanism of direct Mannich-type α-methylenation of ketoesters via electrospray ionization mass spectrometry. Ketoesters were treated with formaldehyde/acetic acid solution and morpholine was utilized as a catalyst. Then the reaction was monitored via ESI-MS(/MS) experiments. They figured out that the reaction key for the mechanism cycle of this reaction is the formation of iminium cation from formaldehyde and morpholine which attacks the ketoester (Mannich pathway), but not the intermediate which form from the catalyst and the ketoester (aldol pathway).

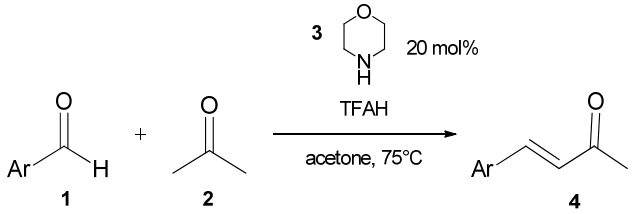

Scheme 6.1 Aldol condensation reaction catalysed by organocatalysis by morpholinium trifluro acetate **3**.

The aim of this study was the investigation of an organocatalytic aldol condensation reaction between acetone and aromatic aldehyde catalysed by morpholinium trifluro acetate **3** as previously reported by List[28] (see Scheme **6.**1). It is necessary to observe the fast changes and the formation of the low concentrated intermediate components to understand the mechanism of such reactions where the catalyst **3** is able to react with both starting materials (acetone and aromatic aldehyde) in the same time.

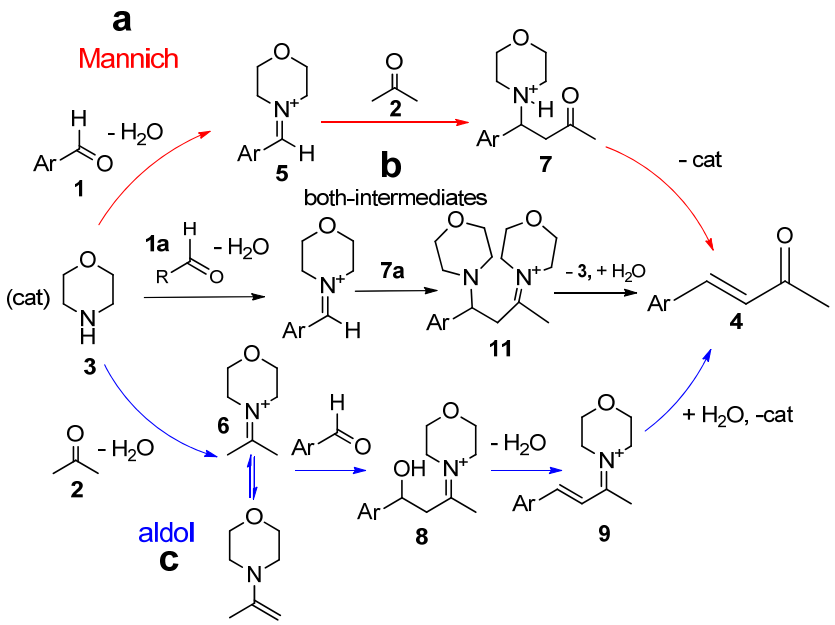

Scheme 6.2 Potential mechanisms of the reaction.

There are three different potential pathways for this reaction as described in Scheme 6.2. The first potential pathway is following a Mannich mechanism. In this pathway the catalyst **3** react first with the carbonyl group of aldehyde **1** to form an iminium cation intermediate **5**, followed by creation of intermediate **7** by attack of acetone molecule on intermediate **5**. The last step is the elimination of catalyst **3** and creation of final product **4**. The other potential pathway is following an aldol mechanism. In this pathway the catalyst **3** reacts first with the acetone molecule to form an enamine intermediate **6**. This intermediate attacks the aldehyde and forms **8**, afterwards water elimination takes place and **9** is created. Finally, after hydrolyzation of **9** the endproduct **4** is being formed**.** It has to be noted that the intermediate **7** of Mannich pathway and **8** of aldol pathway have the same exact mass and elemental composition and therefore, it is a challenging to characterize and differentiate them by using mass spectrometry. The last potential mechanism is a combination of the previous two mechanisms. In this pathway the intermediate **5** of Mannich pathway is attaced by aldol intermediate **6** to from intermediate **11** where two catalyst molecules are involved. Intermediate **11** subsequently produce the final product after a hydrolysis and splitting of catalyst.

6.3. Experimental

6.3.1. Mass spectrometry

MS and MS/MS experiments were done using a Thermo TSQ Quantum Ultra AM triple quadrupole mass spectrometer (Thero Scientific, Dreieich, Germany) equipped with an ESI source which was controlled by Xcalibur software. The ESI spray voltages were set to 4000 V and 3000 V for positive and negative ions, respectively. The heated capillary temperature was adjusted to 270 °C. For MS/MS analysis, the collision energy was increased in steps from 10 eV to 50 eV. The mass spectrometer was operated in the Q1 scan and product ion scan modes, with the mass width for Q1 set at 0.5 Da and for Q3 at 0.7 Da. The collision cell, Q2, contained argon and was adjusted to a pressure of 1.5 mTorr to induce CID. Spectra were collected by averaging 10 scans with a scan time of 1 s. The Mass range was adjusted between 50 and 1500 Da.

High resolution MS data were acquired using a research-type LTQ-Orbitrap Elite mass spectrometer (Thermo Scientific, Bremen, Germany). All experimental parameters were the same as for the triple quadrupole experiments, except that MS/MS measurements were carried out with an isolation window of 1 Da and at different collision energies.

6.3.2. Reaction

For a better understanding of the reaction and to study the influence of substitutions on the aromatic aldehydes, different aromatic aldehydes have been used which leads to changes in the mass spectral fingerprint (Table 6.1 shows the used aromatic aldehydes). The aromatic aldehyde **1** (**1a, 1b, 1c**) (5 mmol) was dissolved in acetone (12.5 mL). To this solution catalyst morpholinium trifluoroacetate **3** (20 mol%) was added. The reaction mixture was stirred at 75 °C in a sealed vial for 24 h. Samples were taken from the reaction mixture in the course of time for measuring by electrospray mass spectrometry (ESI-MS) after dilution with methanol (1:250).

Table 6.1 morpholinium- trifluoroacetate-catalyzed aldol condensation reaction.

Entry	aldehyde 1	Ketone 2	Product 4
1	1a 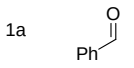		4a 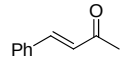
2	1b 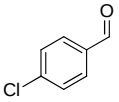		4b 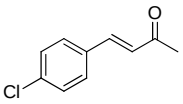
3	1c 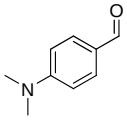		4c 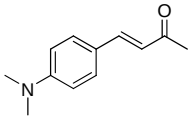

6.3.3. Retro-reactions

The conditions of the retro-reaction are the same as the direct reaction but the starting material in this case is the condensation product **4** (*E*)-4-aryllbut-3-en-2-one. To a solution of condensation product **4** (5 mmol) in acetone (12.5 mL) catalyst **3** (20 mol%) was added. The reaction mixture was stirred at 75 °C in a sealed vial for 24 h.

Samples of the reaction mixture were collected in course of time, diluted with methanol (1:250) and measured by MS.

6.3.4. Online micro-flow reactor

For the online micro-flow reactor experiments two syringes **A** and **B** were used. In the first experiment syringe **A** has been filled with catalyst **3** (40 mol%) in acetone, syringe **B** with corresponding aldehyde 10 mmol in acetone. In the second experiment syringe **A** has been filled with the corresponding aldehyde 10 mmol and catalyst **3** (40 mol%) in DCM, syringe **B** with acetone. The flows (flow rate 10 µL/min each) from both syringes **A** and **B** are combined in a mixing chamber (T-mixer1) and afterwards the reaction takes place in a PEEK (poly etheretherketone) capillary (diameter r= 0.375 mm). A second mixing chamber (T-mixer2) has been used to dilute the reaction mixture with methanol at flow rate 50 µL/min. The reaction time can be adjusted by varying the length of capillary from T-mixer1 to T-mixer2 as well as adjusting the flow rate of the syringe pumps. . A micro-splitter has been used to reduce the flow rate of the diluted reaction mixture to 5 µL/min Figure 6.2. That results in a reaction time of about 15 seconds.

6.3.5. Ion/ molecule gas phase experiment

An ion molecule reaction between intermediate **5a** and acetone in collision cell of the mass spectrometer has been first achieved by preparing **5a** by mixing the catalyst **3** (20 mol%) and benzaldehyde **1a** in dichloromethane at 75°C for 10 min. This reaction solution was diluted with methanol (1:250) and injected into an ESI(+)-MS (Thermo TSQ Quantum Ultra AM triple quadrupole mass spectrometer). Intermediate **5a** was isolated using product scan modus. Acetone vapour was injected with Argon into the collision cell at 1.5 mTorr. CID energy was adjusted at 10 eV. The reaction products were scanned in Q3

6.3.6. Labeling experiments

Chloro-labeling experiments:

First reaction:

5 mmol benzaldehyde **1a** (0.53 g, 0.51 mL), 5 mmol condensation product (E)-4-(4-chlorophenyl)but-3-en-2-one **4b** (0.90 g) were dissolved in acetone (12.5 mL). To this solution catalyst morpholinium trifluroacetate **3** 20 mol% (0.20 g) was added. The reaction mixture was stirred at 75 °C in a sealed vial. Samples were taken from the reaction mixture in the course of time for measuring by ESI-MS after dilution with methanol (1:250).

Second reaction:

5 mmol 4-chlorobenzaldehyde **1a** (0.70 g), 5 mmol condensation product (*E*)-4-aryllbut-3-en-2-one **4a** (0.73 g) were dissolved in acetone (12.5 mL). To this solution catalyst morpholinium trifluroacetate **3** 20 mol% (0.20 g) was added. The reaction mixture was stirred at 75 °C in a sealed vial. Samples were taken from the reaction mixture in the course of time for measuring by ESI-MS after dilution with methanol (1:250).

Deuterium exchange experiments:

Three retro-reaction experiments were carried out using (20 mol%) of three different catalysts: morphlinium trifluro acetate **3** (0.20 g), morpholine (0.09 g, 0.08 mL), triflouroacidic acid (0.11 g, 0.07 mL).

The general procedure:

Catalyst 20 mol% was added to a solution of condensation product **4a** 5 mmol (0.73 g) in 6d-acetone (12.5 mL). The reaction mixture was stirred at 75 °C in a sealed vial.

Samples of reaction mixture were collected in the course of time, diluted with methanol (1:250) and measured by ESI-MS.

^{18}O exchange experiment

4-(dimethylamino)benzaldehyde **1c** 5 mmol (0.74 g, 0.67 mL) was dissolved in ^{18}O-acetone (12.5 mL). To this solution catalyst morpholinium trifluroacetate **3** 20 mol% (0.20 g) was added. The reaction mixture was stirred at 75 °C in a sealed vial. Samples were taken from the reaction mixture in the course of time for measuring by ESI-MS after dilution with methanol (1:250).

6.3.7. NMR experiment

Aldol addition product **10c** 4-(4-(dimethylamino)phenyl)-4-hydroxybutan-2-one 0.4 mmol (0.08 g) was added to an NMR tube containing catalyst **3** 20 mol% (0.01 g) in deuterated acetone (1 mL) and kept at 75°C. The conversion was monitored by ^{1}H-NMR in the course of time.

6.4. Results and discussion

The aim of this study is using different mass spectrometric methods to investigate a very unique and complicated organocatalyzed reaction and find mechanistic evidence about the formation pathways and eliminate side reactions that can occur. Additionally to the mechanistic studies influences that could occur in the gas phase during the ionization were studied to exclude them from mechanistic evaluations. Here, especially labeling experiments allow a direct access to chemical reactions because the labeled site of the molecule can easily being identified.

For the mechanistic investigation of such reactions it is necessary to observe the fast changes and the formation of small amounts of intermediate components especially in a case like this where there are three different potential mechanisms that could describe the reaction. Usually the best way to study such a reaction is the use of ESI-MS and ESI-MS/MS methods.

6.4.1. ESI-MS and ESI-MS/MS studies

A first experimental overview is shown in Figure 6.1a, where the spectrum of the reaction mixture of **1a** with acetone in the presence of catalyst **3** is displayed, after 1 h reaction time at 75°C. In addition to the catalyst **3** at *m/z* 88 and the condensation product at *m/z* 147 the spectrum shows reactive intermediates **5a**, **6** at *m/z* 176, *m/z* 128, respectively, which are first step intermediates of both Mannich and aldol pathways **a**, **b**. The intermediate **9a** of the aldol pathway appears in the spectrum at *m/z* 216.

As can be seen in Scheme 6.2 intermediates **7** and **8** represents two key intermediates that are able to define the mechanistic pathway. Unfortunately both have the same elemental composition and are therefore cannot directly be assigned. A signal at *m/z* 234 was detected with high intensity that could be either or both of those intermediates. Since it is not possible to differentiate the signal CID studies of the intermediate was carried out to allow a structural characterization.

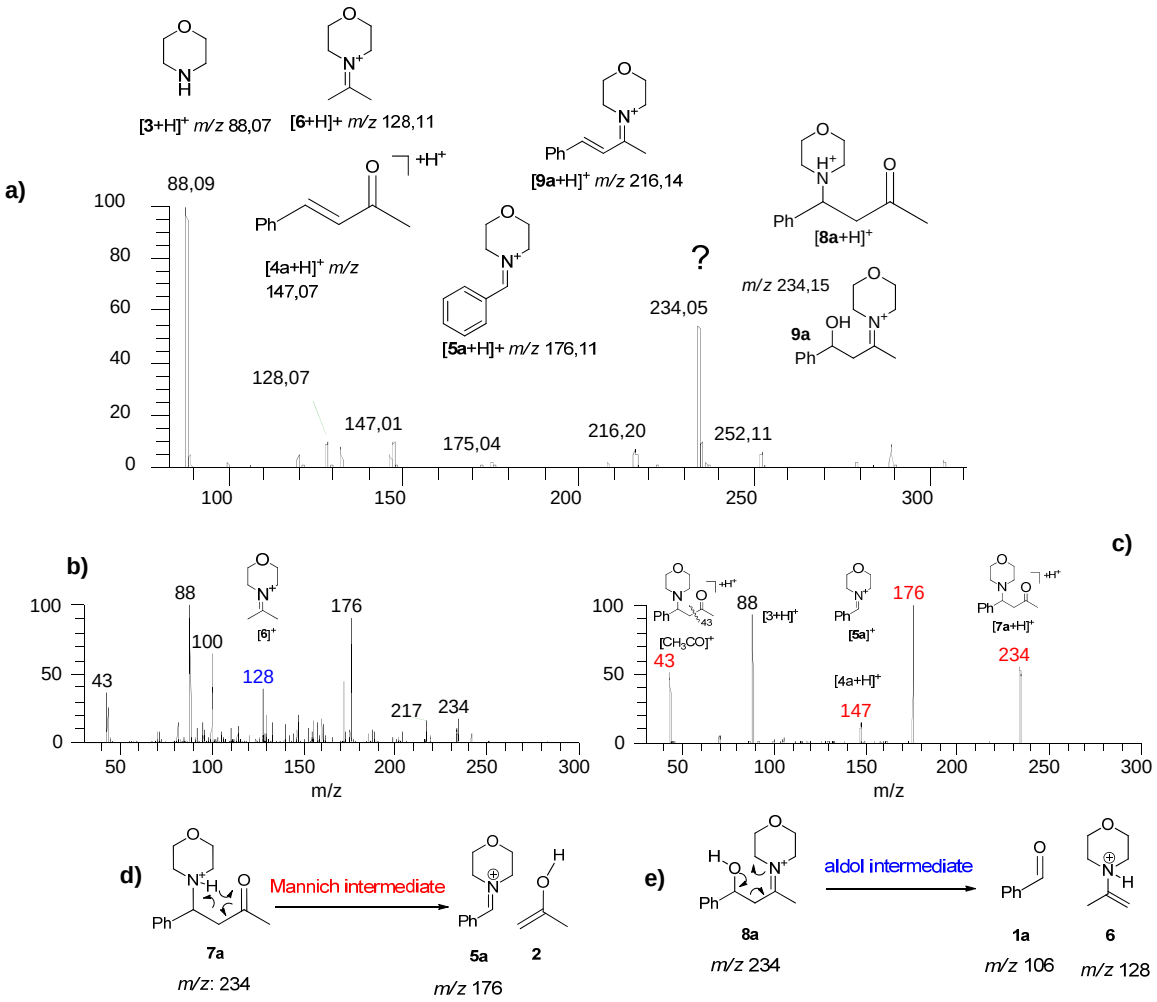

Figure 6.1 a) ESI(+)-MS of aldol condensation reaction of **1a** with acetone in prensence of catalyst **3** 20 mol % at 75°C after 1h, **b)** ESI(+)-MS/MS of *m/z* 234 after 1 min at RT, **c)** ESI(+)-MS/MS of *m/z* 234 after 1h at 75°C, **d, e)** Fragmentation mechanism of **7a** and **8a** respectively by McLafferty rearrangement.

In Figure 6.1c the results from the fragmention of the signal at *m/z* 234 is shown. The resulting fragmentation pattern with a fragment at *m/z* 43 (CH_3CO) makes it possible to assign this to the intermediate **7a**. Additional fragments were detected at *m/z* 88 and *m/z* 147 which resemble the fragment of **3** and **4a**, respectively. The fragment at *m/z* 176 is the intermediate cation **5a** which react with acetone in the reaction mixture to form the intermediate **7a**. There was no trace of characteristic fragments of aldol intermediates **8a** in this MS/MS experiment.

Another MS/MS experiment of *m/z* 234 was performed after much shorter reaction time (1 min) and only at room temperature. Here, a fragment at *m/z* 128 was detected that is characteristic for the aldol intermediate **8a** as can be seen in Figure 6.1b. This fragment at *m/z* 128 can be interpreted as reactive intermediate **6** which can be considered as a diagnostic fragment of intermediate **8a** (see Figure 6.1b). Figure 6.1(d, e) explain the fragmentation mechanisms of both intermediates **7a** and **8a** respectively.

The difficulty to be able to observe the fragment at *m/z* 128 was that it could only be detected in the reaction after 1 min reaction time and at lower reaction temperature and not in a reaction sample after longer reaction times or at higher temperatures. This can have different reasons. One, this intermediate is low concentrated and has very short life time because it is converted immediately to the intermediate **9a** by water elimination especially at higher temperatures. Another reason could be that a suppression effect of intermediate **7a** which obviously has the same *m/z* value but higher intense than **8a**. Obviously intermediate **7a** needs longer time to be formed than **8a** but it is seems to be more stable. Additional ESI(+)MS(/MS) measurements are shown in the appendix (Figures A6.1, A6.2) for other aromatic aldehydes **1b**, **1c** with acetone and catalyst **3.** The MS signals of the reactive intermediates and the fragmentation patterns of the corresponding aldol and Mannich intermediates **7**, **8** of these aldehydes were analogous to the previous experiments.

According to these results it seems that diagnostic fragments for both the Mannich **a** and aldol **c** pathways can be detected in this reaction while no evidence could be found for pathway **b**. To be certain that the diagnostic intermediates are actually formed according to the pathways described in Scheme 6.2 a potential retro-reaction from product **4** needs to be considered. Therefore, the product was cleaned after synthesis and used as starting material for a retro-reaction. The results show that some small signals appear in the MS spectrum of the reactive intermediates of both aldol and Mannich pathways. This experiment illustrates that the end product of the reaction **4a** which is formed in the reaction solution of aldehyde **1a** and acetone can react with the catalyst **3** to form the reactive intermediates of both Mannich and aldol pathways. That is confusing the determination of the reaction pathway as long as the reactive

intermediates could be formed not only from the direct reaction but also from the retro-reaction although the MS signals of the reactive intermediates in the retro reaction are not as intensive as in the direct reaction. Still, due to this result it is still not really possible to assign a mechanistic pathway to the reaction from these results alone.

6.4.2. Micro-reactor studies

One way to really determine the formation pathway of this reaction is to eliminate the retro-reaction. This could be done in different ways. One way is to use a method that allows intercepting the reactive intermediates of the reaction of aldehyde **1a** with acetone in the presence of catalyst **3** before the formation of the end product **4a** to avoid the retro reaction effect.

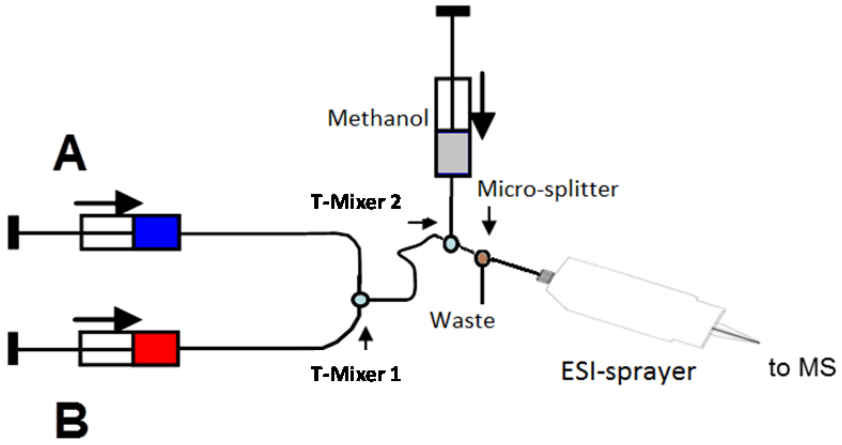

Figure 6.2 Schematic drawing of the online micro-flow reactor.

This has been shown by Metzger and co-workers[17] who were using a micro-flow reactor technique where the reaction components are mixed continuously via a T-mixer from two different syringes. The mixed flow continues through a small capillary and the remaining time that the mixed solutions spend in the capillary is the reaction time. The solution is then coupled directly to the sprayer of the electrospray source for online monitoring. When the capillary is short this allows for short reaction times where the reactive intermediates are just formed but where the time is not long enough to form the end product (see Figure 6.2).The set-up used here allows for a reaction time of 15 seconds.

To investigate the aldol pathway in this reaction, acetone and the catalyst **3** were placed in syringe **A** to form reactive intermediate **6** of the first stage of aldol pathway, while syringe **B** contained a solution of benzaldehyde **1a** in acetone as solvent. The results are shown in Figure 6.3. It can be seen that it is not possible to detect the intermediate **8a** at *m/z* 234

because of its low concentration and its short life time but it was possible to find a strong signal of the more stable reactive intermediate **9a** at *m/z* 216 (Figure 6.3.a). This intermediate is being formed after the water elimination step of **8a** and is a much more stable and intense intermediate than **8a**. This confirms that **9a** is formed by direct reaction rather than by retro reaction and aldol pathway controls this formation. For more examples of other aldehydes, please see the appendix (Figures A6.3-A6.6).

In order to investigate the Mannich pathway, a solution of benzaldehyde **1a** and the catalyst **3** were mixed in syringe **A** forming the first Mannich intermediate **5a**. Syringe **B** contained only acetone. In this experiment there was no detection of the expected reactive intermediate **7a** of Mannich pathway at *m/z* 234 but only a small signal of reactive intermediate **9a** at *m/z* 216 (Figure 6.3.b).

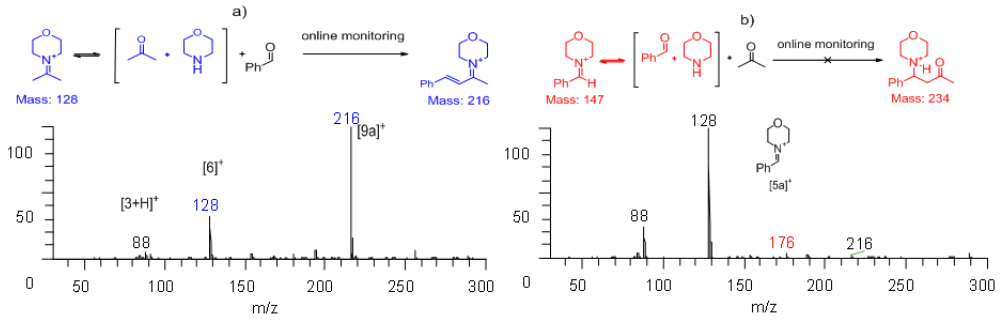

Figure 6.3 ESI(+)-MS of the micro flow reactor of: **a)** aldol intermediate **6** *m/z* 128 in the syringe A with benzaldehyde **1a** in syringe **B** to form intermediate **9a, b)** Mannich intermediate **5a** *m/z* 176 in the syringe **A** with acetone in syringe **B** to form intermediate **7a** *m/z* 234, but no trace detected of **7a** *m/z* 234.

These results show that the formation of the Mannich intermediate **7a** needs more time and a higher temperature than what is provided in the micro-flow reactor set-up unlike aldol intermediates **8a, 9a** which are formed much faster. Another technique would be needed to exclude the occurrence of the retro-reaction for the Mannich intermediates

6.4.3. Labeling experiments

The results shown here still do not allow getting a clear picture of the reaction. While the diagnostic intermediates are characterized, the impact of the retro-reaction still is a mystery. To evaluate such chemical changes usually labeling experiments are carried out, often using isotopic enriched labels. Here, a labeling procedure is shown with a chloro-group used for labeling.

For a better evaluation of the impact of the retro-reaction on the diagnostic intermediates an experiment is needed that allows distinguishing between the forward and the retro-reaction.

Therefore two different experiments were set-up where both the product **4** and the starting aldehyde **1** were reacted with the catalyst.

In order to differentiate the reaction rates of forming the reactive intermediate **7a** of the Mannich pathway from the direct and the retro-reactions the condensation product was labeled in the first step with a chloro-atom **4b** while benzaldehyde **1a** was used. By doing so, it is possible to differentiate if the intermediate is being formed by direct reaction or along the retro-reaction pathway because the amount of the chlorinated compound allows to determine the difference. Such an approach can be affected by the addition of the chloro-atom to the product that could cause a different reactivity. Therefore, we repeated this experiment while not labeling the product but the aldehyde. The results from both experiments are shown in Figure 6.4 in addition with time dependency curves that show the changes in pattern of the two signals according to the reaction time.

Sample was collected after 10 min of reaction time a and measured by ESI(+)MS. The major signals are the chlorinated intermediate **7b** at *m/z* 268 and the not-chlorinated intermediate **7a** at *m/z* 234. In the first reaction set-up, **7a** is being formed from benzaldehyde, the chlorinated compound is being formed in the retro-reaction. The results of the time dependency curve shows that the signal from the retro-reaction is really low, comparing to **7a** at *m/z* 234. This indicates that **7a** is formed mostly by the direct-reaction pathway via the Mannich mechanism and its retro-reaction background is negeligble. Figure 6.4a shows the comparison of the intensities of **7a**, **7b** in course of time. The cross-check experiment with the chlorinated benzaldehyde confirms these results because here the chlorinated intermediate is being formed. To see the full spectra, please refer to the appendix Figures A6.7, A6.8.

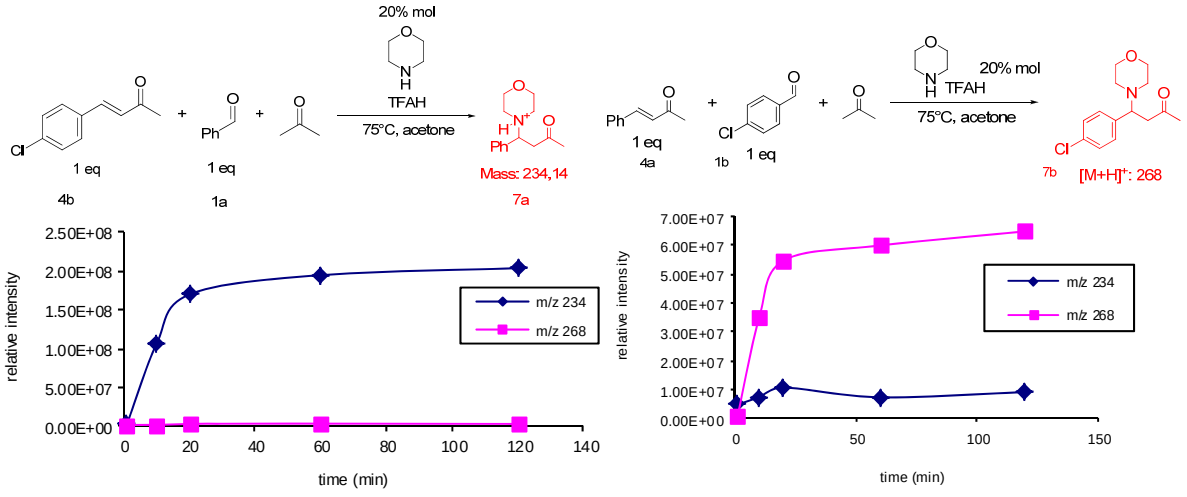

Figure 6.4 Time dependency of a) **7a** *m/z* 234 (direct-reaction), **7b** *m/z* 268 (retro-reaction), b) **7b** *m/z* 268 (direct-reaction), **7a** *m/z* 234 (retro-reaction).

To investigate any acidic or basic effect of catalyst **3** upon the catalytic process in addition to the organocatalytic process (as long as the aldol condensation reaction could be catalyzed by acid or base), three retro-reaction experiments were carried out using the condensation product **4a** as reactant for each experiment with catalyst **3**, morpholine, and triflouroacidic acid in deuterated acetone at 75°C. Samples from the reaction mixtures are sampled each hour and diluted in methanol and measured by ESI(+)-MS. In Figure 6.5 the differences in the deuterium exchange pattern from **4a** at *m/z* 147, 148, 149, 150 for each catalyst is shown. In the case of the acidic catalyst (trifluoroacidic acid) or basic catalyst (morpholine) the exchange happens one per one deuterium atom exchange during 8 h of reaction time while the reaction using catalyst **3** (morpholinium trifloro acidic acid) were an exchanged of the methyl group can be determined all atoms at one.

In the case of using catalyst **3** the catalyst forms aldol intermediate **9a** with **4a**. This intermediate has very active protons in the α-methyl group via iminium/enamine equilibrium. Because of high concentration of D^+ in the solution which came from acetone-d6, the protons of the α-methyl group of **9a** were exchanged at once then hydrolysed to **4a**-d3 at *m/z* 150. In the case of acidic or basic catalyst the α-methyl group of **4a** has been activated via the keto-enol tautomerism which leads to a gradual deuterium-exchange of **4a** to finally form **4a**-d3 at *m/z* 150, **4a**-d4 at *m/z* 151 for trifluoroacidic acid and morpholine respectively. The addition deuterium-exchange in the case of the basic catalyst (morpholine) is because its ability to deprotonate **4a** at the β-carbon atom i.e. exchanging 3 protons on α-methyl group plus 1 proton on β-carbon atom (see Scheme A6.1-4). Again, the deuterium exchange pattern of **4a** using catalyst **3**, it is possible to just observe tiny signals at *m/z* 148, 149, 151 in addition to the natural ^{13}C- isotope pattern which allows excluding any acidic or basic effect for catalyst **3**.

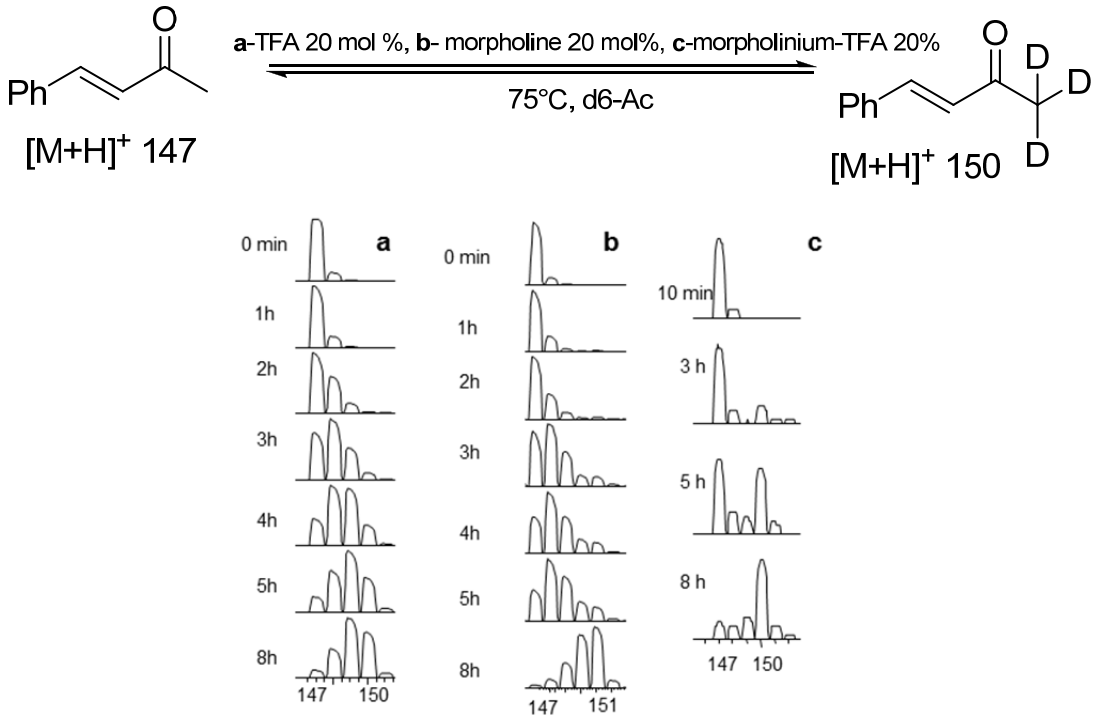

Figure 6.5 ESI(+)-MS of deuterium exchange rate of condensation reaction **4a** *m/z* 147 with deuterated acetone using **a)** acidic catalyst trifluroacidic acid 20 mol%, **b)** basic catalyst 20 mol% morpholine, **c)** organocatalyst **3** morpholinium-trifluroacidic acid 20mol%.

To investigate the reaction rate of the formation of the first intermediates for the aldol and Mannich mechanism **5**, **6** aldehyde **1c** was added to catalyst **3** in the presence of ^{18}O-acetone instead of normal acetone at 75°C. Samples were taken from the reaction mixture every 5 min, diluted with methanol and measured with ESI(+)MS. The aldehyde **1c** at *m/z* 150 was chosen due to its high response with ESI(+)MS. First the catalyst **3** reacts with both aldehyde **1c** and ^{18}O-acetone to form intermediates **5c**, **6** respectively with releasing of excess ^{18}O-water from ^{18}O-acetone to the reaction medium in addition to the normal water from **1c**. Because of the equilibrium in intermediates forming, intermediate **5c** hydrolysed in the presence of excess ^{18}O-water to ^{18}O-**1c** *m/z* 152. In only 20 min **1c** *m/z* 150 is fully converted to ^{18}O-**1c** at *m/z* 152, which means the formation of the intermediates **5c** and **6** is quite fast. For more mass spectra see Appendix Figure A6.9.

6.4.4. Gas-phase studies

In general, ESI-MS studies of a chemical reaction suffer from the fact that under ESI conditions gas phase associates can be formed that are not really liquid phase products. The differentiation of such effects of what is liquid phase chemistry or what is gas phase association is often difficult. One way to solve such a problem is the induction of slight collision voltages in the ion source region of the mass spectrometer that cause some minor

fragmentation. On the other side, such collisions can destroy compounds such as weak intermediates that are formed during the chemical step.

The reactive intermediate of Mannich pathway **7a** is just an addition product of the reactive intermediate **5a** with acetone**.** For a confirmation that **7a** is formed in the reaction solution and not in the gas phase from **5a** and acetone during the measurement with ESI-MS a reaction mixture of aldehyde **1c** and **3** in acetone at 75°C was prepared (aldehyde 1c was chosen because of the high response of its reaction intermediates by MS). A sample of 5 µL of the previous reaction mixture was diluted with 1 mL methanol and 20 µL of labeled ^{18}O-acetone were added to the diluted solution and measured by ESI(+)-MS. No significant signal at *m/z* 279 was detected, which means the intermediate **7c** at *m/z* 277 was formed in the solution and not in the gas phase (See Figure A6.10).

Ion/molecule reaction is a unique MS-technique where a reaction takes place in the collision cell of the mass spectrometer between an isolated ion from Q1 and a chemical reagent which can be introduced in the collision cell with the collision gas. The reaction components and product(s) are measured subsequently by Q3. The big advantage of this technique is the ability to control the reaction and combine the reaction components precisely (See Scheme A6.4 in the appendix).

This technique has been applied in this investigation to compare the different reactivity of intermediate **5x** where **x** is **a**, **b** or **c** dependently on the corresponding aromatic aldehyde **1a**, **1b** and **1c** in term of the reaction with acetone to form **7x**.

Three different ion/molecule reactions have been performed with the different reactive intermediates **5x** which prepared in a separated reaction solution of the corresponding aromatic aldehyde in the presence of **3**. **5x** cations were isolated by the first quadrupole Q1 at the product scan modus and the acetone vapor was introduced with Ar gas in the collission cell at pressure of 1.5 mTorr. The reactive intermediate **7x** was formed at the corresponding *m/z* value. We noticed that the activity of the intermediate **5c** increased because of electron donating group comparing to electron withdrawing group **5b** figure 6.6.

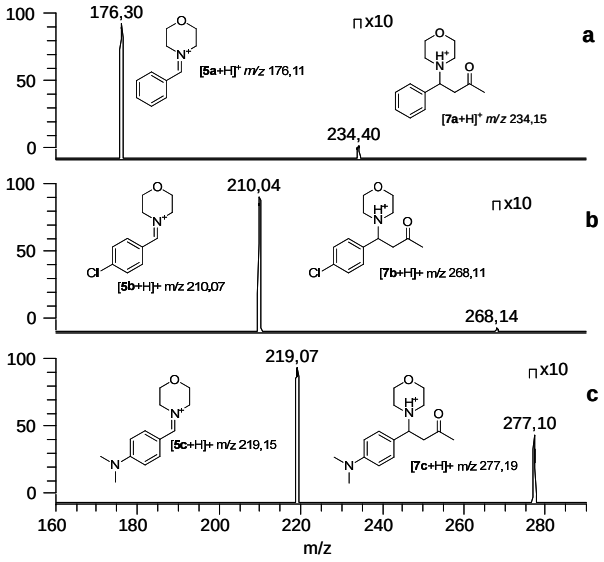

Figure 6.6 Building of Mannich intermediate **7** via ESI(+)-MS/MS gas phase ion/molecule experiment of different aldehyde intermediates **5** with acetone a) **5a** , b) **5b**, c) **5c**. Here we can see the different intensity of **7** because of the effect of substitution group of the aldehyde.

From previous results, the sequence of intermediate forming of 7 from **5** as Mannich pathway could be confirmed, in addition to study the substitution effect on the reactivity of **5**.

For more deep understanding of aldol pathway an experiment by NMR has been added to confirm the formation sequence from intermediate **8** to **9** and finally product **4**. Aldol addition product **10c** was added to an NMR tube containing catalyst **3** in deuterated acetone and kept at 75°C. The conversion was monitored by ^{1}H-NMR. Catalyst **3** forms intermediate **8c** with reactant **4c** followed with water molecule elimination to **9c**, a hydrolysis of **9c** takes place and the condensation product **4c** is formed. Conversion was completed in 8h. No conversion was seen without addition of catalyst **3**. (see Figure 6.7).

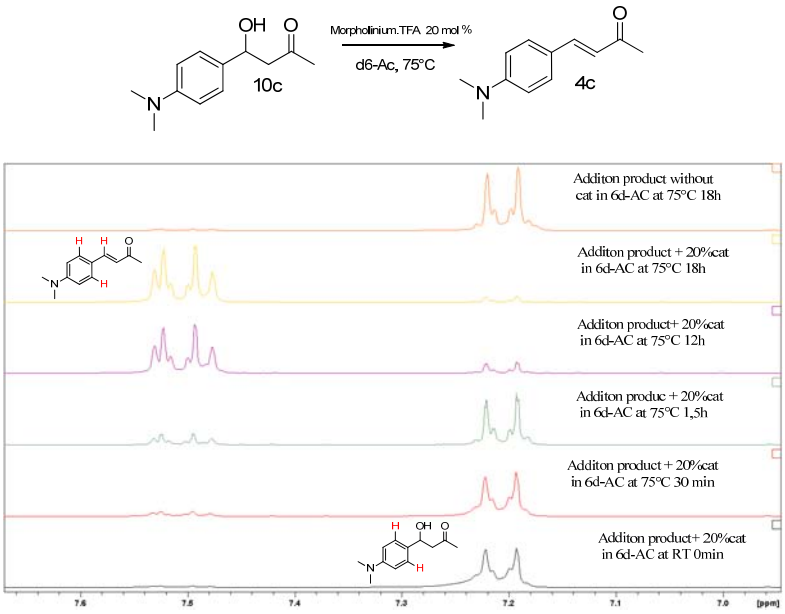

Figure 6.7 NMR monitoring of conversion of aldol addition compound **5c** to condensation product **4C** in the present of catalyst **3** 20 mol% in deuterated acetone at 75°C in NMR tube.

All things considered, these results indicate that the reaction seems to follow both Mannich and aldol pathways to form the same product. The reactive intermediates of the aldol pathway appear immediately even at room temperature (which could be a kinetically controlled pathway), while the other reactive intermediate **7a** of Mannich pathway needs more time and higher temperature (which could be a thermodynamically controlled pathway).

6.5. Conclusions

This work presents applications of different mass spectrometric tools to solve the mechanistic evaluation of a unique organocatalyzed reaction which has different potential reaction pathways. Different examples of the experiments and techniques of mass spectrometry have been given for focusing on each step of the reaction. It was possible to characterize the intermediates in two different pathways of the aldol condensation reaction of aromatic aldehydes with acetone catalyzed by morpholinium trifluoroacetate **3** as organocatalyst using ESI(+)-MS(/MS). The first mechanism is an aldol pathway which seems like a kinetically controlled mechanism and the second one is the Mannich mechanism which could be a more thermodynamically controlled mechanism.

Different MS techniques were implemented such as a micro-flow reactor, ion/molecule isotope labeling experiments with mass spectrometry and NMR to determine the properties of the mechanisms i.e. rate, reversibility, reactivity. The first step of the aldol and Mannich mechanisms to forming **5**, **6** is very fast and was investigated by using ^{18}O-isotope exchange

from ^{18}O-acetone to the aldehyde in the presence of catalyst **3**. We successfully exclude any acidic or basic catalytic effect of **3** on the reaction comparing the mass spectra of the retro-reaction of the condensation product with trifluor acidic acid, morpholine and our catalyst **3**.

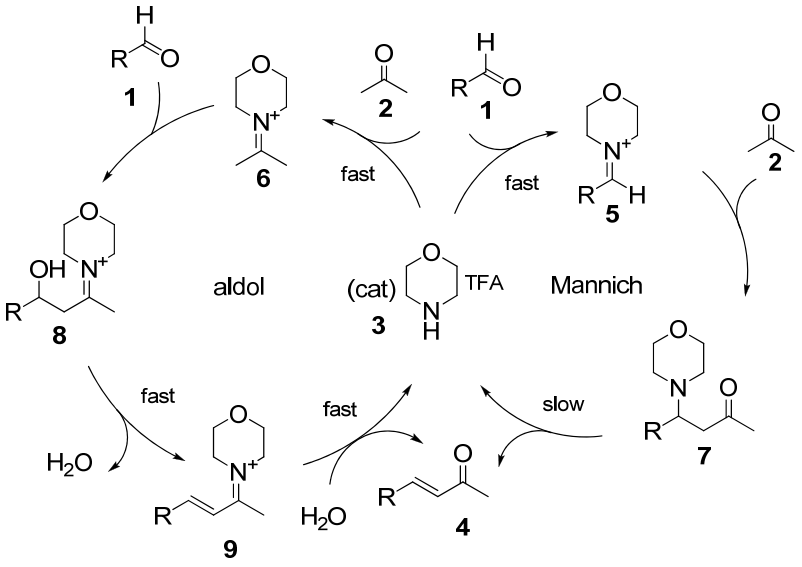

Scheme 6.3 The proposed mechanisms and intermediates of morpholinium- trifluoroacetate-catalyzed aldol condensation reaction (arrows may be considered equilibria).

References

[1] P. I. Dalko, in *Wiley-VCH Verlag GmbH & Co. KGaA, Weinheim, Germany, Vol. Vol. 1*, **2007**.

[2] B. List, *Chemical Communications* **2006**, 819.

[3] B. List, R. A. Lerner, C. F. Barbas, *Journal of the American Chemical Society* **2000**, *122*, 2395.

[4] K. A. Ahrendt, C. J. Borths, D. W. C. MacMillan, *Journal of the American Chemical Society* **2000**, *122*, 4243.

[5] Z. G. Hajos, D. R. Parrish, *Journal of Organic Chemistry* **1974**, *39*, 1615.

[6] U. Eder, G. Sauer, R. Weichert, *Angewandte Chemie-International Edition* **1971**, *10*, 496.

[7] H. Budzikiewicz, *Analytical and Bioanalytical Chemistry* **2005**, *381*, 1319.

[8] J. Seayad, B. List, *Organic & Biomolecular Chemistry* **2005**, *3*, 719.

[9] P. I. Dalko, L. Moisan, *Angewandte Chemie-International Edition* **2004**, *43*, 5138.

[10] P. I. Dalko, L. Moisan, *Angewandte Chemie-International Edition* **2001**, *40*, 3726.

[11] J. B. Fenn, M. Mann, C. K. Meng, S. F. Wong, C. M. Whitehouse, *Science* **1989**, *246*, 64.

[12] C. M. Whitehouse, R. N. Dreyer, M. Yamashita, J. B. Fenn, *Analytical Chemistry* **1985**, *57*, 675.

[13] C. Trage, D. Schroder, H. Schwarz, *Chemistry-a European Journal* **2005**, *11*, 619.

[14] D. Schroeder, *European Journal of Mass Spectrometry* **2012**, *18*, 139.

[15] S. M. Polyakova, R. A. Kunetskiy, D. Schroeder, *International Journal of Mass Spectrometry* **2012**, *314*, 13.

[16] W. Schrader, P. P. Handayani, J. Zhou, B. List, *Angewandte Chemie-International Edition* **2009**, *48*, 1463.

[17] C. Marquez, J. O. Metzger, *Chemical Communications* **2006**, 1539.

[18] L. S. Santos, L. Knaack, J. O. Metzger, *International Journal of Mass Spectrometry* **2005**, *246*, 84.

[19] T. D. Fernandes, B. G. Vaz, M. N. Eberlin, A. J. M. da Silva, P. R. R. Costa, *Journal of Organic Chemistry* **2010**, *75*, 7085.

[20] A. O. Aliprantis, J. W. Canary, *Journal of the American Chemical Society* **1994**, *116*, 6985.

[21] J. Griep-Raming, S. Meyer, T. Bruhn, J. O. Metzger, *Angewandte Chemie-International Edition* **2002**, *41*, 2738.

[22] J. W. Sam, X. J. Tang, R. S. Magliozzo, J. Peisach, *Journal of the American Chemical Society* **1995**, *117*, 1012.

[23] N. Iranpoor, F. Kazemi, *Tetrahedron* **1998**, *54*, 9475.

[24] B. List, L. Hoang, H. J. Martin, *Proceedings of the National Academy of Sciences of the United States of America* **2004**, *101*, 5839.

[25] M. B. Schmid, K. Zeitler, R. M. Gschwind, *Journal of the American Chemical Society* **2011**, *133*, 7065.

[26] M. B. Schmid, K. Zeitler, R. M. Gschwind, *Angewandte Chemie International Edition* **2010**, *49*, 4997.

[27] C. D. F. Milagre, H. M. S. Milagre, L. S. Santos, M. L. A. Lopes, P. J. S. Moran, M. N. Eberlin, J. A. R. Rodrigues, *Journal of Mass Spectrometry* **2007**, *42*, 1287.

[28] K. Zumbansen, A. Doehring, B. List, *Advanced Synthesis & Catalysis* **2010**, *352*, 1135.

Appendix

4-Chlorobenzaldehyde **1b**, 4-dimethylaminobenzaldehyde **1c** are also used for the organocatalyzed reaction with acetone in the presence of catalyst **3**. Reaction mixture have been measured with ESI(+)-MS to detect the reaction intermediates

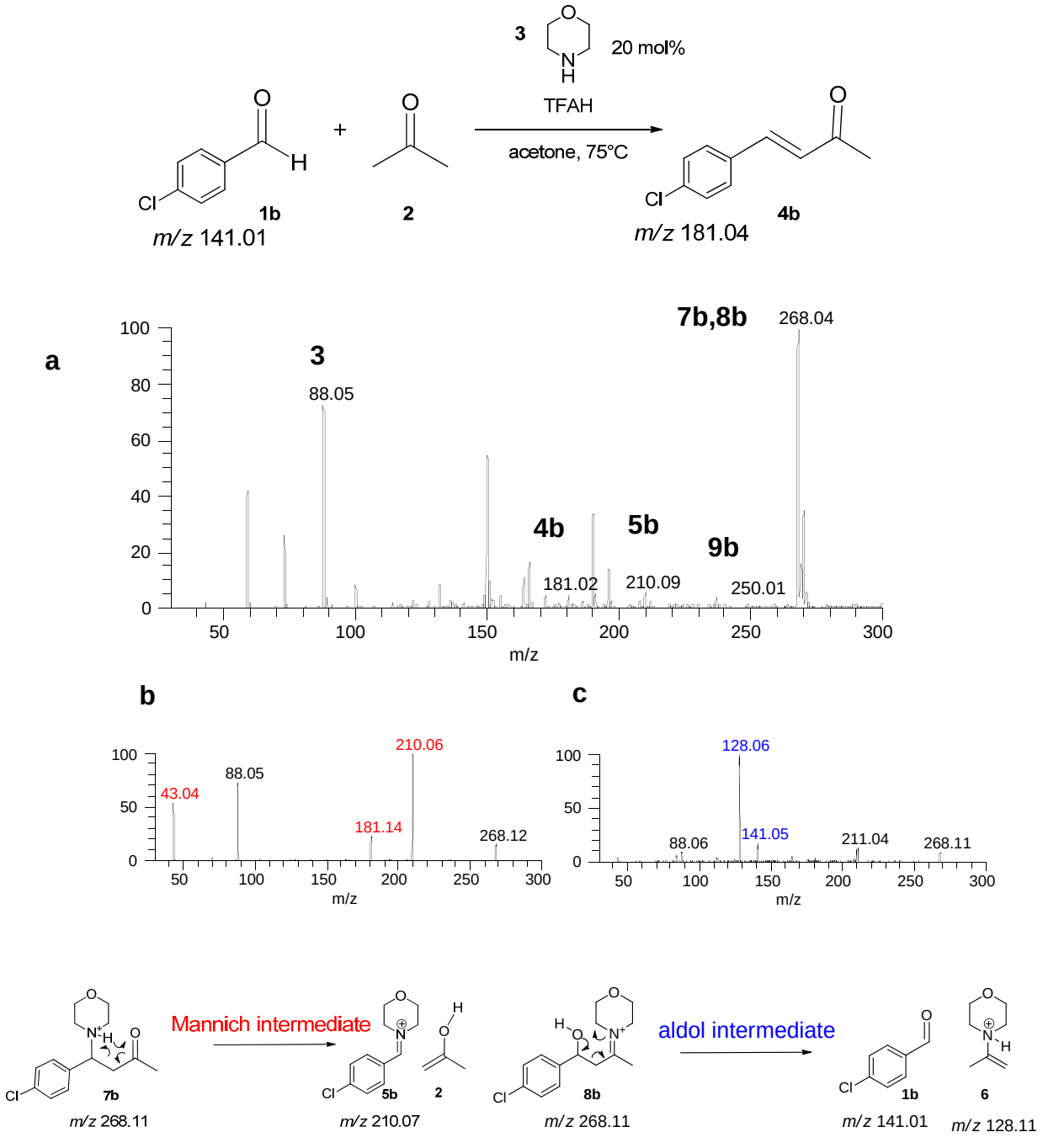

Figure A 6.1 a) ESI(+)-MS of reaction entry (2) at 75°C after 1h. **b)** ESI-(+)-MS/MS of *m/z* 268 after 1h at 75°C (Mannich intermediate **7b**) **C)** ESI-(+)-MS/MS of *m/z* 268 after 1 min at RT (aldol intermediate **8b**).

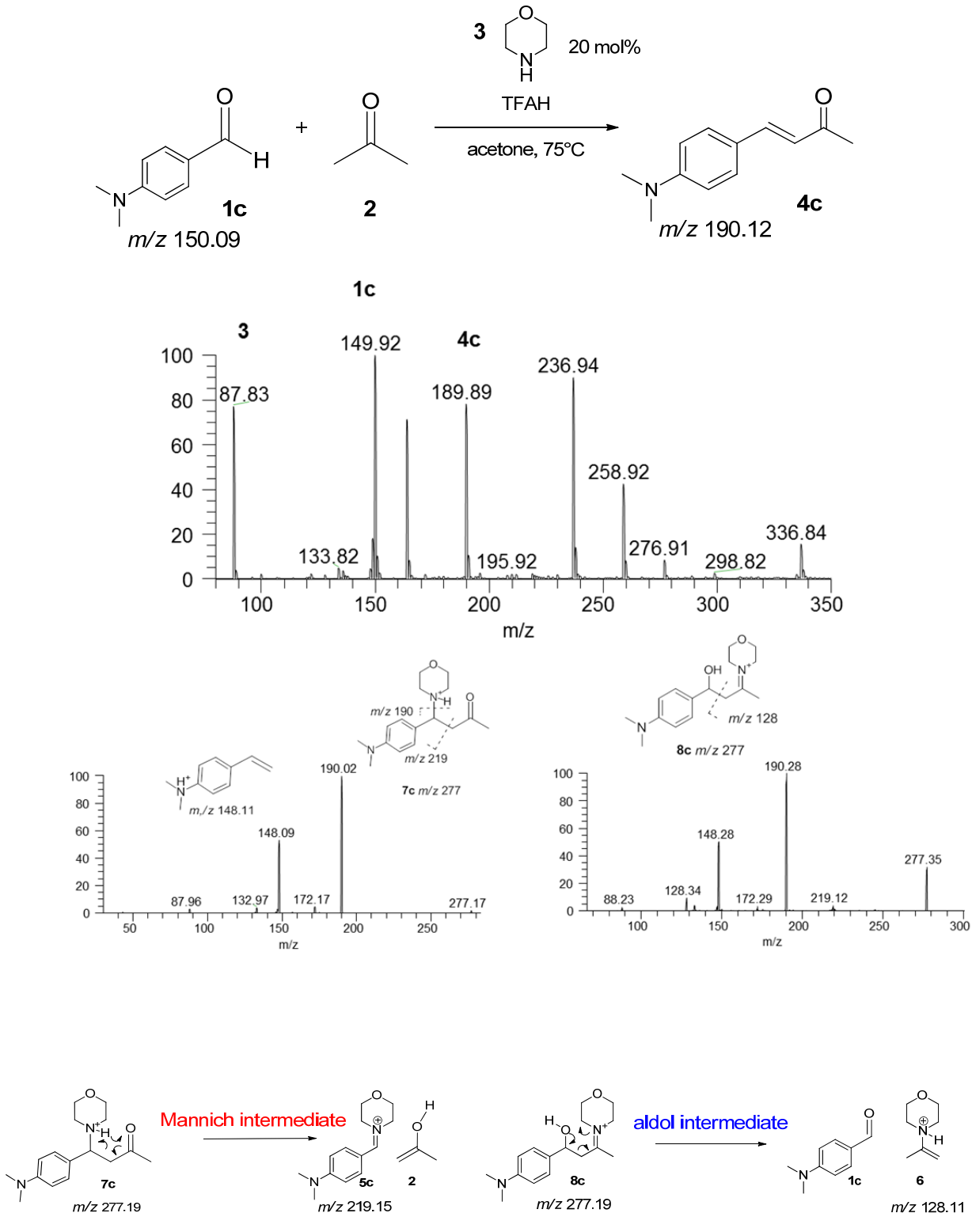

Figure A 6.2 a) ESI-(+)-MS of reaction entry (3) at 75°C after 1h. **b)** ESI-(+)-MS/MS of *m/z* 277 after 1h at 75°C (Mannich intermediate **7**). **c)** ESI-(+)-MS/MS of *m/z* 277 after 1 min at RT (aldol intermediate **8c**).

The online monitoring experiment has been repeated using aromatic aldehydes **1b**, **1c**, with the same results as experiment with **1a**

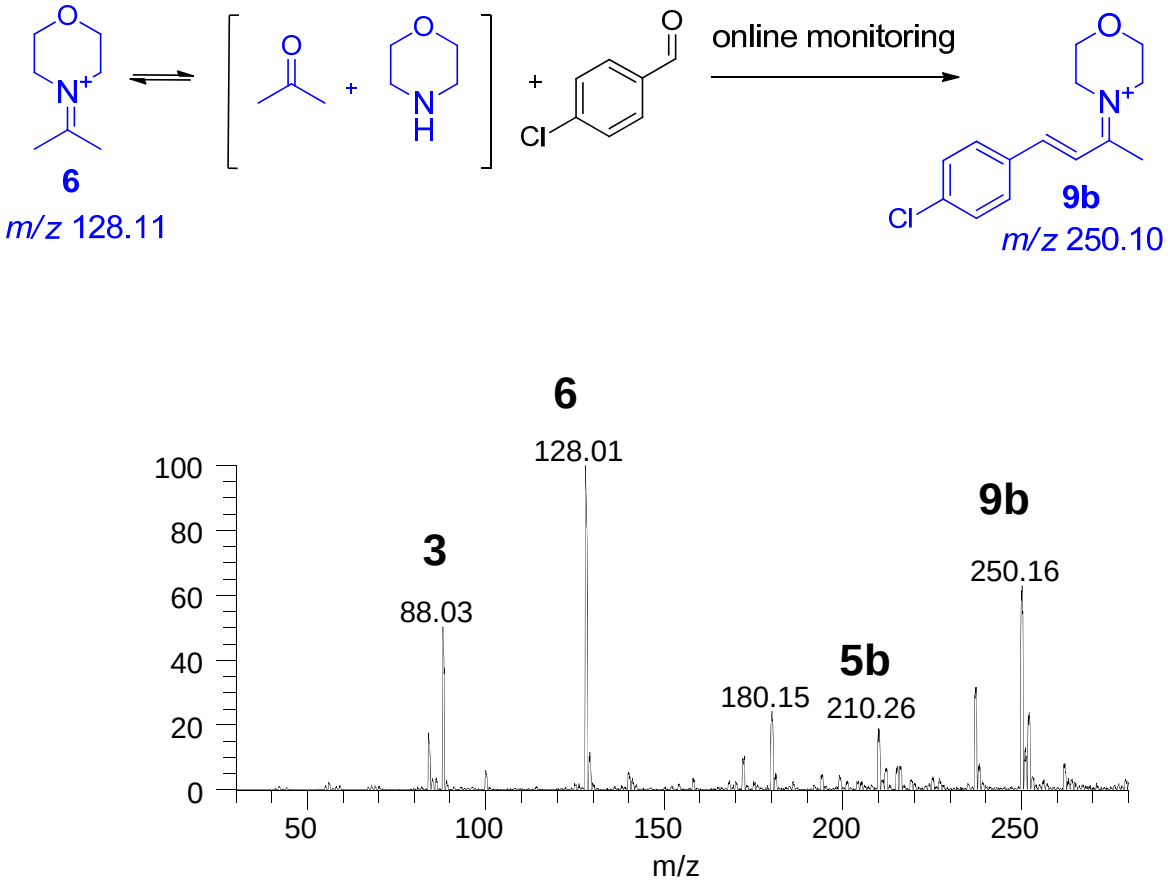

Figure A 6.3 a) A mixture of acetone and catalyst **3** in the first syringe to form aldol intermediate **6** *m/z* 128, aldol intermediate **6** mixed with the aldehyde **1b** in the tee-peace to form aldol intermediates **9b** *m/z* 250 continuously. Micro-flow reactor coupled directly to the ESI-MS. **b)** ESI-(+)-MS spectrum of the online monitoring reaction (no trace of the expected Mannich intermediate **7b** at *m/z* 268).

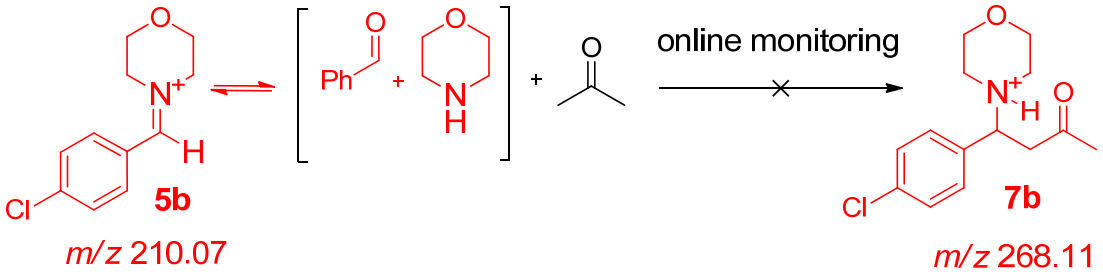

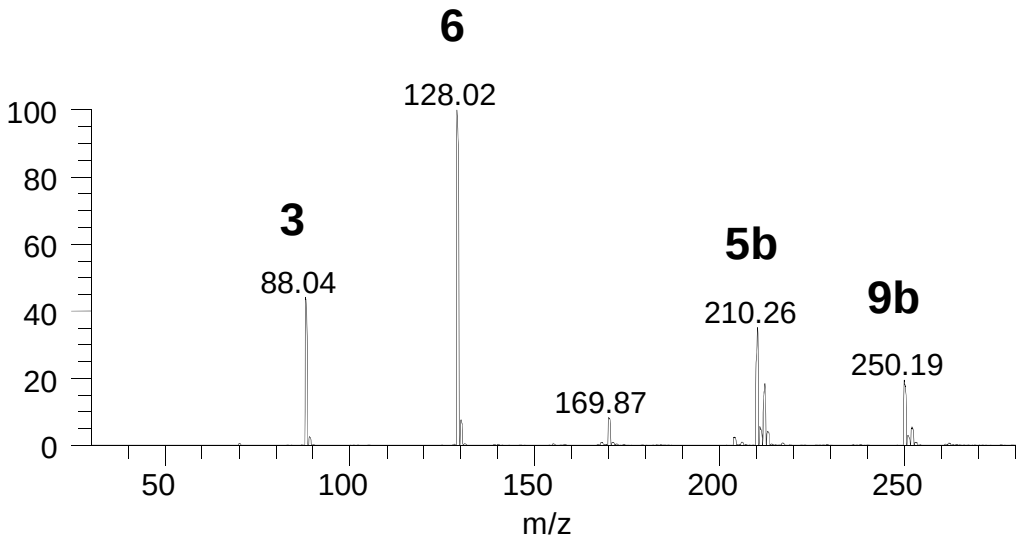

Figure A 6.4 a) a mixture of aldehyde **1b** and catalyst **3** in the first syringe to form Mannich intermediate **5** *m/z* 210, aldol intermediate **5** mixed with acetone in the tee-peace to form Mannich intermediate **7b** continuously. Micro-flow reactor coupled directly to the ESI-MS **. b)** ESI-(+)-MS spectrum of the online monitoring reaction (no trace of the expected Mannich intermediate **7b** at *m/z* 268).

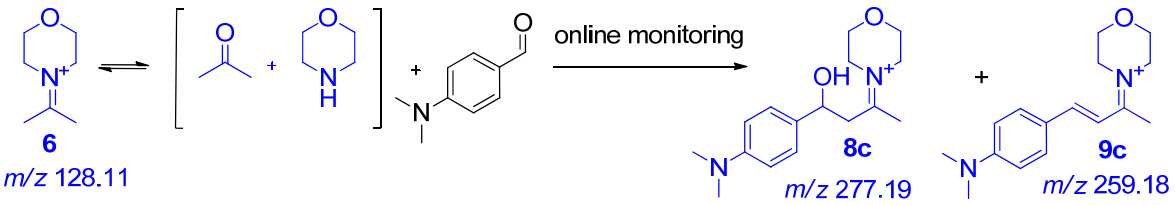

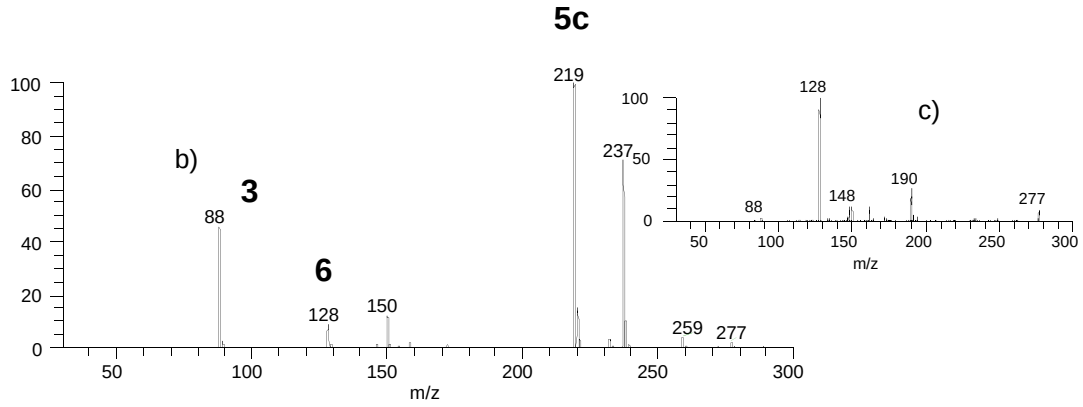

Figure A 6.5 a) a mixture of acetone and catalyst **3** in the first syringe to form aldol intermediate **6** *m/z* 128, aldol intermediate **6** mixed with the aldehyde **1c** in the tee-peace to form aldol intermediates **8c**, **9c** continuously. Micro-flow reactor coupled directly to the ESI-MS . **b)** ESI-(+)-MS of the online monitoring reaction of scheme 6.5. **c)** ESI-(+)-MS/MS of *m/z* 277 at CID energy 20 eV (aldol intermediate fragmentation pattern **8c** with diagnostic fragment *m/z* 128).

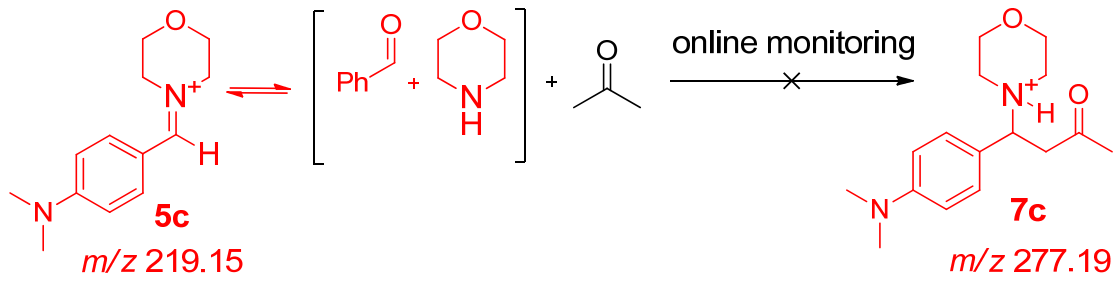

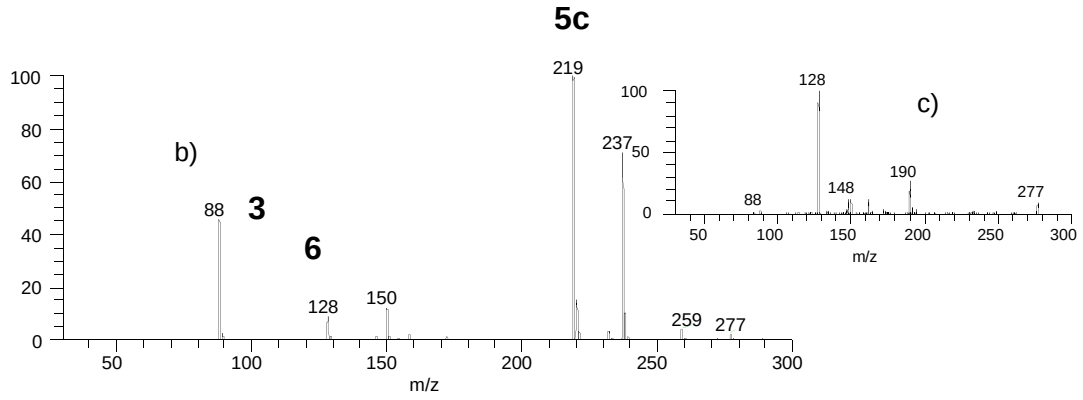

Figure A 6.6 a) a mixture of aldehyde **1c** and catalyst **3** in the first syringe to form Mannich intermediate **5** *m/z* 219, aldol intermediate **6** mixed with acetone in the tee-peace to form Mannich intermediate **7c** continuously. Micro-flow reactor coupled directly to the ESI-MS **. b)** ESI-(+)-MS of the online monitoring reaction. **c)** ESI-(+)-MS/MS of *m/z* 277 at CID energy 20 eV (aldol intermediate fragmentation pattern **8c** with *m/z* 128 and small trace of Mannich intermediate).

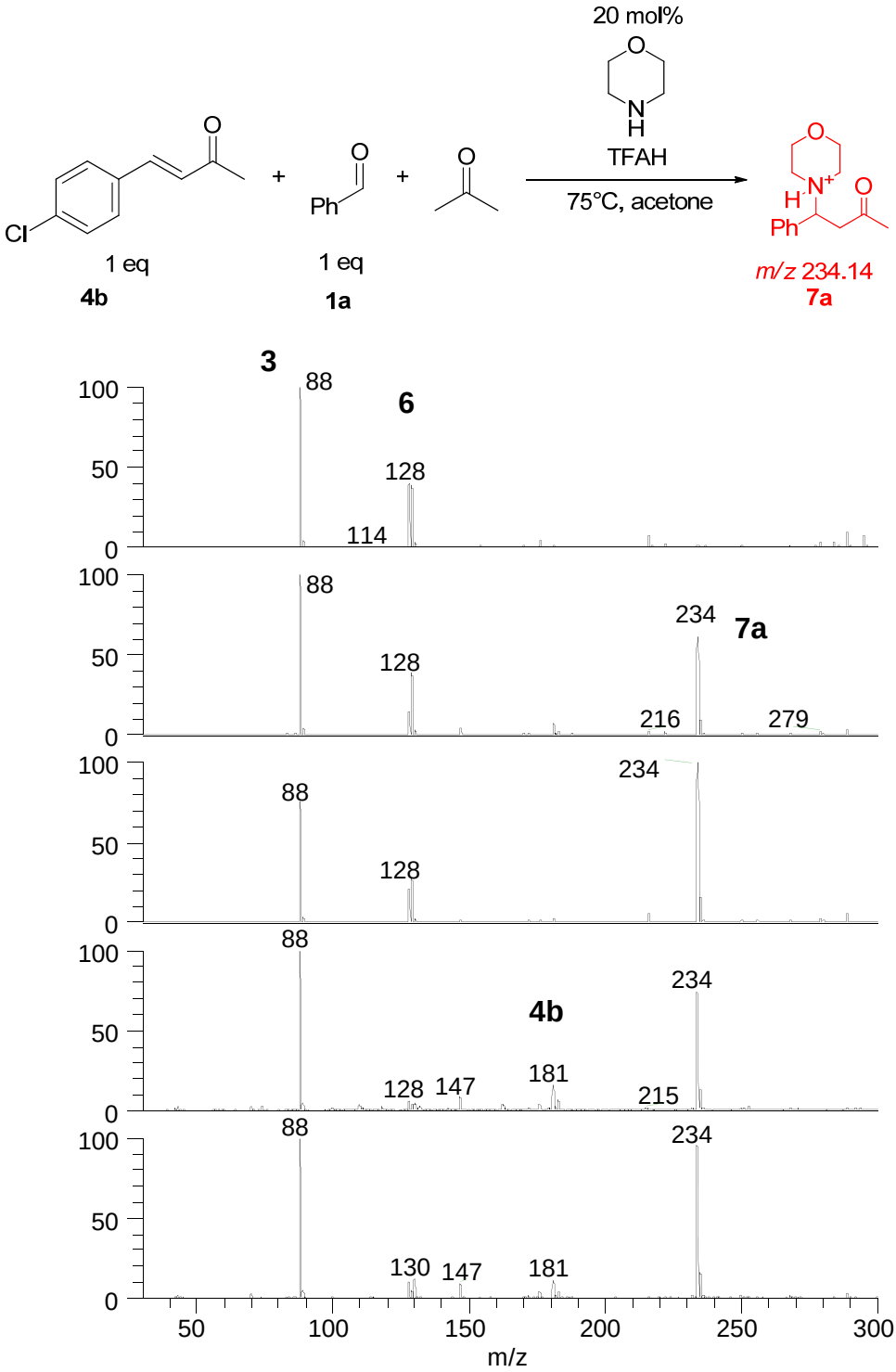

Figure A 6.7 ESI(+)-MS of the **1a** in acetone and 20 mol% of **3** in the present of 1 equivalent **4b** at 75°C in course of time.

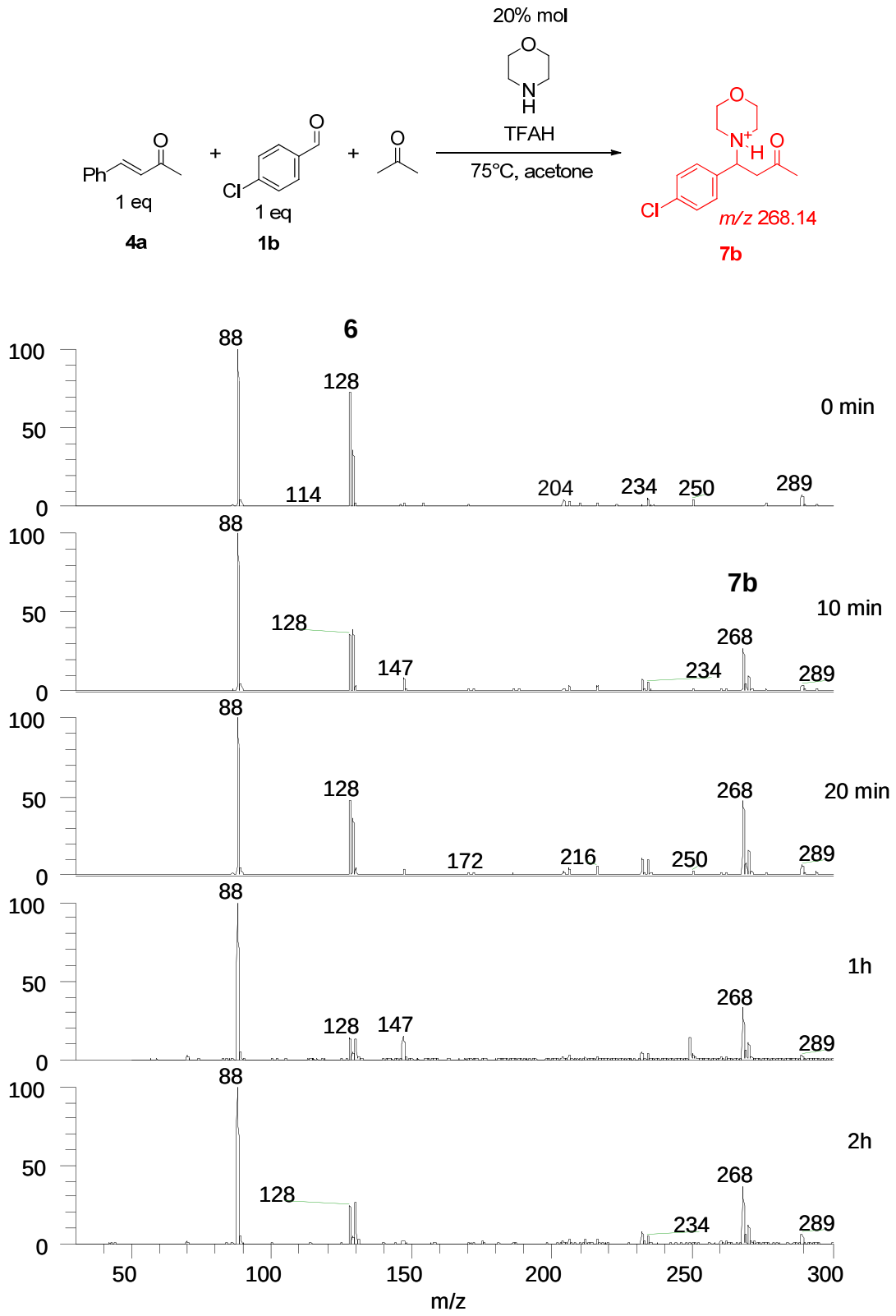

Figure A 6.8 ESI(+)-MS of the 1b in acetone and 20% of **3** in the present of 1 equivalent **4a** at 75°C in course of time.

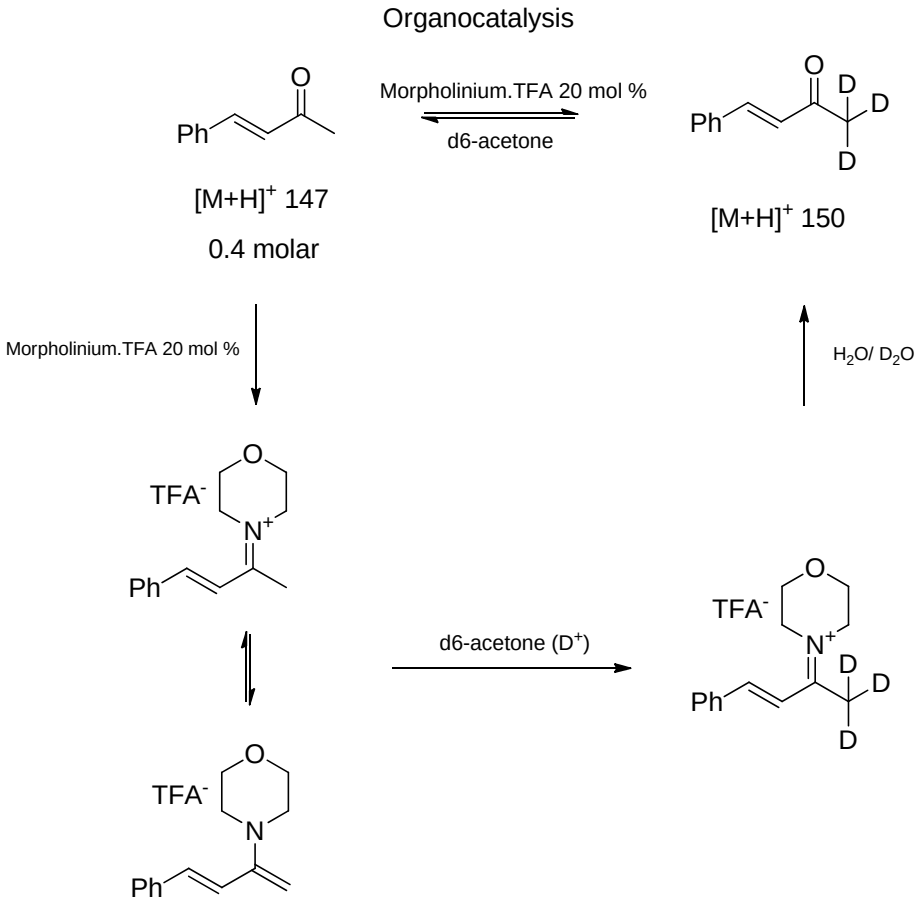

Scheme A 6.1 Deuterium exchange mechanism of **1a** in the presence of trifouroacetic acid (organocatalyst) in d6-acetone.

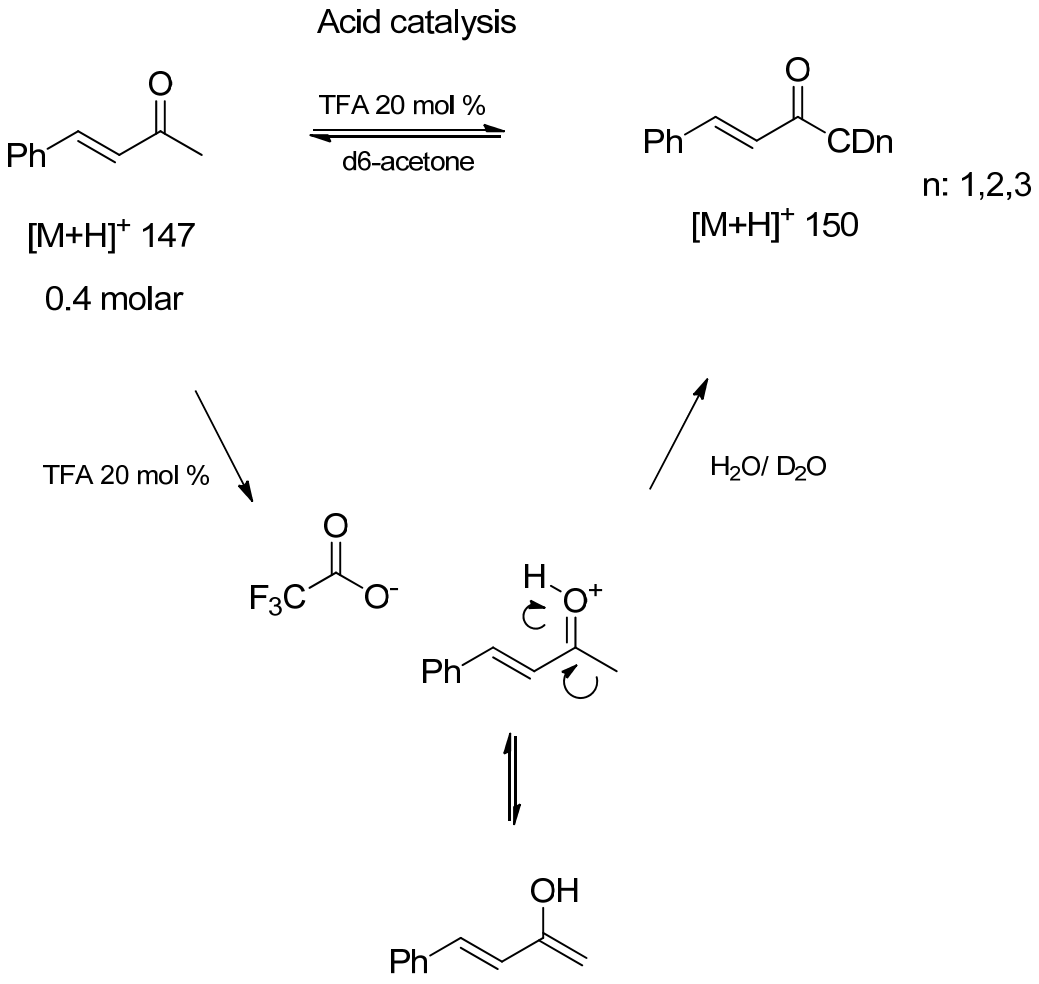

Scheme A 6.2 Deuterium exchange mechanism of **1a** in the presence of trifluoroacetic acid (acid catalyst) in d6-acetone.

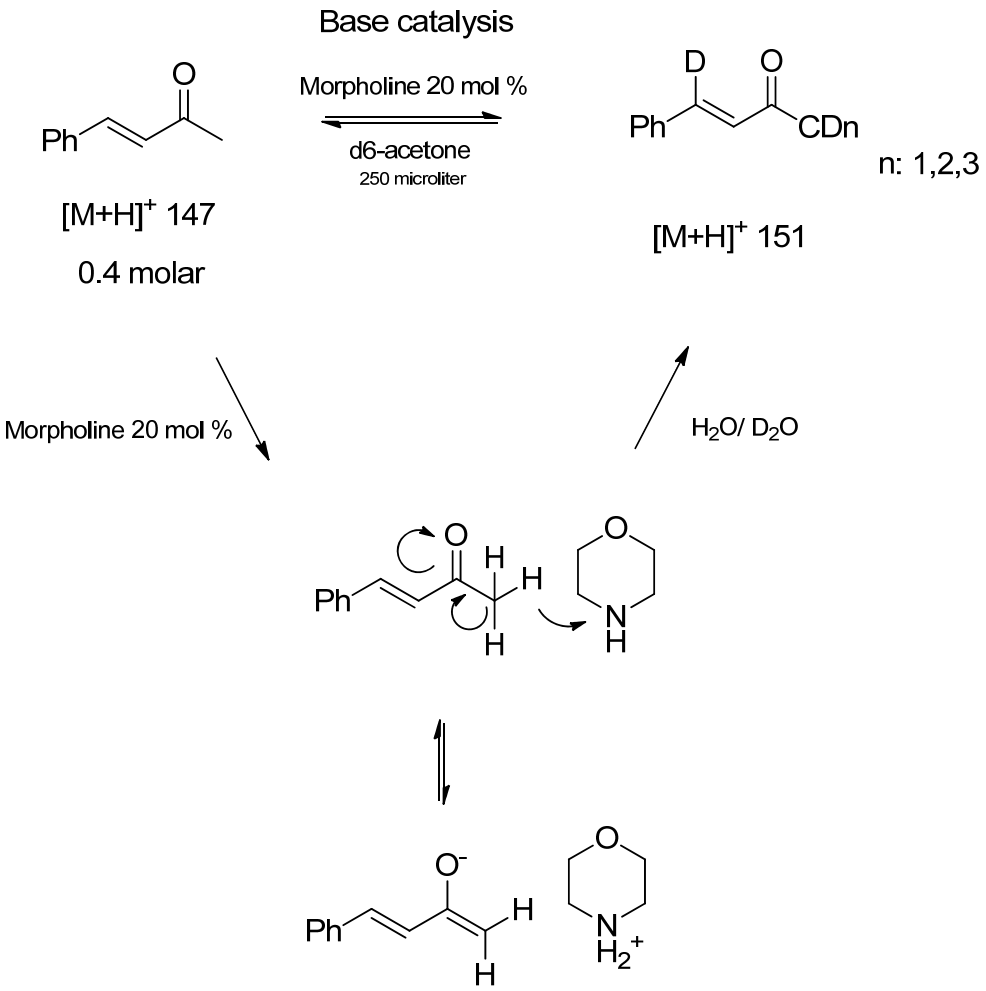

Scheme A 6.3 Deuterium exchange mechanism of **1a** in the presence of morpholine (base catalyst) acid in d6-acetone.

Full MS spectra of the ^{18}O-atom exchange from ^{18}O-acetone to the aldehyde **1c** in course of time to study the kinetic of the intermediates **5c**, **6**

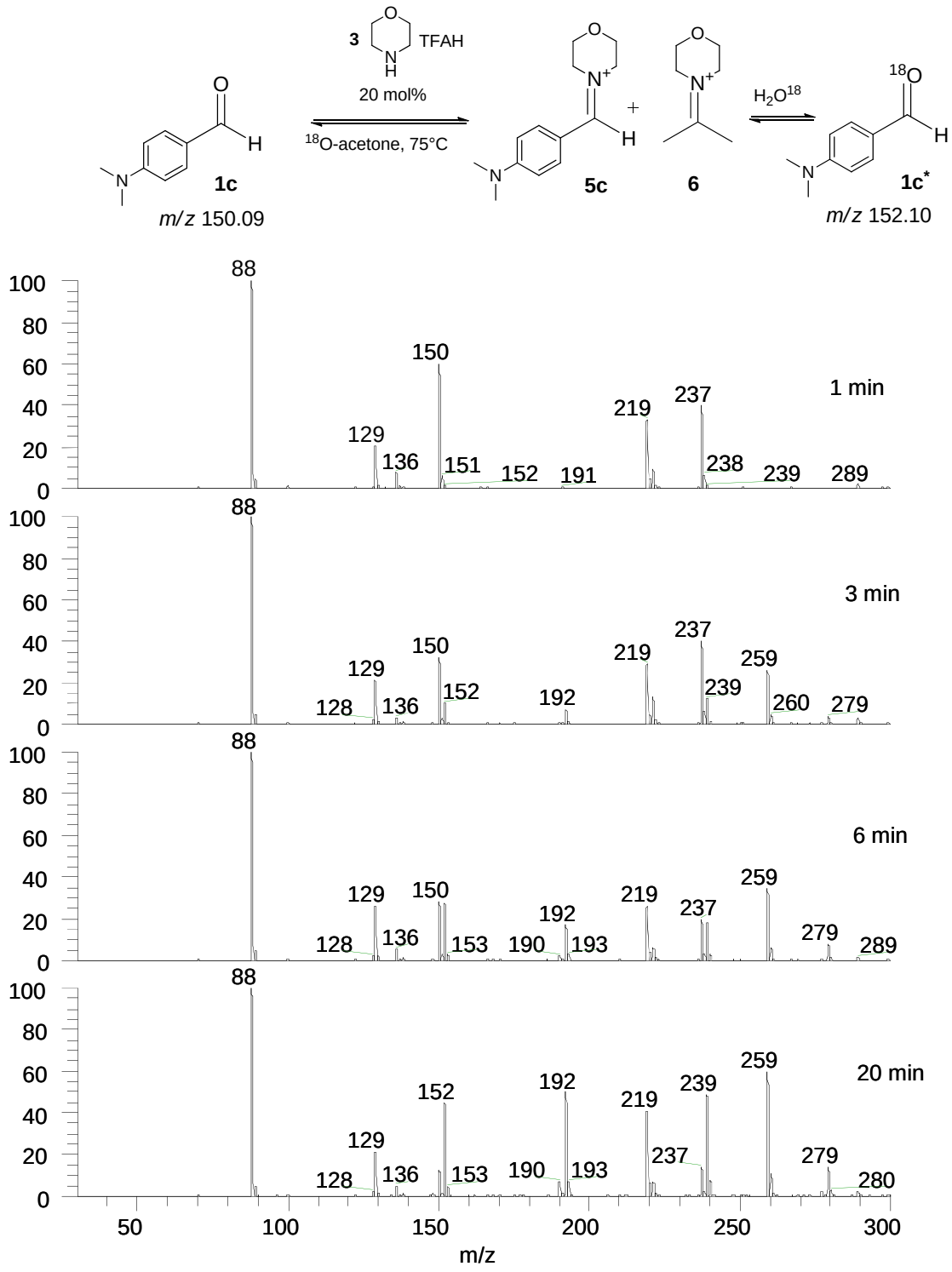

Figure A 6.9 ESI(+)-MS spectra of the conversion of **1c** *m/z* 150 to **1c*** *m/z* 152 in presence of ^{18}O-acetone and catalyst **3** in course of time.

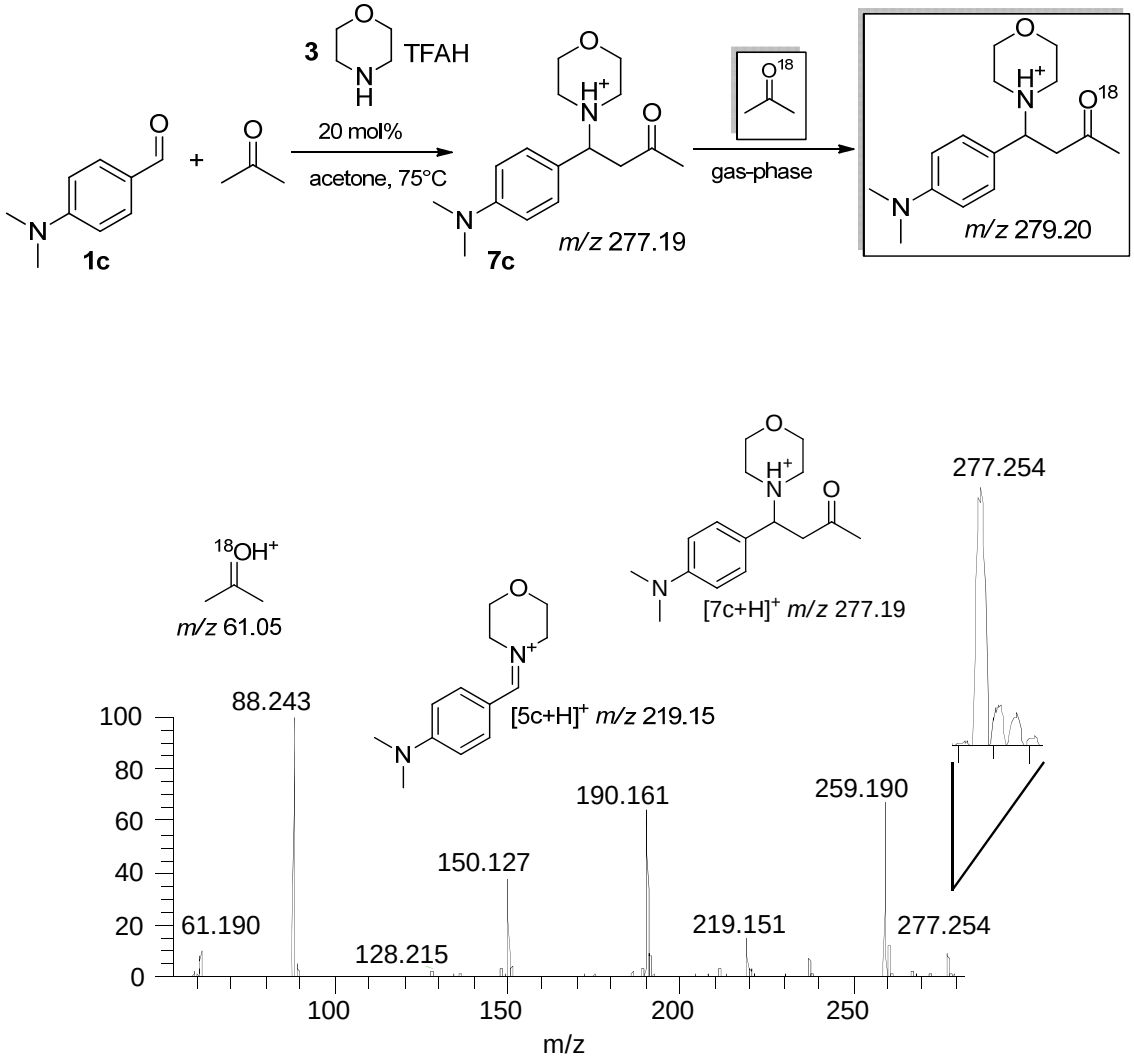

Figure A 6.10 Investigation of adduct formation of intermediate **7c** in the gas-phase by adding ^{18}O-labeled acetone to the diluted measured sample.

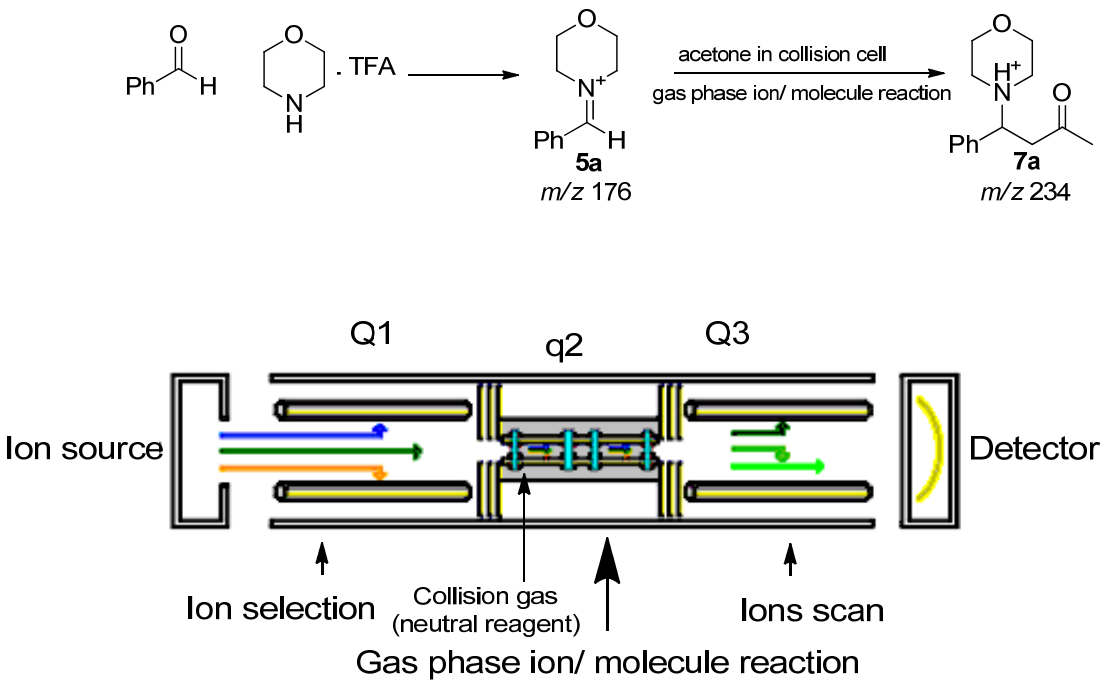

Scheme A 6.4 Schematic representation of the ion/molecule reaction.

7. Summary

In the last decade the field of Organocatalysis emerged as one of the essential method of the asymmetric synthesis. Organocatalysis offers several important advantages over transition metal- and bio-catalysis because they show reduced toxic effects and the catalytic compounds are usually robust, inexpensive, and readily available.
A huge number of organocatalytic reactions have been reported in the last years, but the understanding of the mechanism of these reactions is still in the beginning. Therefore it was necessary to investigate and understand the mechanism of such reactions to optimize the reaction conditions in regard to gain better reaction efficiency.

IR and NMR as the common analytical methods for structural elucidation in organic chemistry have often limitation in characterizing the reactive intermediates of complex reactions, such as multiple steps organocatalytic cascade reactions. The difficulties in such reactions are the limitation to detect the reactive intermediates present in the reaction solution with relatively short life times and low concentrations.

Electrospray ionization mass spectrometry with its tandem version ESI-MS(/MS) was chosen for the study of different organocatalytic reactions in this thesis because of its advantages particularly for the complex reactions.
The mechanistic reaction investigation began with a study of multi-step organocatalytic cascade reactions for the synthesis of tetra-substituted cyclohexene carbaldehydes by ESI-MS and ESI-MS/MS techniques. The mechanism was suggested by intercepting and characterizing of reactive intermediates in the complex reaction solution. The obtained results from this reaction confirmed the possibility to fish intermediates of such complex multi-step cascade reactions with ESI-MS and elucidate structural information by ESI-MS/MS to gain insights into the reaction details. However, the final products could only be detected in low intensities. If an intermediate or a product is not polar enough, it might be difficult to detect the analytes mass spectrometric with ESI, in this case, different ionization methods needed to be used like APCI or APPI, allowed to transform the desired analyte to the ionic form to gain detailed information of it.
After the investigations on the cascade reaction, new methods using electrospray mass spectrometry have been implemented to study the mechanism of aldol reactions of acetone with different aldehydes catalyzed by secondary amine organocatalyst like L-proline,

morpholinium- trifluoroacetate. It was possible to determine the reactive intermediates for this reactions by ESI(+)-MS and ESI(+)-MS/MS. Different techniques have been applied, such as online, -offline monitoring and isotope labeling with regard to deep detailed investigation of the catalytical cycle, as well as the intermediates activity. The results indicate that the reaction mechanism can allow different routes depending on the reaction conditions.

Finally a new organocatalytic concept using a multifunctional catalyst based on a peptide backbone has been investigated fully by electrospray mass spectrometry. Two different reaction systems with two different enantioselective multifunctional organocatalysts have been studied. The first cascade reaction is an enantioselective monoacylation od 1,2 cyclohexanediol followed by an oxidation of the second OH-group. The second reaction system is an epoxidation, hydrolysis and enantioselective monoacylation of cyclohexene. It was possible to determine the modification on the catalysts as well as reactive intermediates, products and side products by ESI(+)-MS and ESI(+)-MS/MS. Their structural elucidation was properly achieved using high resolution mass spectrometry.

At the end of this work it can be concluded that MS is a powerful tool with regard to investigate mechanistic study of organocatalyzed reactions and characterize the reaction components sensitively and selectively with huge possibilities of mass spectrometric techniques and methods to be applied for the requirements of each studied reaction.

List of Figures

List of schemes

List of tables

List of Abbreviations and Symbols

ACN	acetonitrile
APCI	atmospheric pressure chemical ionization
API	atmospheric pressure ionization
APPI	atmospheric pressure photo ionization
CAD	collisionally activated dissociation
CID	collision-induced dissociation
CM	catalytical moiety
CRM	charge residue model
Da	dalton
DC	direct current
ee	enantiomeric excess
EI	electron impact
ESI-MS	electrospray-ionization mass spectrometry
et al.	et alii
eV	electron volt
FAB	Fast atom bombardment
FT-ICR	fourier transform ion cyclotron resonance
i.e.	id est
IEM	Ion Evaporation Model
KV	kilo volt
LTQ	linear trap quadrupole
m/z	mass to charge ratio
MALDI	Matrix-assisted laser desorption/ionization
MeOH	methanol
NMR	nuclear magnetic resonance
pH	potentia hydrogenii
ppm	part per million
QIT	quadrupole ion trap

QqQ	triple quadrupole
R	rectus
RF	radio frequence
RF	triple stage quadrupole
S	sinister
S	ultra violet
SI	secondary ionization method
TOF	time of filght

Erklärung

Hiermit versichere ich, dass ich die vorliegende Arbeit mit dem Titel

„**Development and application of mass spectrometric method for the investigation of organocatalytic reactions**"

selbst verfasst und keine außer den angegebenen Hilfsmitteln und Quellen benutzt habe, und dass die Arbeit in dieser oder ähnlicher Form noch bei keiner anderen Universität eingereicht wurde.

Mülheim an der Ruhr, 9th Juli 2013

UNTERSCHRIFT